Instrumentation: Gamma-ray spectroscopy

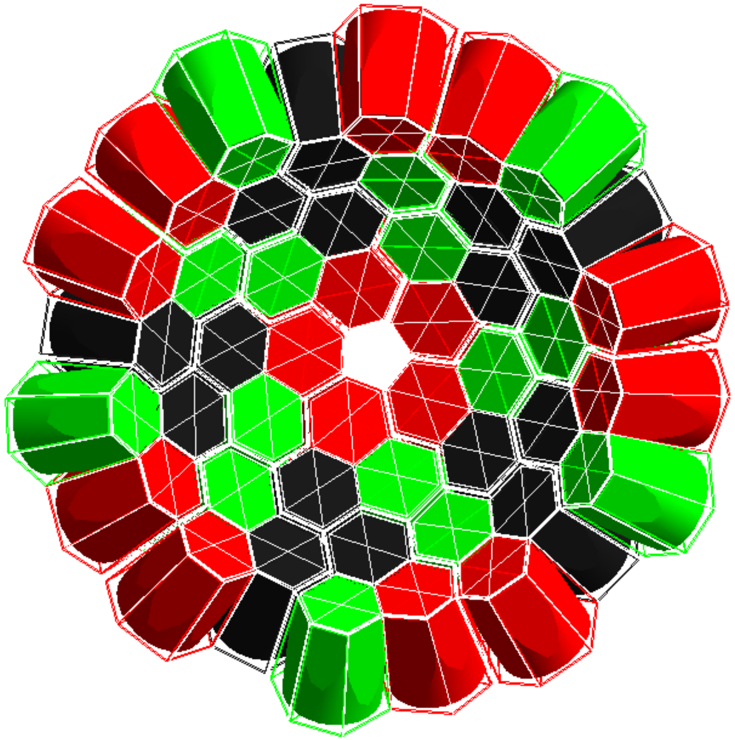

Stefanos Paschalis

22nd STFC Nuclear Physics Summer School

August 2024

Resources and acknowledgements

Sidong Chen, York PDRA, exercises

Slides from several colleagues:
Augusto Macchiavelli, Marina Petri, Pankaj Josi….

GRETA and AGATA collaborations

Glenn F. Knoll. Radiation detection and measurement (John Wiley & Sons, 1979), 4th edition

W.R. Leo: Techniques for Nuclear and Particle Physics Experiments, Springer-Verlag, second revised edition edition, 1994

Zhong He, NIM A 463 (2001) 250–267, Review of the Shockley–Ramo theorem and its application in semiconductor gamma-ray detectors

UK landscape – STFC funded projects

CERN

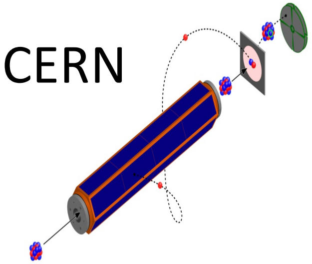

ISS

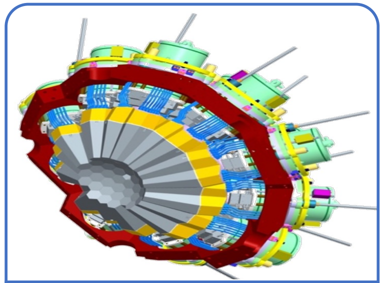

AGATA

FAIR

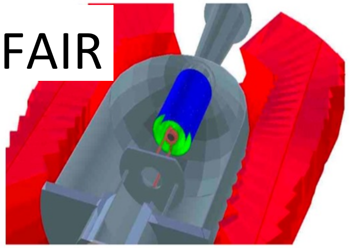

R3B TRT

FRIB

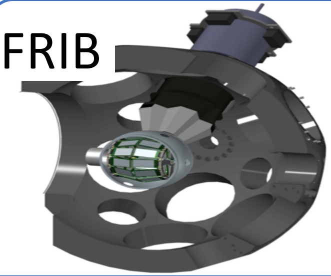

FAUST

RIBF

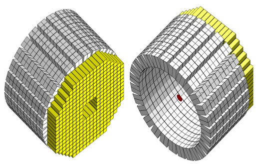

HYPATIA

Detectors for
EIC
JLAB
ALICE

……*

*Apologies to those projects that I may have forgotten

Ionising radiation detectors

All types of detectors are based on the same fundamental principle: the transfer of part or all of the radiation energy to the detector mass where it is converted into some other form more accessible to human perception (W.R. Leo).

One is typically interested in extracting the:

- Energy deposition (of ionising particle)
- Timing (of interaction)
- Position (of interaction within the detector)
- Type of particle (PID)
- Incident rate or dose
- .....

The basic ingredients for detection

- Interactions of ionizing radiation with matter
- Detection technology
- Electronic readout and signal processing
- Data analysis

The basic ingredients ~~for detection~~ of this Lecture

Background and motivation

- Interactions of ionizing radiation with matter — γ rays
- Detection technology — Semiconductors, HPGe arrays
- Electronic readout and signal processing — position sensitive
- Data analysis — for g-ray tracking

ADVANCED GAMMA TRACKING ARRAY

RESOLVING POWER or "finding a needle in the haystack"
The elevator Speech

https://www.triz.co.uk/problem-solving---facilitation-workshops

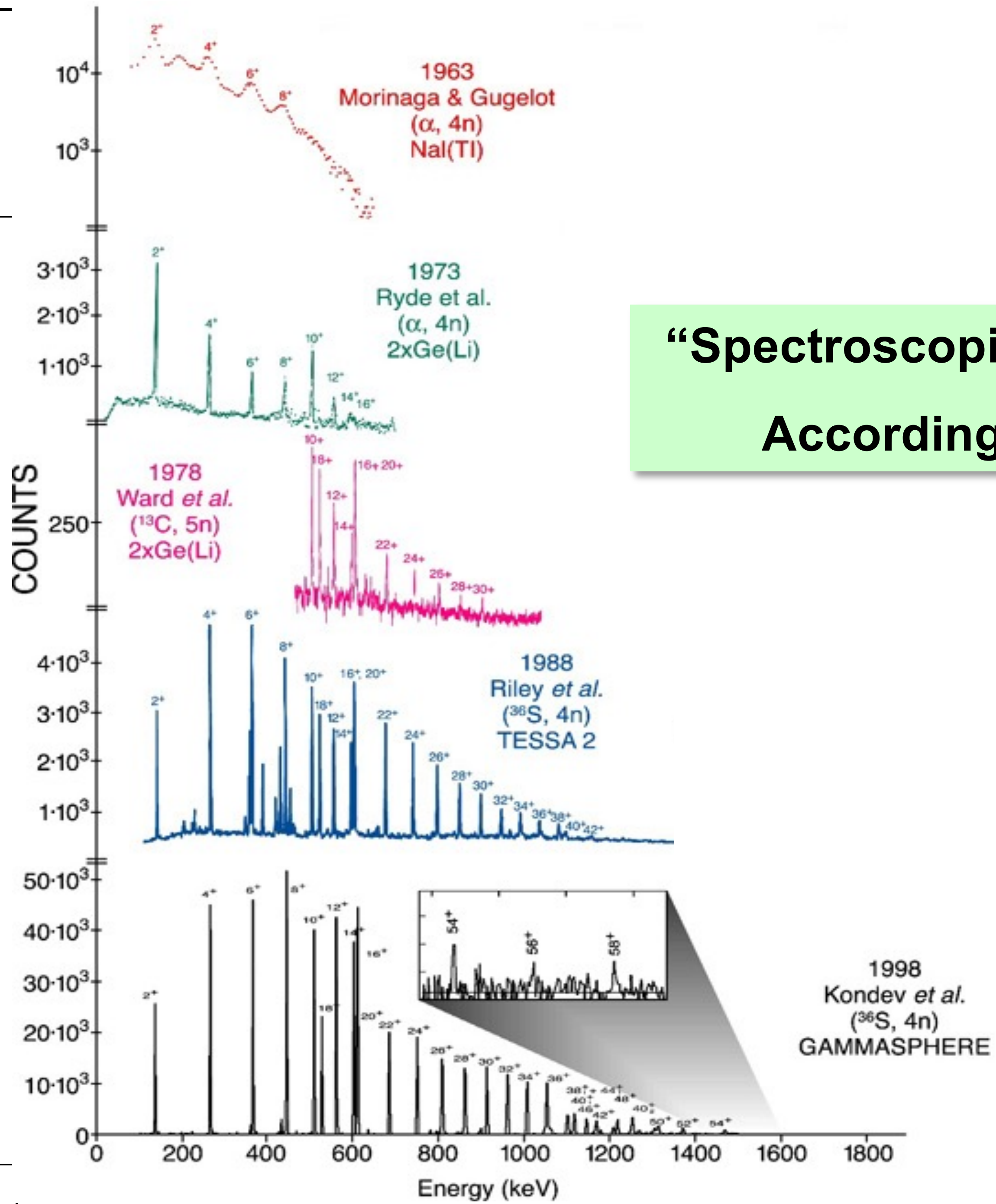

“Spectroscopic history” of ^{156}Dy

According to Mark Riley

Development of new detectors and techniques have always led to discoveries of new and unexpected phenomena.

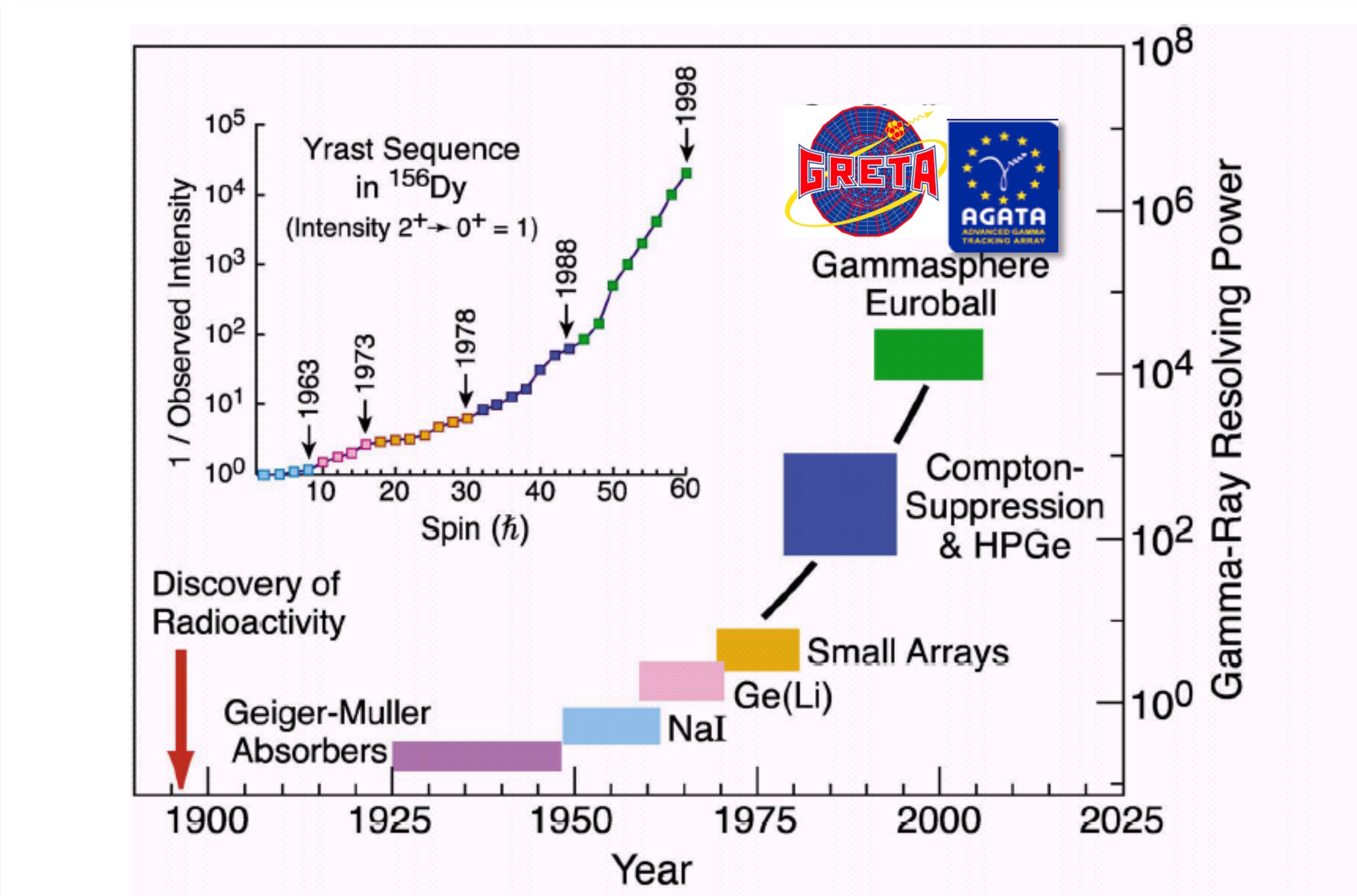

Interactions of ionizing radiation with matter

γ rays

Detection technology

Electronic readout and signal processing

Data analysis

Interaction of γ rays with matter

Photo effect

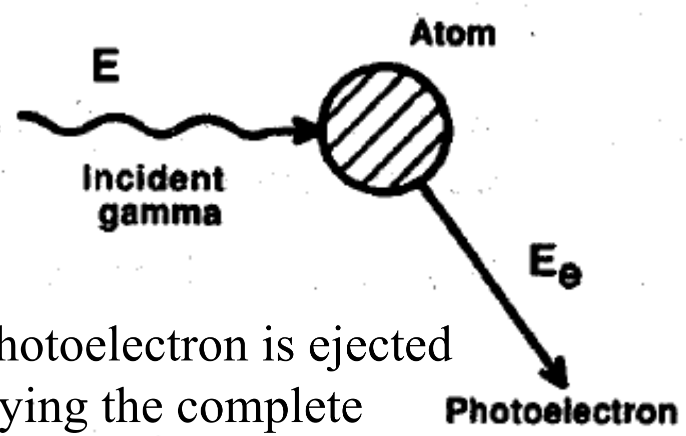

A photoelectron is ejected carrying the complete gamma-ray energy (- binding)

Compton scattering

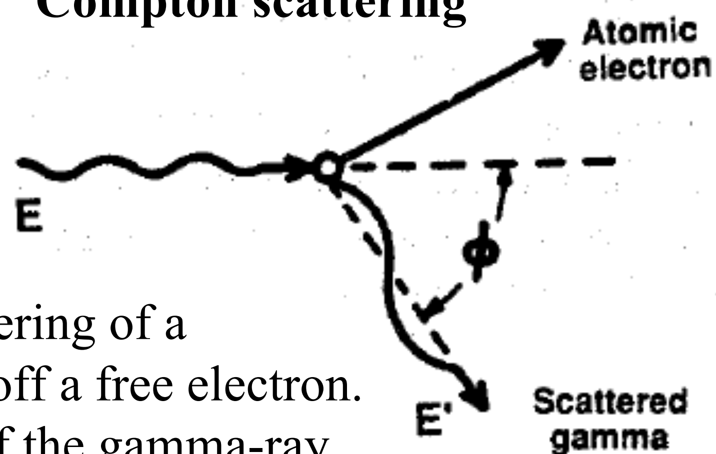

Elastic scattering of a gamma ray off a free electron. A fraction of the gamma-ray energy is transferred to the Compton electron

Pair production

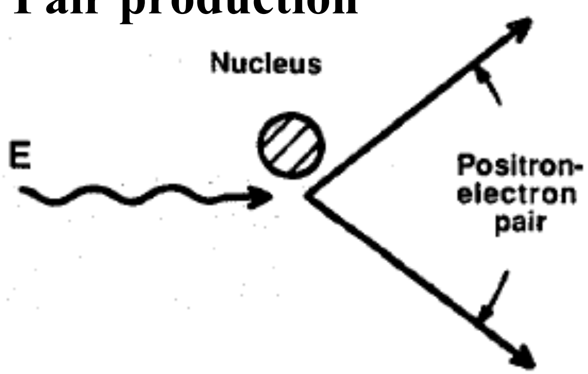

If gamma-ray energy is >> 2 m_oc^2 (electron rest mass 511 keV), a positron-electron can be formed in the strong Coulomb field of a nucleus. This pair carries the gamma-ray energy minus 2 m_oc^2 .

Exercise 1:
Anatomy of a high resolution gamma-ray spectrum

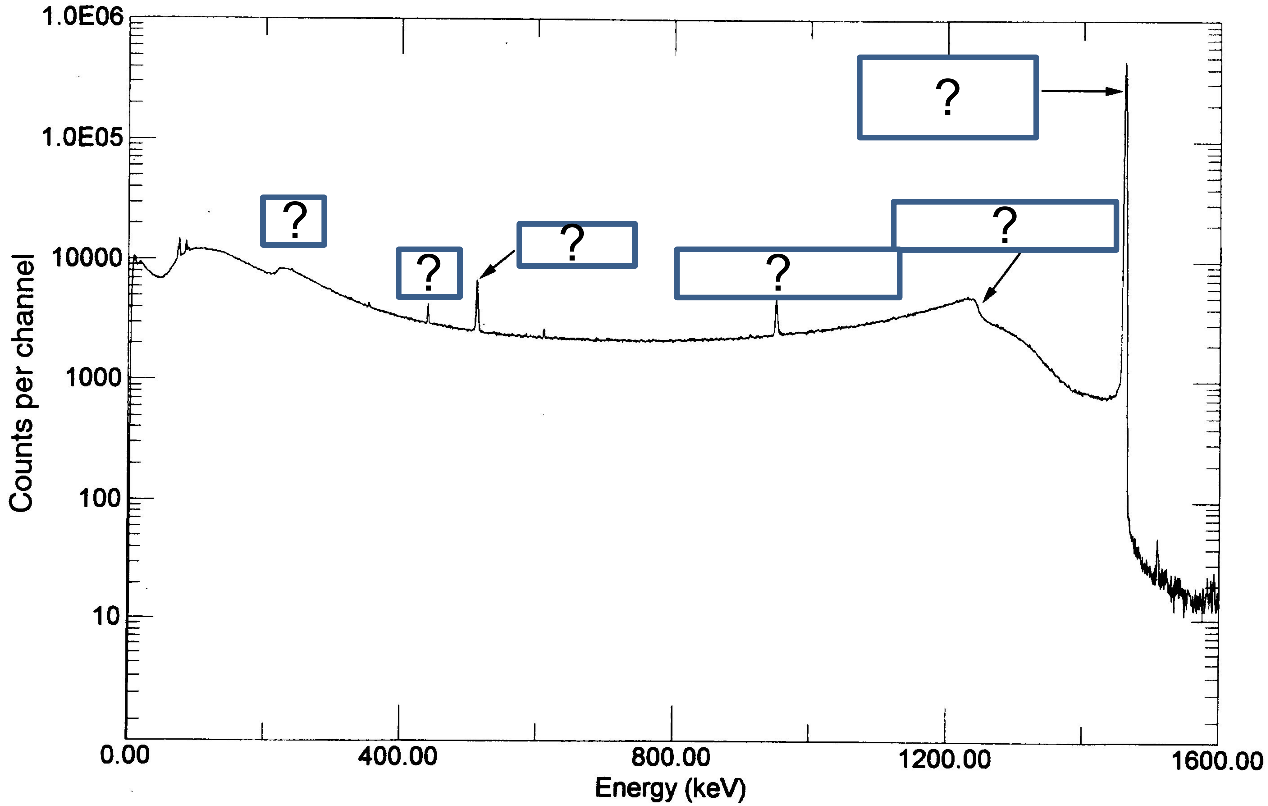

What are the characteristic features?

Think of the origin of all characteristic peaks and structures, all based on the previous slide!

Analysing a high resolution gamma-ray spectrum

Full energy peak (photo-peak)

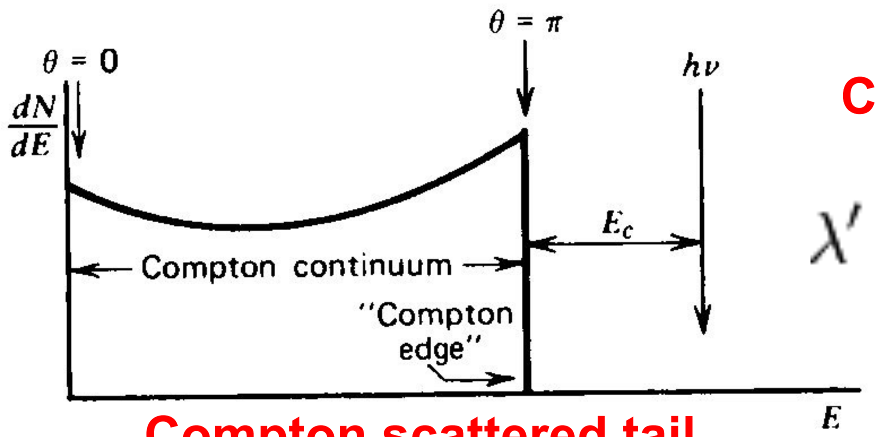

Compton scattered tail

Compton scattering formula

$$\lambda' - \lambda = \frac{h}{m_e c}(1 - \cos\theta),$$

The concept of Compton Suppression

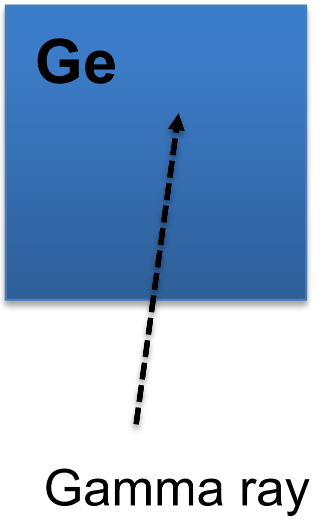

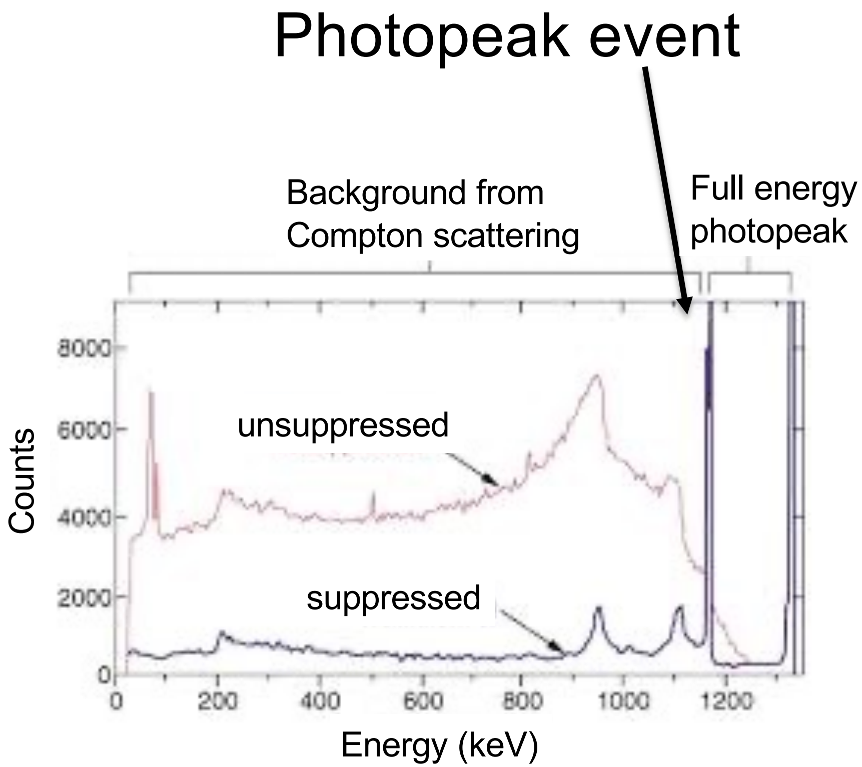

The concept of Compton Suppression

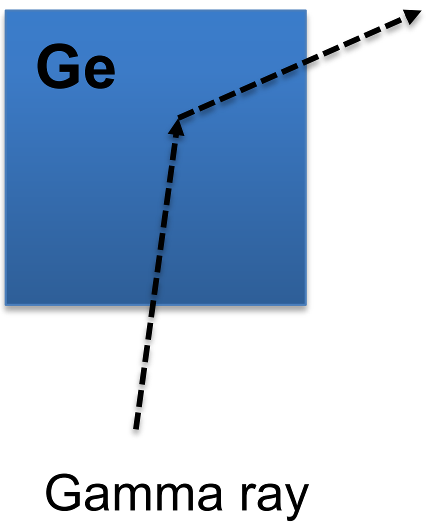

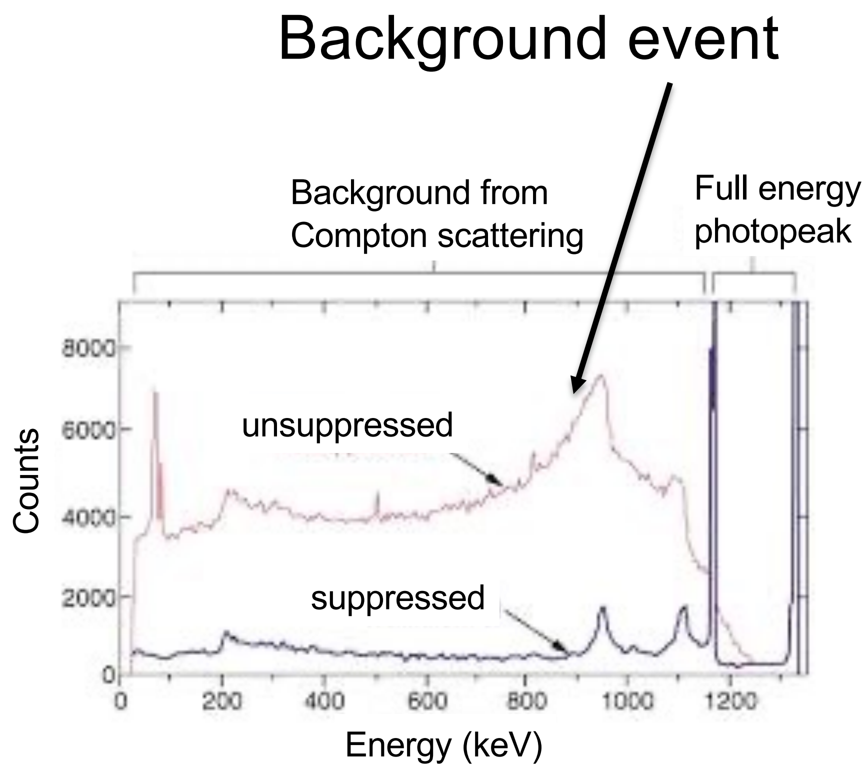

The concept of Compton Suppression

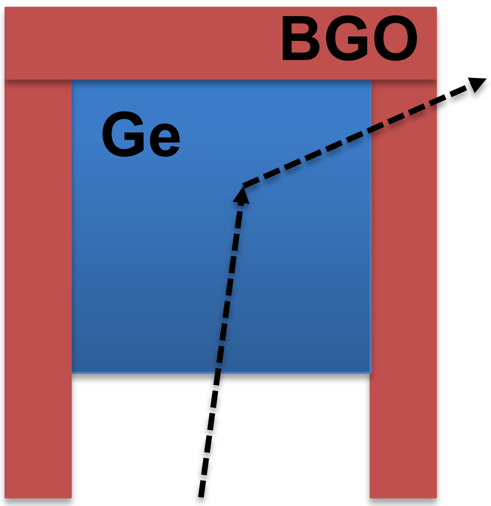

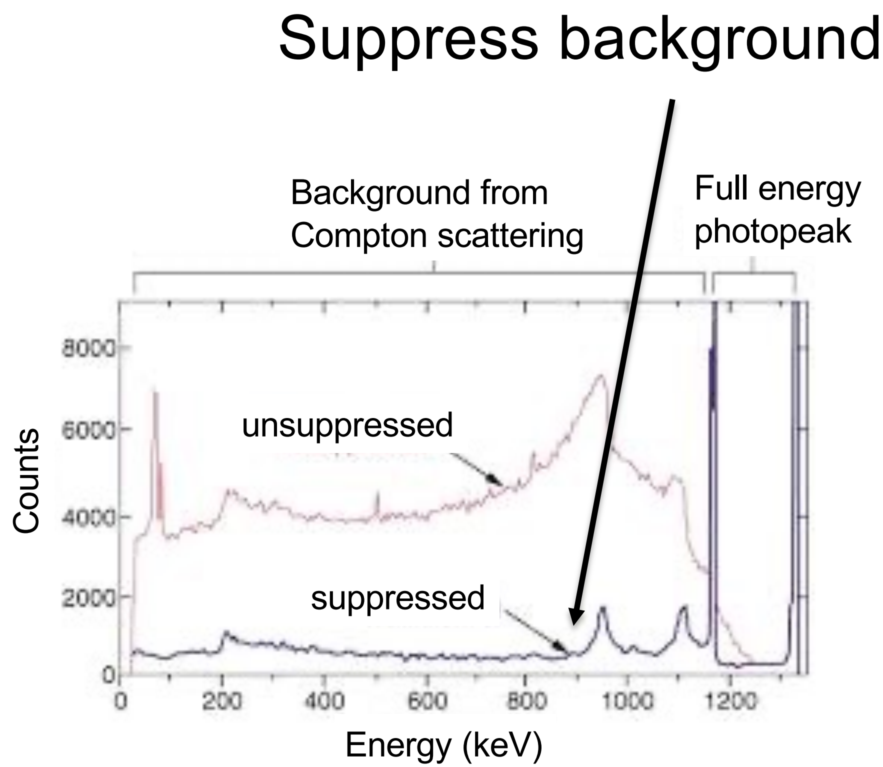

Improves peak-to-total ratio considerably!

The concept of Compton Suppression

Compton suppressed arrays:
Excellent peak-to-total ratio <u>but</u> limited efficiency

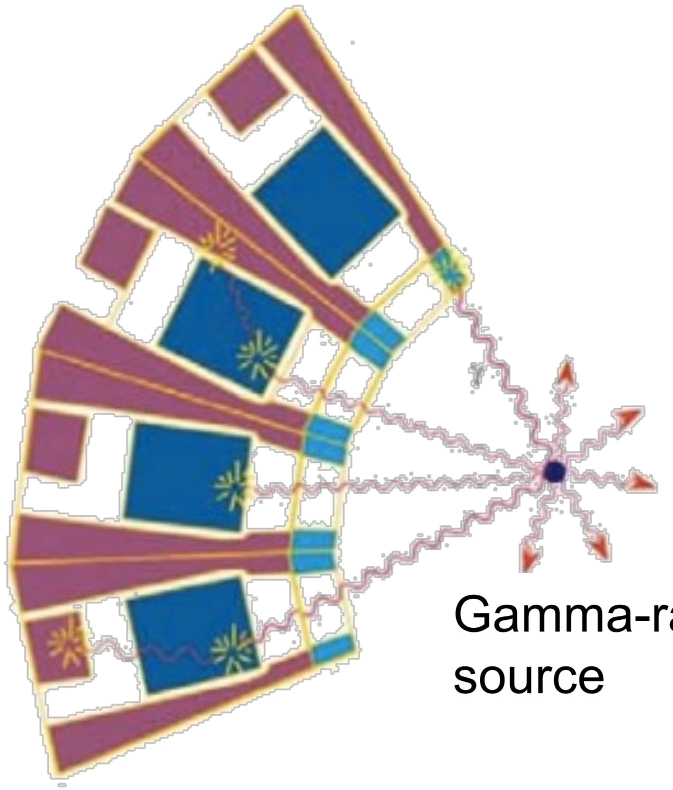

Gamma-ray source

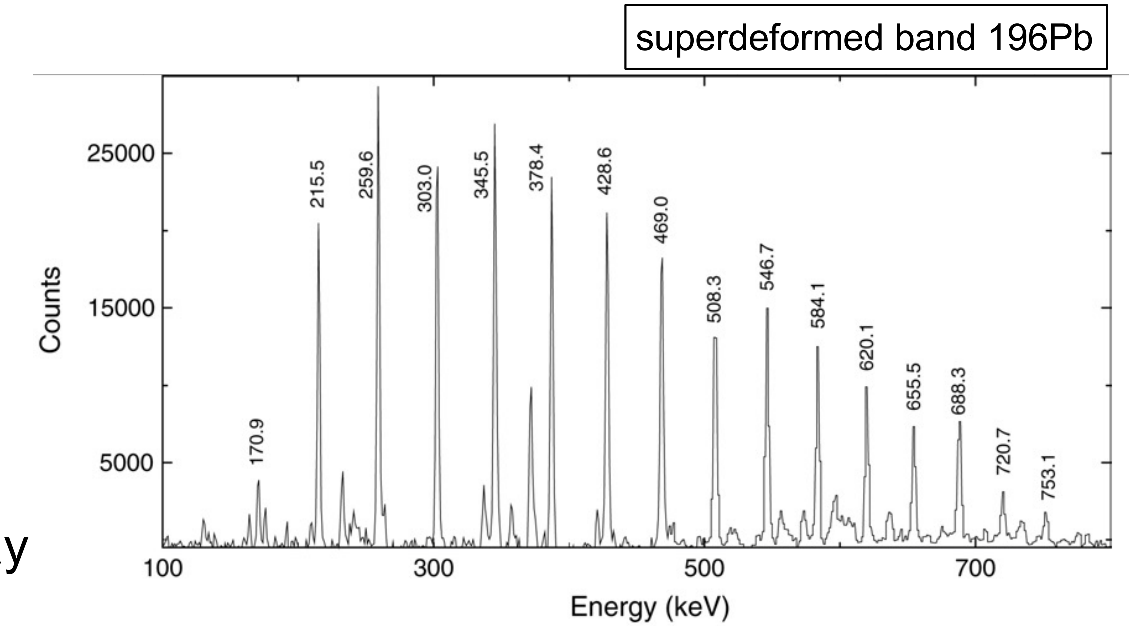

A.K. Singh *et al.*, Nucl. Phys. A 707, 3 (2002

Widely used quantities for high res. gamma-ray detectors

Peak to Compton = $\frac{Height\ of\ photopeak}{Aver.\ counts\ in\ Compt.\ plateau}$

P/T = Peak to Total = $\frac{Counts\ in\ the\ peak\ area}{Total\ counts\ in\ the\ spectrum}$

Resolution (δE)

average spacing between gammas (SE_{γ})

and resolving power (RP)

Efficiency
(often relative to a 3”x3” NaI (cylinder))

Suppress background

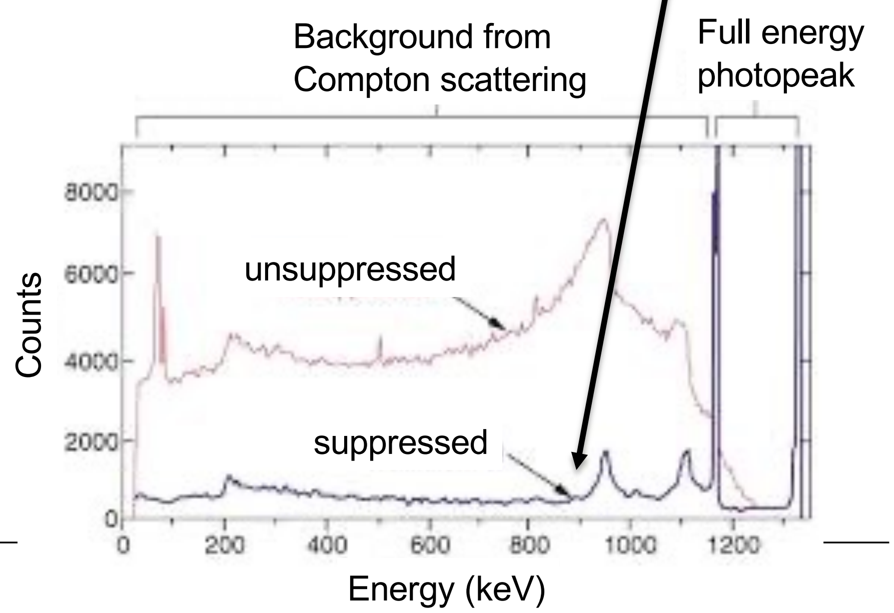

Array Capabilities and Future Arrays

D.C. Radford

Physics Opportunities with Large Ge Detector Arrays: Present and Future
Asilomar, October 1993

2. $R = (SE_\gamma/\delta E_\gamma)\ PT$

$R \propto$ average improvement in peak-to-background as a function of increased coincidence fold.

SE_γ = average spacing between gammas in cascade ($\approx$ 60 keV for (HI,xn) reactions)

δE_γ = energy resolution (FWHM) (typically 4 – 6 keV at E_γ = 1 MeV)

PT = photopeak-to-total ratio for the Compton-suppressed HPGe detectors

Evolution of gamma-ray detection technology

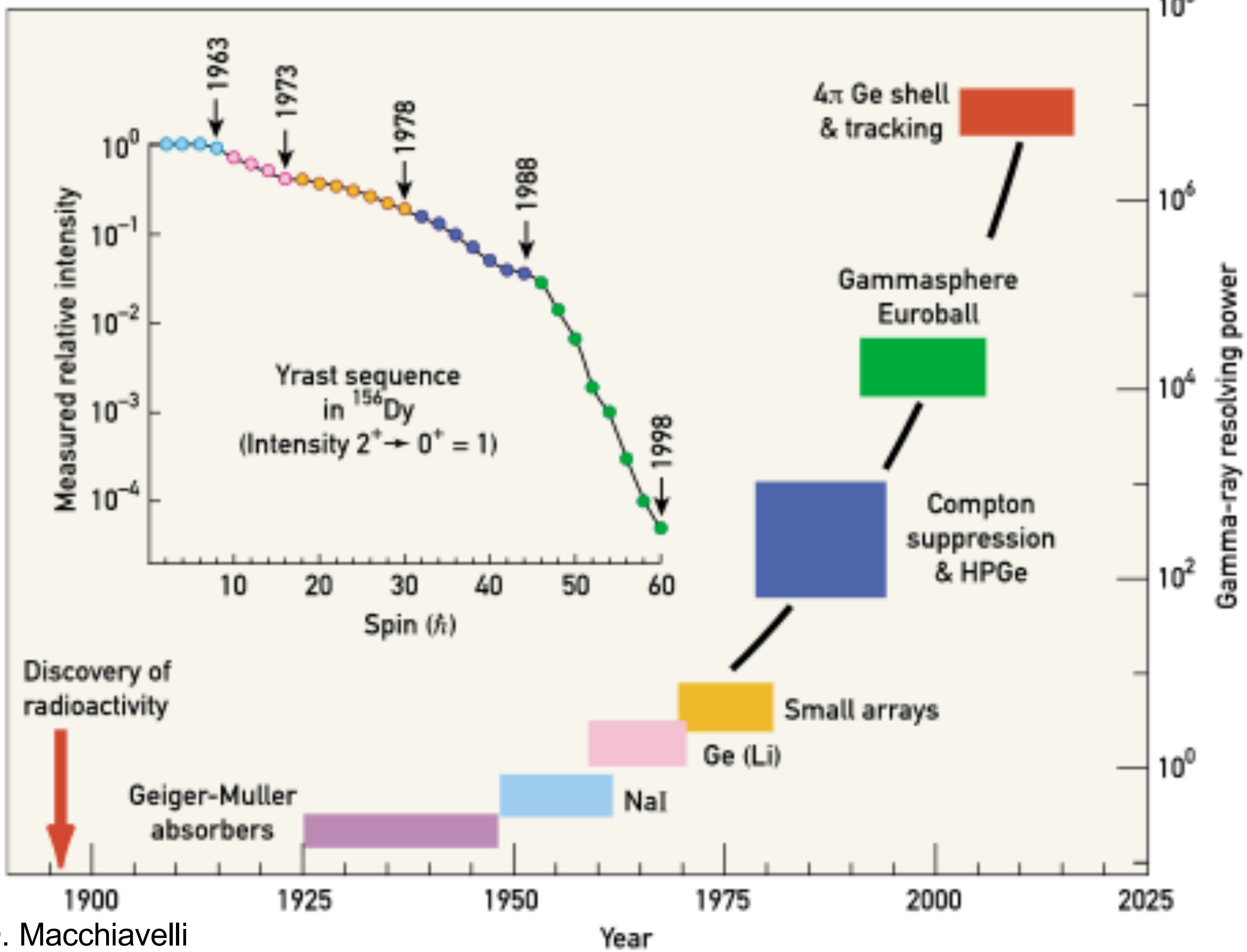

Resolving power:
Energy resolution (δE),
Efficiency (ε),
Peak-to-total (P/T)

A.O. Macchiavelli

Evolution of gamma-ray detection technology

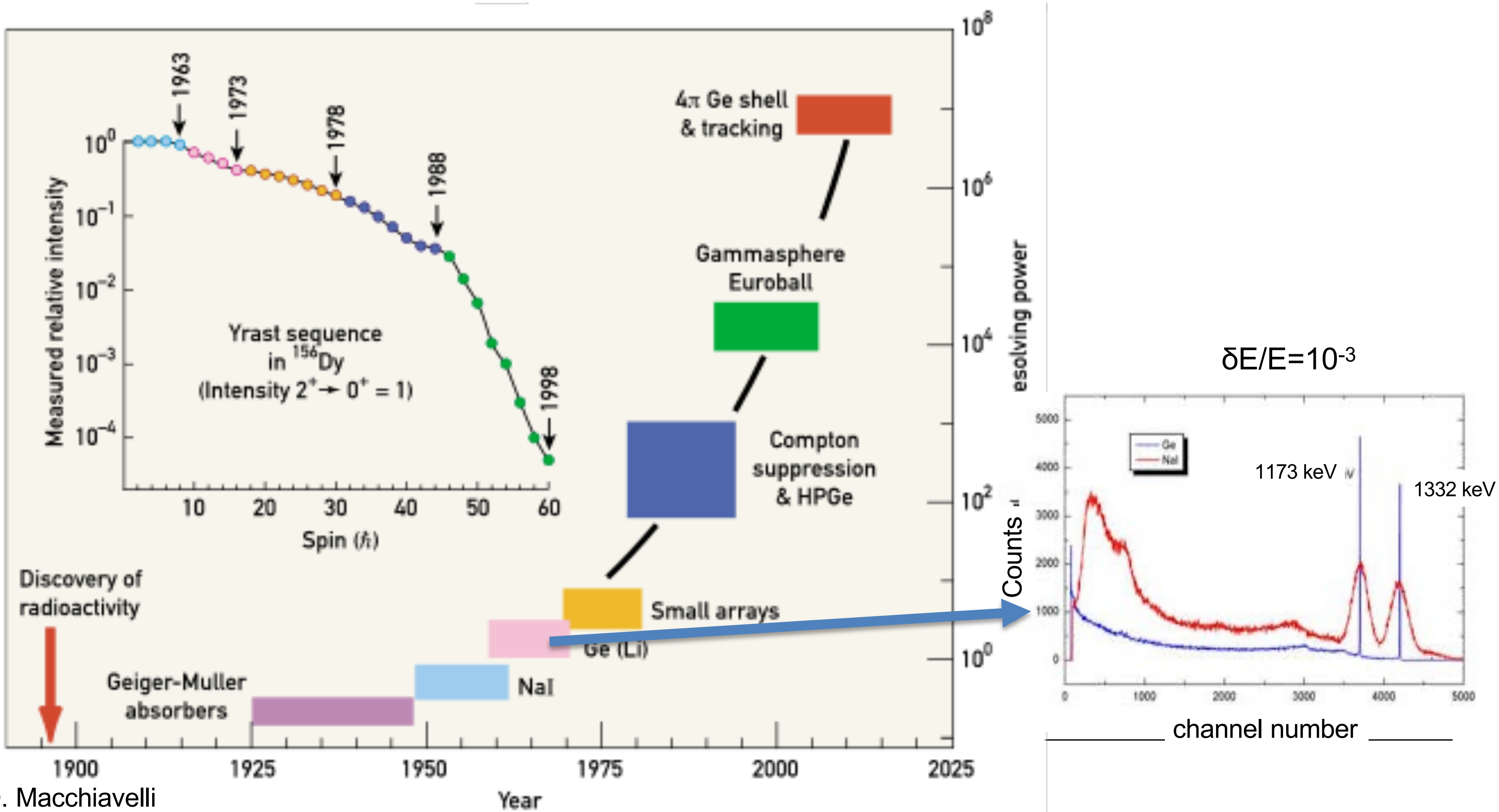

A.O. Macchiavelli

Evolution of gamma-ray detection technology

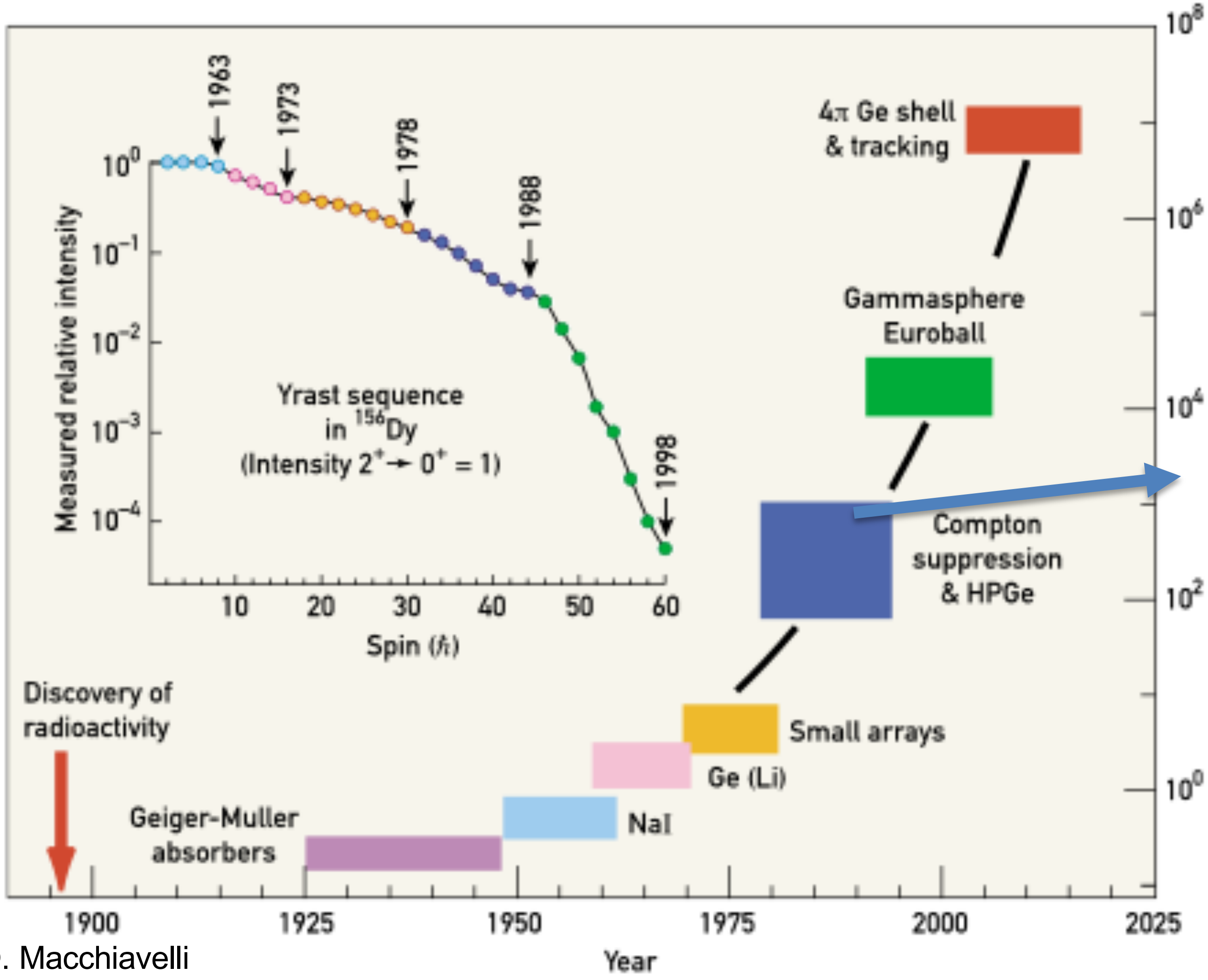

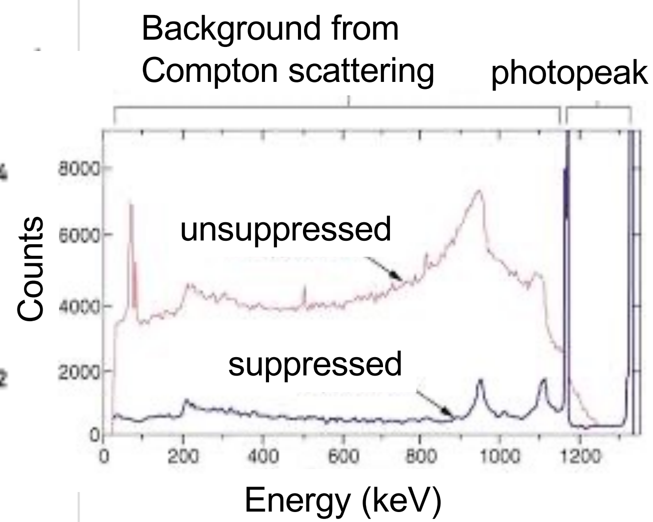

A.O. Macchiavelli

Evolution of gamma-ray detection technology

Gamma-ray tracking arrays

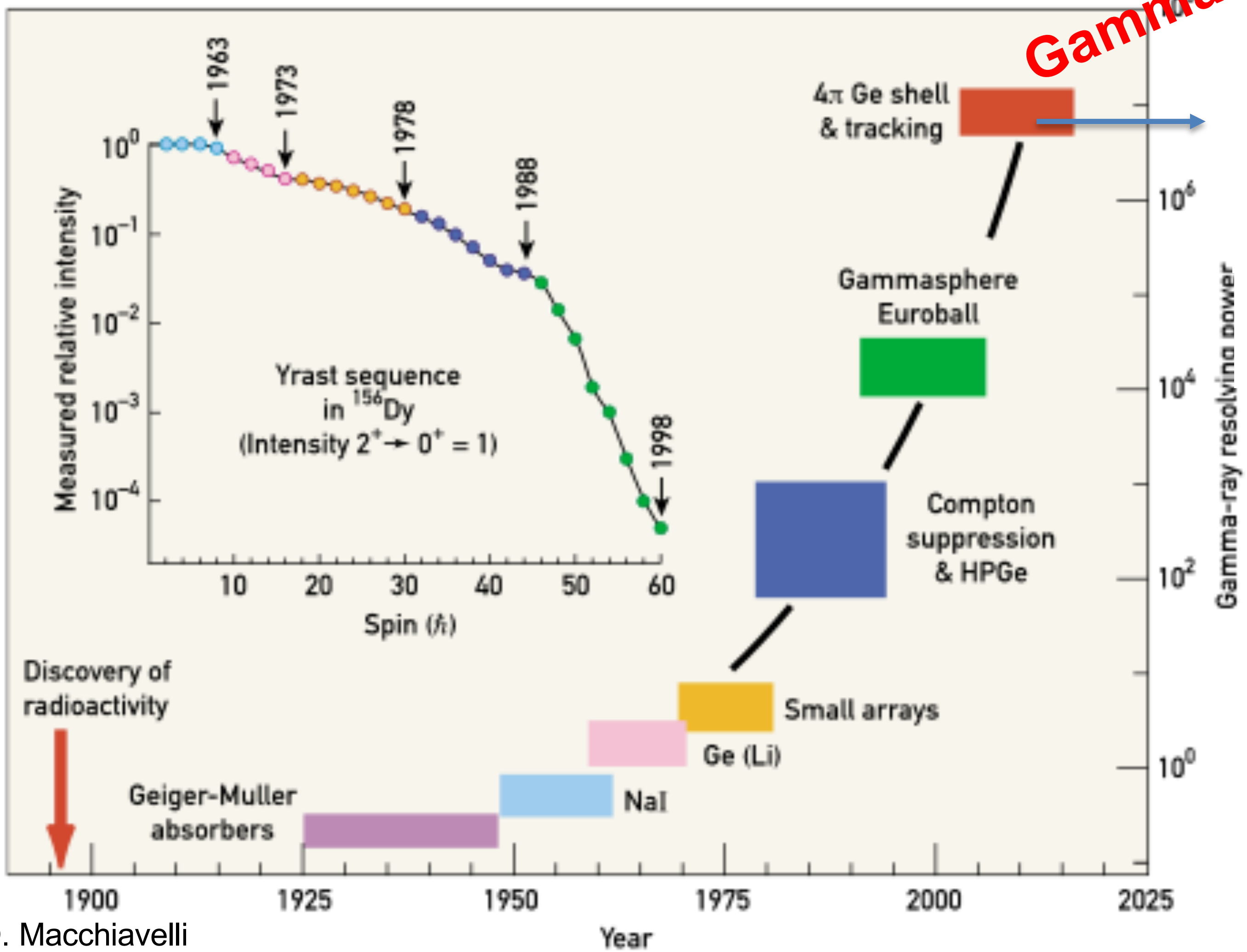

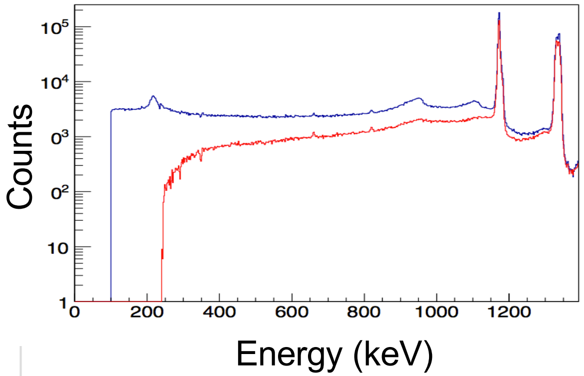

A.O. Macchiavelli

Gamma-ray tracking:
Principle of operation

The idea is: Do not to reject but track instead!

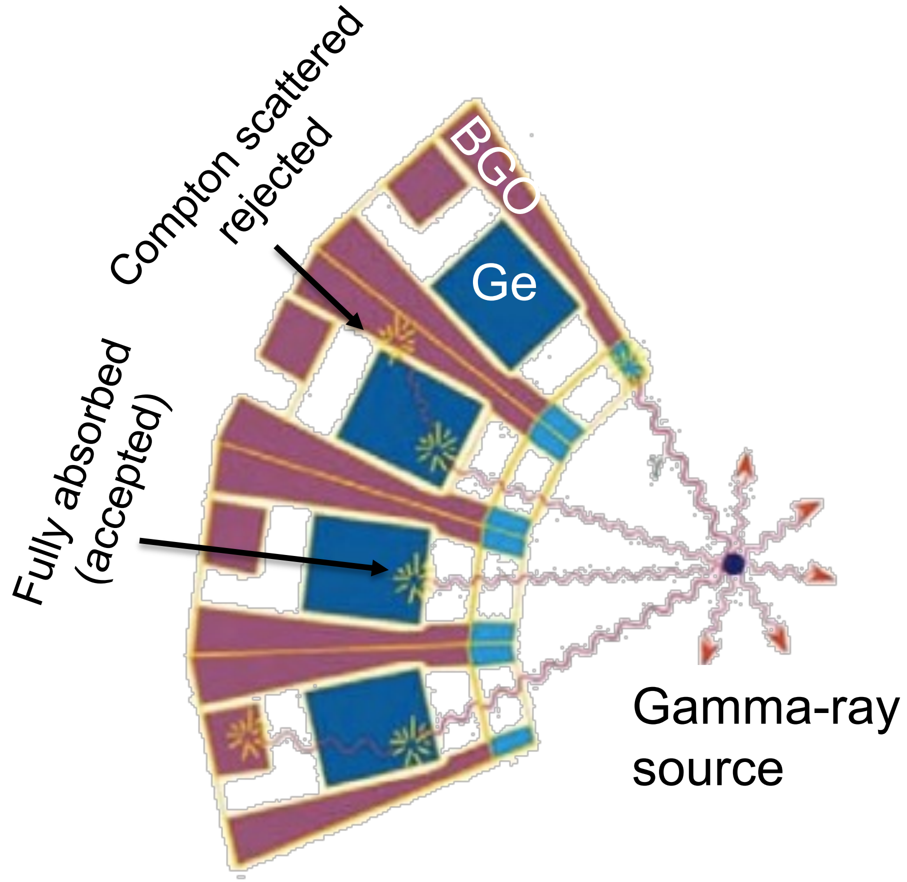

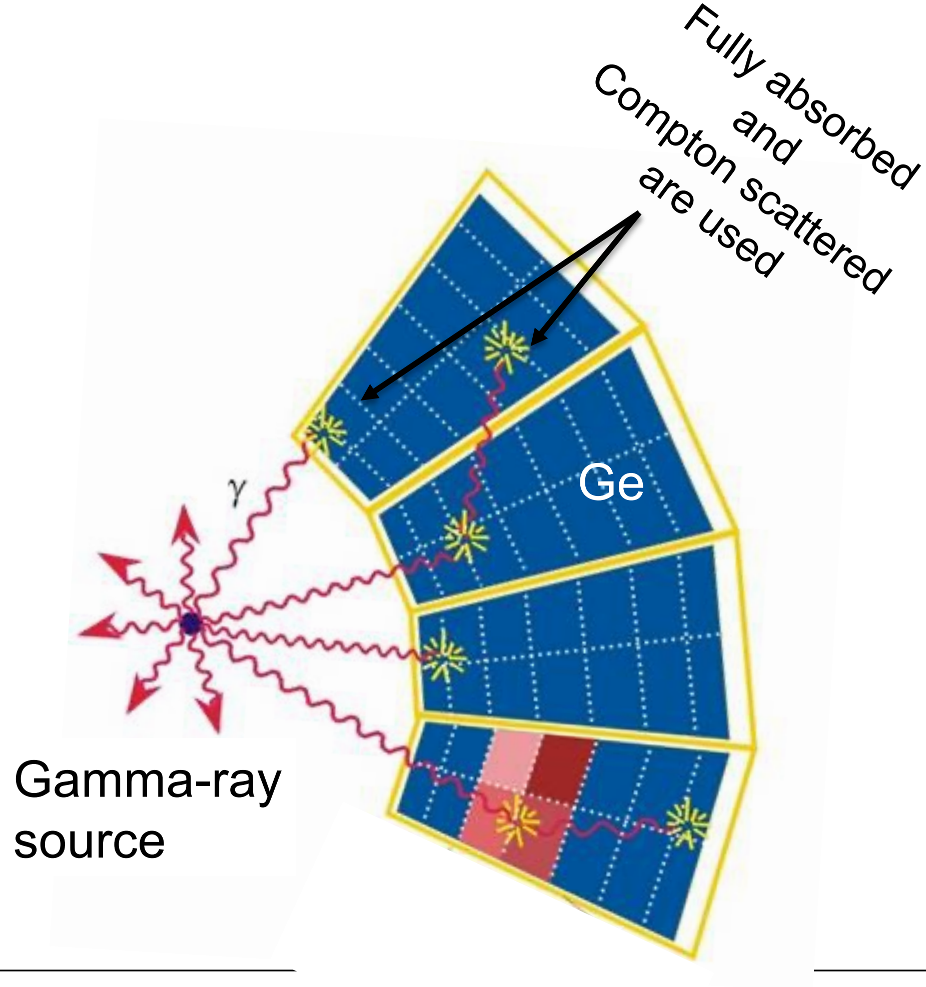

Gamma-ray tracking:
Principle of operation

(x, y, z, e) + Compton formula → Tracking

needs a 3D position sensitive Ge detector

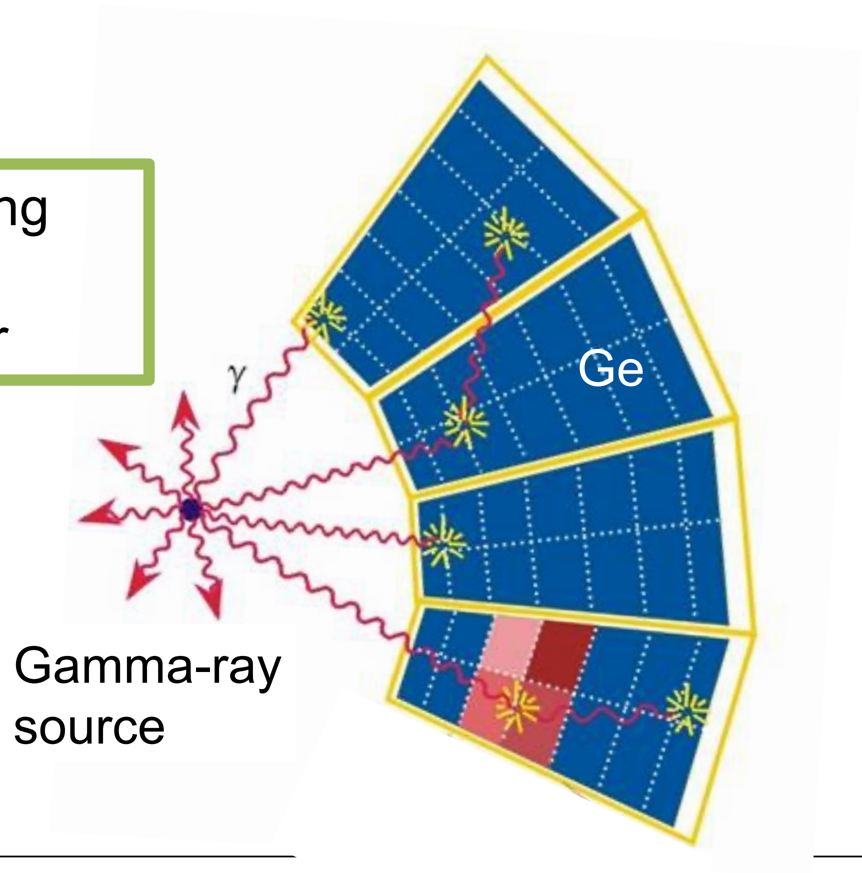

Gamma-ray tracking:
Principle of operation

To proceed from here we should look back at the basics

(x, y, z, e) + Compton

needs a 3D position sensitive Ge d

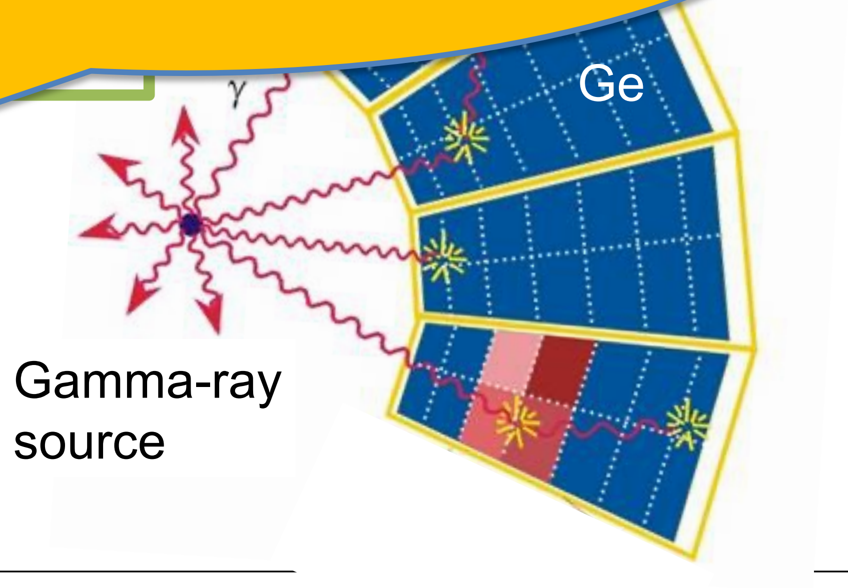

The basic ingredients ~~for detection~~ of this Lecture

- Interactions of ionizing radiation with matter
- Detection technology — Semiconductors
- Electronic readout and signal processing
- Data analysis

Ge crystal

Fig. 5.14 Germanium ingot and Ge detector elements. Figure by courtesy of CANBERRA – an AREVA company

Semiconductor Detectors

- These are predominantly group IV elements; C, Si and Ge based.

PERIODIC TABLE OF THE ELEMENTS

1 IA	2 IIA	3 IIIB	4 IVB	5 VB	6 VIB	7 VIIB	8	9 VIII	10	11 IB	12 IIB	13 IIIA	14 IVA	15 VA	16 VIA	17 VIIA	18 VIIIA
1 H Hydrogen 1.008																	2 He Helium 4.002602
3 Li Lithium 6.94	4 Be Beryllium 9.012182											5 B Boron 10.81	6 C Carbon 12.0107	7 N Nitrogen 14.007	8 O Oxygen 15.999	9 F Fluorine 18.998403163	10 Ne Neon 20.1797
11 Na Sodium 22.98976928	12 Mg Magnesium 24.305											13 Al Aluminum 26.9815385	14 Si Silicon 28.085	15 P Phosphorus 30.973761998	16 S Sulfur 32.06	17 Cl Chlorine 35.45	18 Ar Argon 39.948
19 K Potassium 39.0983	20 Ca Calcium 40.078	21 Sc Scandium 44.955908	22 Ti Titanium 47.867	23 V Vanadium 50.9415	24 Cr Chromium 51.9961	25 Mn Manganese 54.938044	26 Fe Iron 55.845	27 Co Cobalt 58.933195	28 Ni Nickel 58.6934	29 Cu Copper 63.546	30 Zn Zinc 65.38	31 Ga Gallium 69.723	32 Ge germanium 72.630	33 As Arsenic 74.921595	34 Se Selenium 78.971	35 Br Bromine 79.904	36 Kr Krypton 83.798
37 Rb Rubidium 85.4678	38 Sr Strontium 87.62	39 Y Yttrium 88.90584	40 Zr Zirconium 91.224	41 Nb Niobium 92.90637	42 Mo Molybd. 95.95	43 Tc Technetium (97.907212)	44 Ru Ruthenium 101.07	45 Rh Rhodium 102.90550	46 Pd Palladium 106.42	47 Ag Silver 107.8682	48 Cd Cadmium 112.414	49 In Indium 114.818	50 Sn Tin 118.710	51 Sb Antimony 121.760	52 Te Tellurium 127.60	53 I Iodine 126.90447	54 Xe Xenon 131.293
55 Cs Caesium 132.90545196	56 Ba Barium 137.327	57–71 lantha-nides	72 Hf Hafnium 178.49	73 Ta Tantalum 180.94788	74 W Tungsten 183.84	75 Re Rhenium 186.207	76 Os Osmium 190.23	77 Ir Iridium 192.217	78 Pt Platinum 195.084	79 Au Gold 196.966569	80 Hg Mercury 200.592	81 Tl Thallium 204.38	82 Pb Lead 207.2	83 Bi Bismuth 208.98040	84 Po Polonium (208.98243)	85 At Astatine (209.98715)	86 Rn Radon (222.01758)
87 Fr Francium (223.01974)	88 Ra Radium (226.02541)	89–103 Actinides	104 Rf Rutherford. (267.122)	105 Db Dubnium (268.126)	106 Sg Seaborgium (271.134)	107 Bh Bohrium (270.133)	108 Hs Hassium (277.152)	109 Mt Meitnerium (278.156)	110 Ds Darmstadt. (281.165)	111 Rg Roentgen. (282.169)	112 Cn Copernicium (285.177)	113	114 Fl Flerovium (289.190)	115	116 Lv Livermorium (293.204)	117	118

Lanthanide series	57 La Lanthanum 138.90547	58 Ce Cerium 140.116	59 Pr Praseodym. 140.90766	60 Nd Neodymium 144.242	61 Pm Promethium (144.91276)	62 Sm Samarium 150.36	63 Eu Europium 151.964	64 Gd Gadolinum 157.25	65 Tb Terbium 158.92535	66 Dy Dysprosium 162.500	67 Ho Holmium 164.93033	68 Er Erbium 167.259	69 Tm Thulium 168.93422	70 Yb Ytterbium 173.054	71 Lu Lutetium 174.9668
Actinide series	89 Ac Actinium (227.02775)	90 Th Thorium 232.0377	91 Pa Protactinium 231.03588	92 U Uranium 238.02891	93 Np Neptunium (237.04817)	94 Pu Plutonium (244.06420)	95 Am Americium (243.06138)	96 Cm Curium (247.07035)	97 Bk Berkelium (247.07031)	98 Cf Californium (251.07959)	99 Es Einsteinium (252.0830)	100 Fm Fermium (257.09510)	101 Md Mendelevium (258.09843)	102 No Nobelium (259.1010)	103 Lr Lawrencium (262.110)

Taken from the Particle Data Group review of particle properties: http://pdg.lbl.gov

Crystal

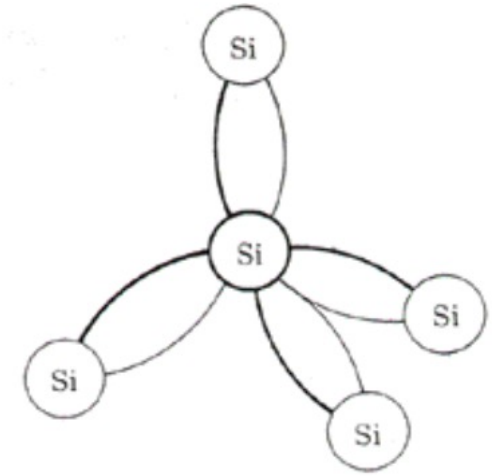

Figure 1. Covalent bonds of silicon

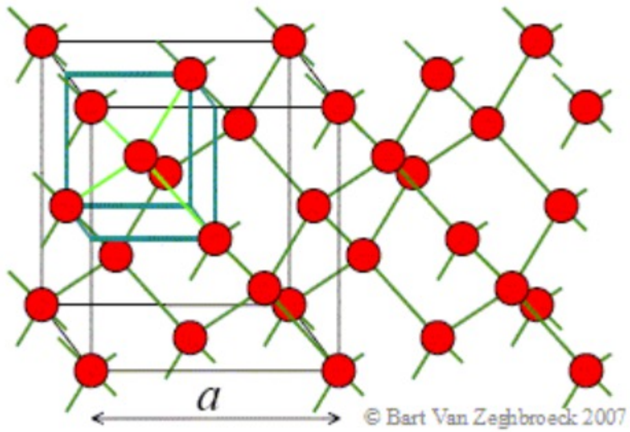

Figure 2.2.5.: The diamond lattice of silicon and germanium

Each Si atom forms four covalent bonds with four neighbouring silicon atoms. These four neighbours are located at the corners of a regular tetrahedron surrounding the atom.

Crystal

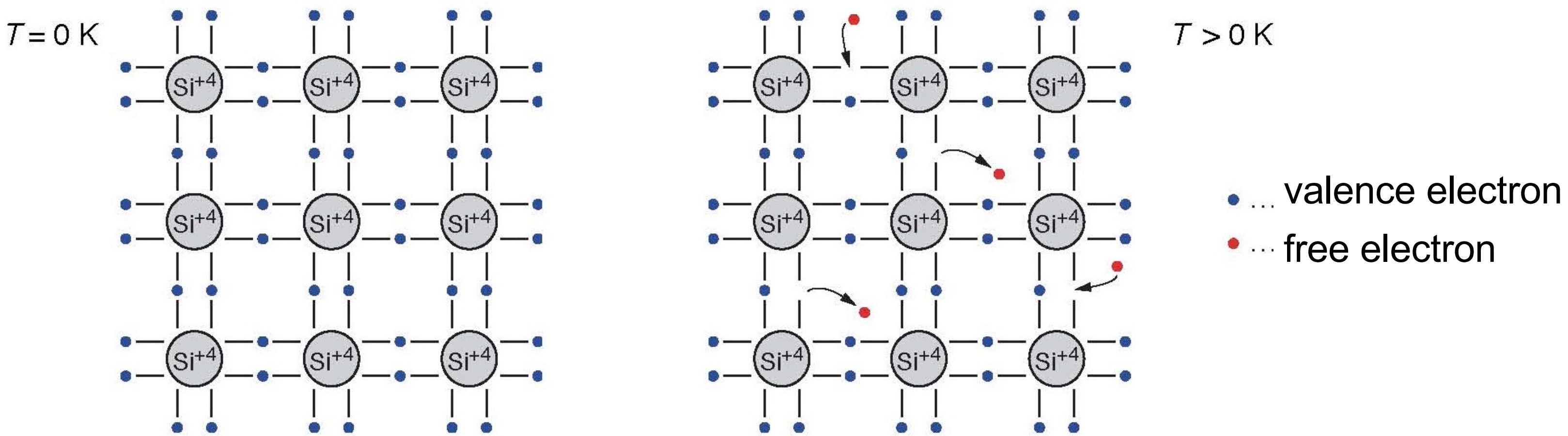

Each Si atom forms four covalent bonds with four neighbouring silicon atoms. These four neighbours are located at the corners of a regular tetrahedron surrounding the atom.

Energy Band Structure

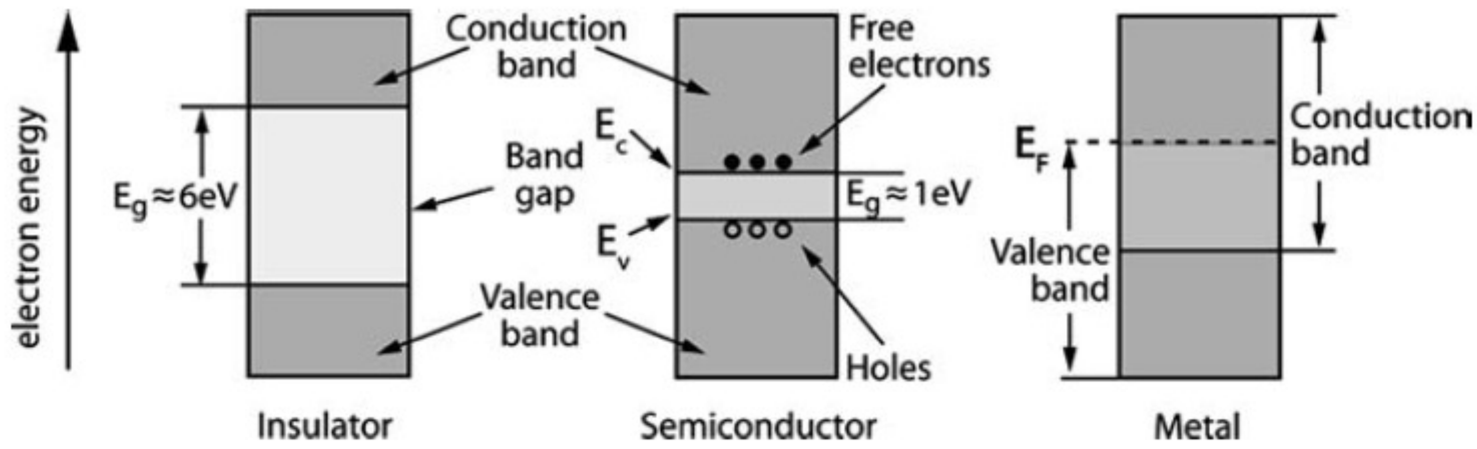

Fig. 5.2 Energy band structure of conductors, insulators and semiconductors. The vertical axis represents the electron energy, the horizontal axis the position in the lattice

	Si	**Ge**
Energy gap [eV]	~1.2	~0.75

SD detector characteristics

Average energy per electron-hole creation in Si & Ge

	Si	**Ge**
300 K	3.62 eV	-
77 K	3.81 eV	2.96 eV

In principle, using these numbers we can estimate the number of electron-hole pairs per incident gamma-ray (e.g. for 1 MeV energy deposition) which dictates also the statistical variation often dominates the resolution (but note the need for the **Fano Factor!**)

Exercise 2: Fano Factor

Fano factor is introduced as a factor to relate the observed variation (σ^2_{exp}) to that predicated by the Poisson distribution (σ^2_{calc} = n_o)

Assume a detector measures a 60 keV gamma ray with a 1 keV FHWM resolution
and a 662 keV gamma ray with a 2.3 keV resolution.

→ Estimate the Fano Factor.

Charge carriers

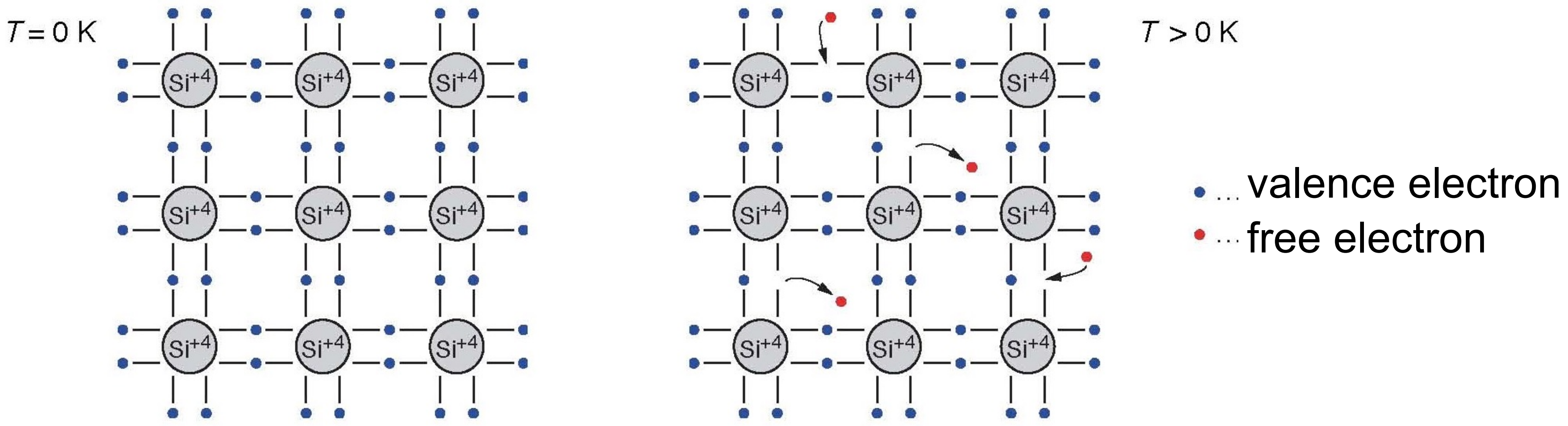

- At T=0 K, all electrons in the valence band participate in covalent bonding between the lattice atoms.
- Si & Ge have four valence electrons, four covalent bonds are formed.
- At T > 0 K (normal temperatures) electrons thermally excite to the conduction band.
- The hole can be filled by neighboring valence electrons and so on.
- The electric current in a semiconductor arises from:
  - Movement of free electrons in conduction band
  - Movement of holes in valence band

Probability (Fermi-Dirac) that an energy level is occupied:

$$f(E) = \frac{1}{e^{\frac{E-E_F}{kT}} + 1}$$

Drift and Mobility

The mobility of electrons and holes is defined as :

$v_e = \mu_e E$ E – magnitude of Electrical Field applied
$v_h = \mu_h E$ v – drift velocity

e.g. in Si@300K μ_e=1350 $cm^2\ V^{-1}\ s^{-1}$
μ_h= 480 $cm^2\ V^{-1}\ s^{-1}$

@77K μ_e= 21400 $cm^2\ V^{-1}\ s^{-1}$
μ_h= 11000 $cm^2\ V^{-1}\ s^{-1}$

Compare with electron-ion mobilities in gas detectors

Drift and Mobility

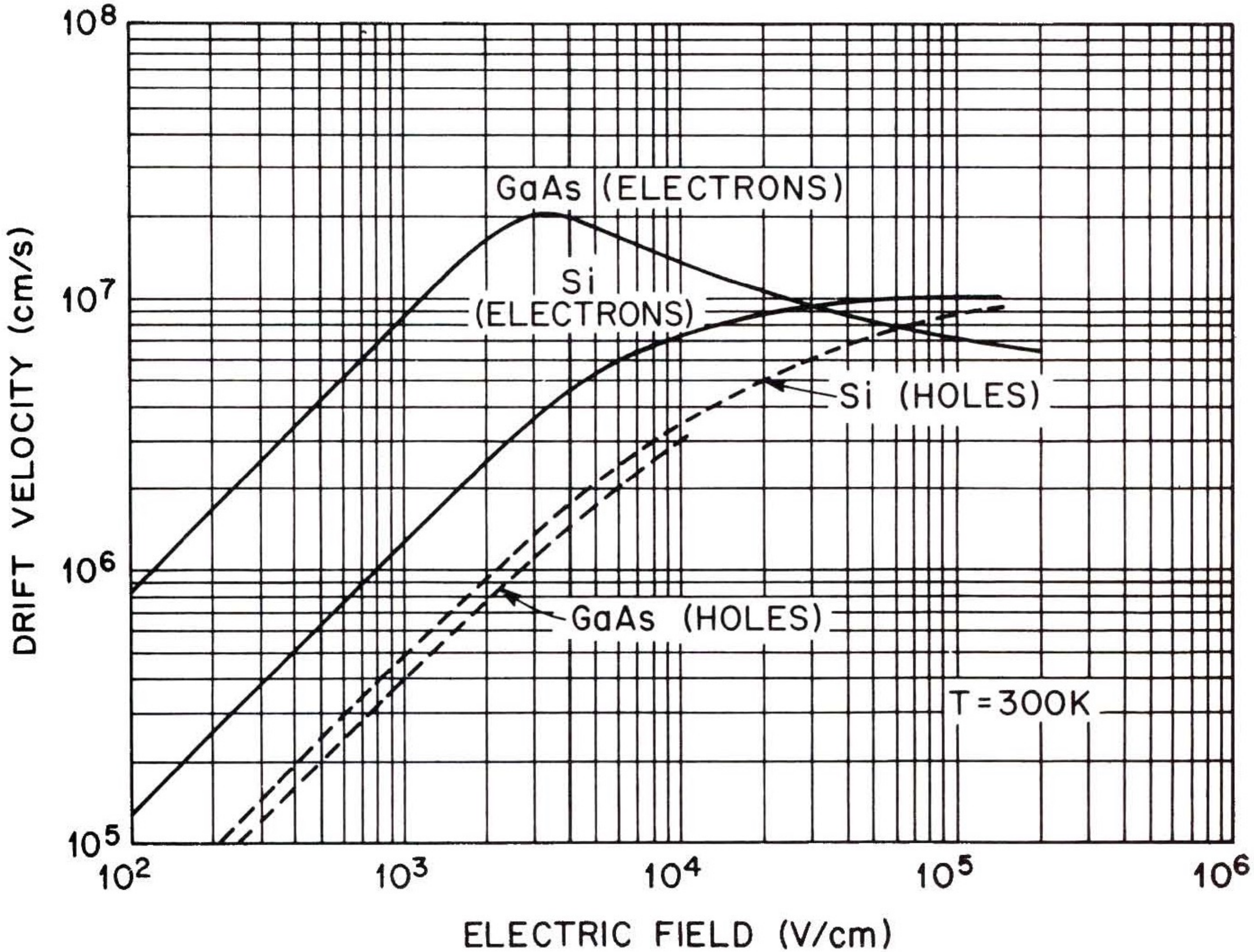

Drift and Mobility

Table 11.1 Properties of Intrinsic Silicon and Germanium

	Si	Ge
Atomic number	14	32
Atomic weight	28.09	72.60
Stable isotope mass numbers	28-29-30	70-72-73-74-76
Density (300 K); g/cm^3	2.33	5.32
Atoms/cm^3	4.96×10^{22}	4.41×10^{22}
Dielectric constant (relative to vacuum)	12	16
Forbidden energy gap (300 K); eV	1.115	0.665
Forbidden energy gap (0 K); eV	1.165	0.746
Intrinsic carrier density (300 K); cm^{-3}	1.5×10^{10}	2.4×10^{13}
Intrinsic resistivity (300 K); $\Omega \cdot cm$	2.3×10^5	47
Electron mobility (300 K); $cm^2/V \cdot s$	1350	3900
Hole mobility (300 K); $cm^2/V \cdot s$	480	1900
Electron mobility (77 K); $cm^2/V \cdot s$	2.1×10^4	3.6×10^4
Hole mobility (77 K); $cm^2/V \cdot s$	1.1×10^4	4.2×10^4
Energy per electron–hole pair (300 K); eV	3.62	
Energy per electron–hole pair (77 K); eV	3.76	2.96
Fano factor (77 K)	0.143 (Ref. 7)	0.129 (Ref. 9)
	0.084 (Ref. 8)	0.08 (Ref. 10)
	0.085 to 0.137 (Ref. 12)	< 0.11 (Ref. 11)
		0.057 0.064 (Ref. 12)
	0.16 (Ref. 13)	0.058 (Ref. 14)

Source: G. Bertolini and A. Coche (eds.), *Semiconductor Detectors*, Elsevier-North Holland, Amsterdam, 1968, except where noted.

•**Saturation velocity** (velocity becomes independent of further increase in the electrical field)

In SD the time required to collect charge carriers over typical dimension of 0.1 cm or less is <10 ns, i.e. thin semiconductor detectors can be used for fast timing purposes

Doped Semiconductors

n-type Semiconductors

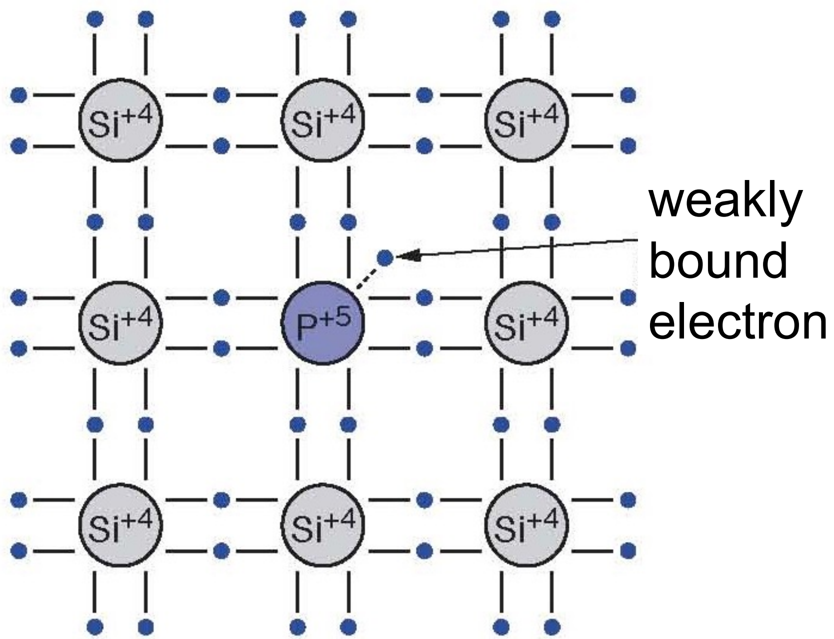

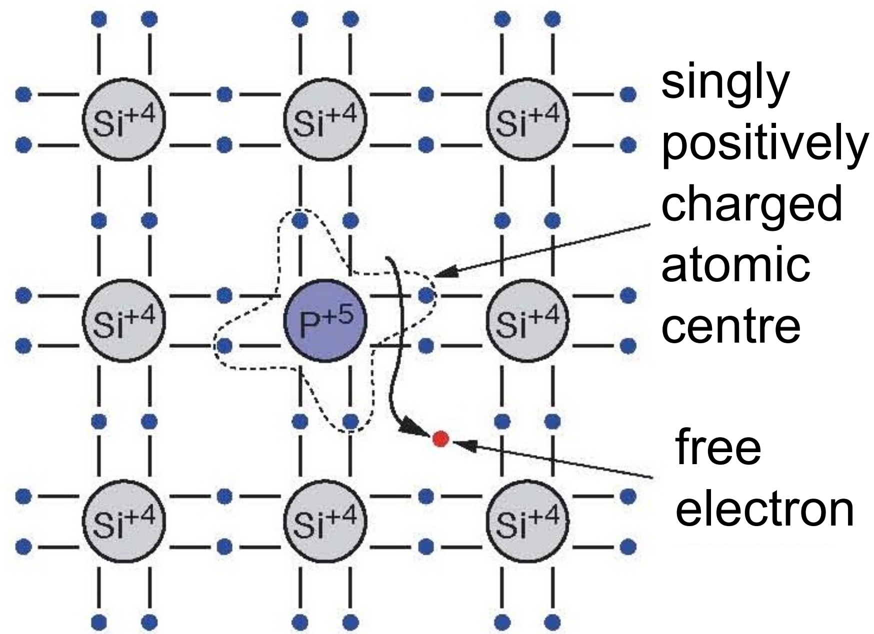

n-type Semiconductors: Energy Band Structure

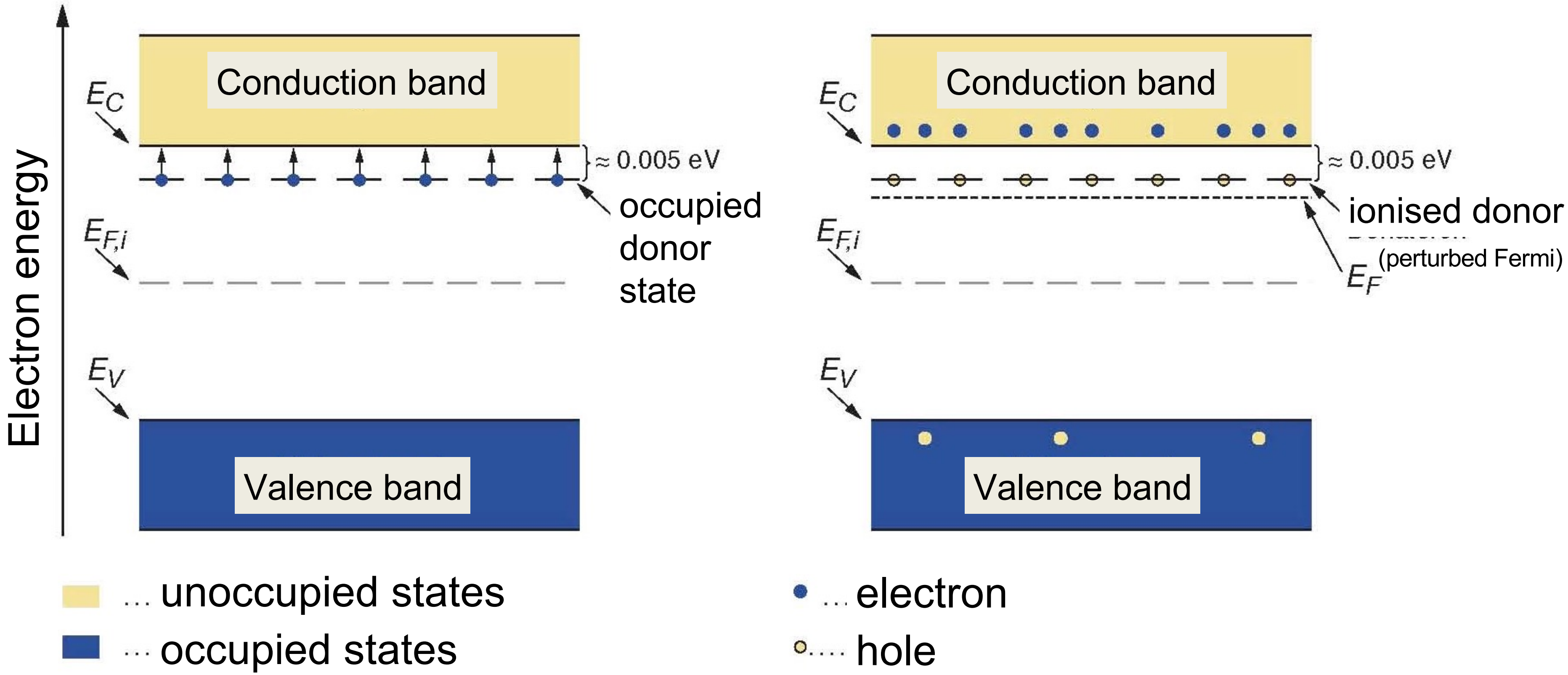

p-type Semiconductors

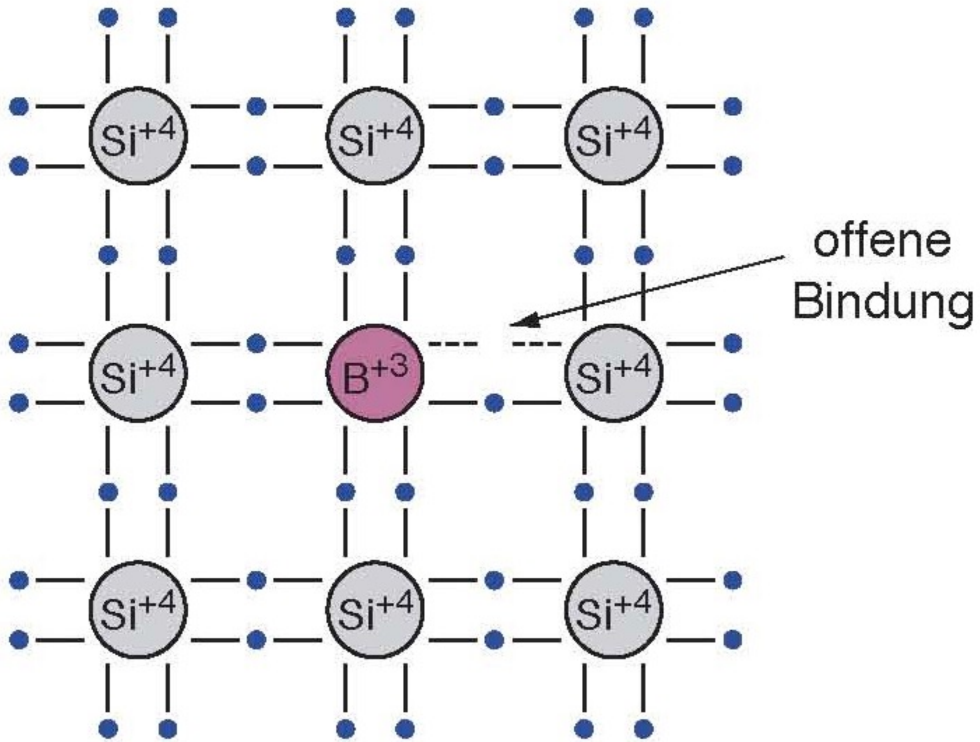

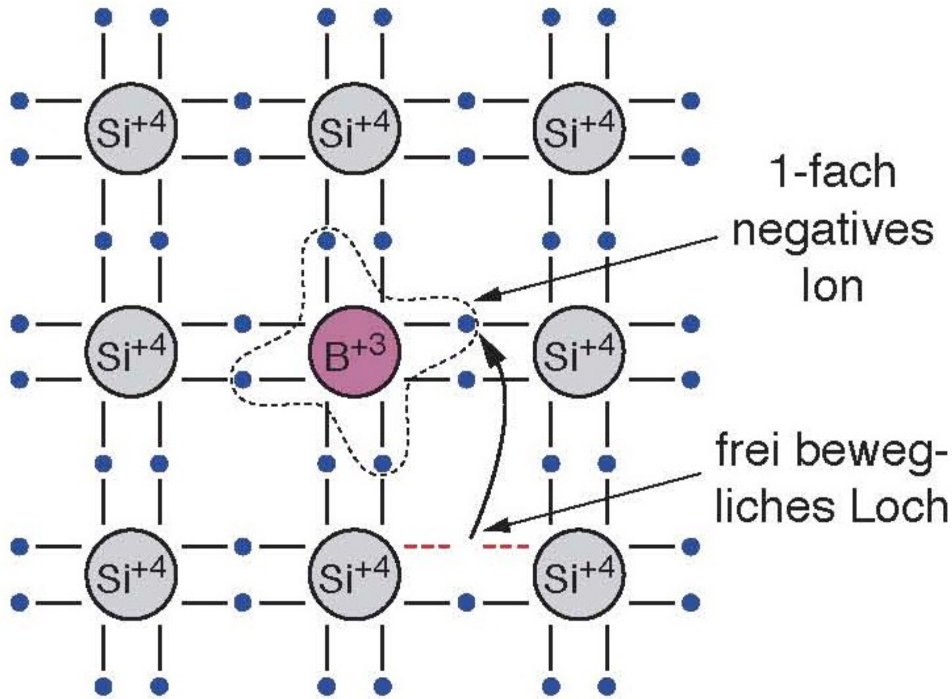

p-type Semiconductors: Energy Band Structure

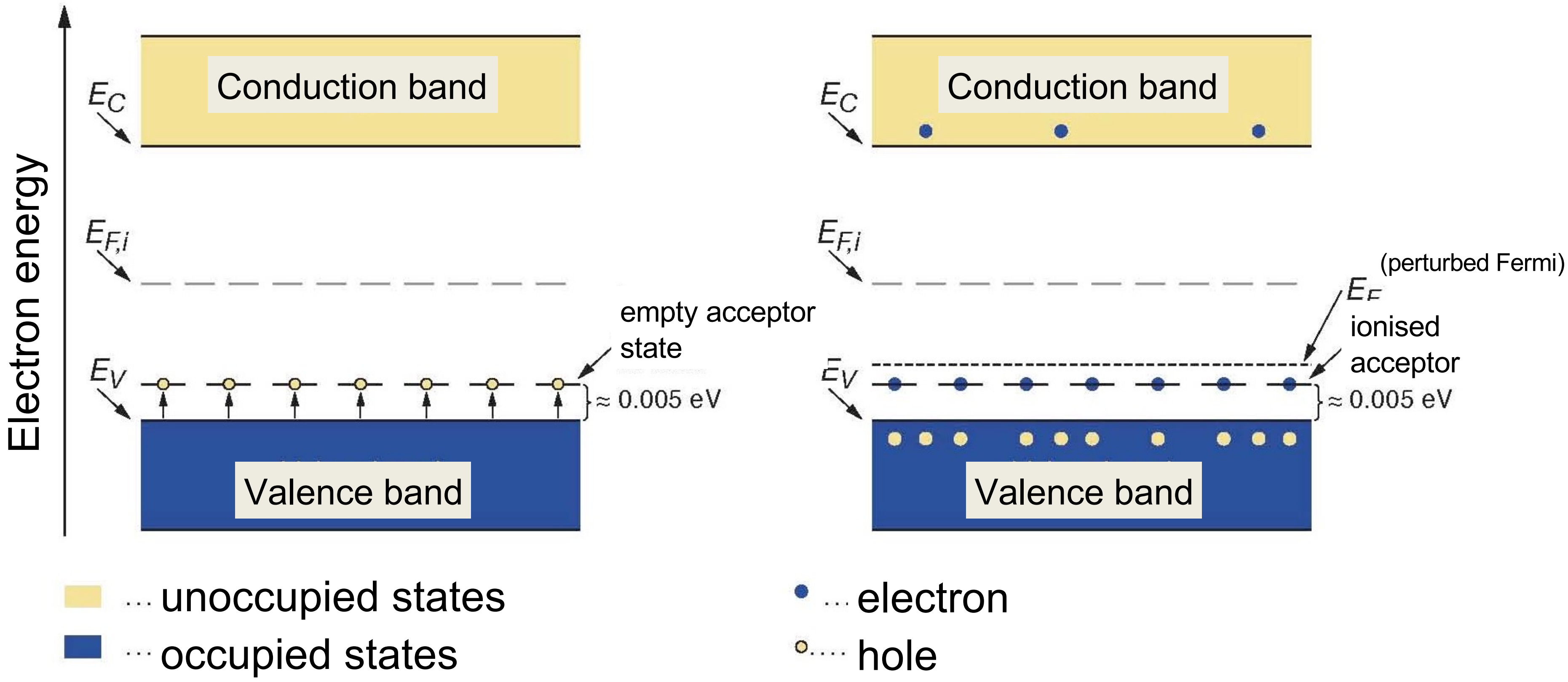

Semiconductor junctions

- The functioning of a SD is based on the formation of a SD “junction”
- Junctions can be formed in several ways
- pn junction (simple configuration)

pn junction

- pn junction is formed by between a p-type material with an n-type material (in practice from a single crystal)
- Because of the difference in the concentration of electrons and holes, there is an initial diffusion of holes towards the n-region and electrons towards the p-region
- Holes capture electrons on the n-side
- Electrons fill up holes on the p-side
- Charge build up on either side of the junction
    - p-region becomes negative
    - n-region becomes positive
- electric field across the junction which eventually halts the diffusion process → region of immobile space charge

See schematic plot of pn junction in the next slide

pn junction (no bias)

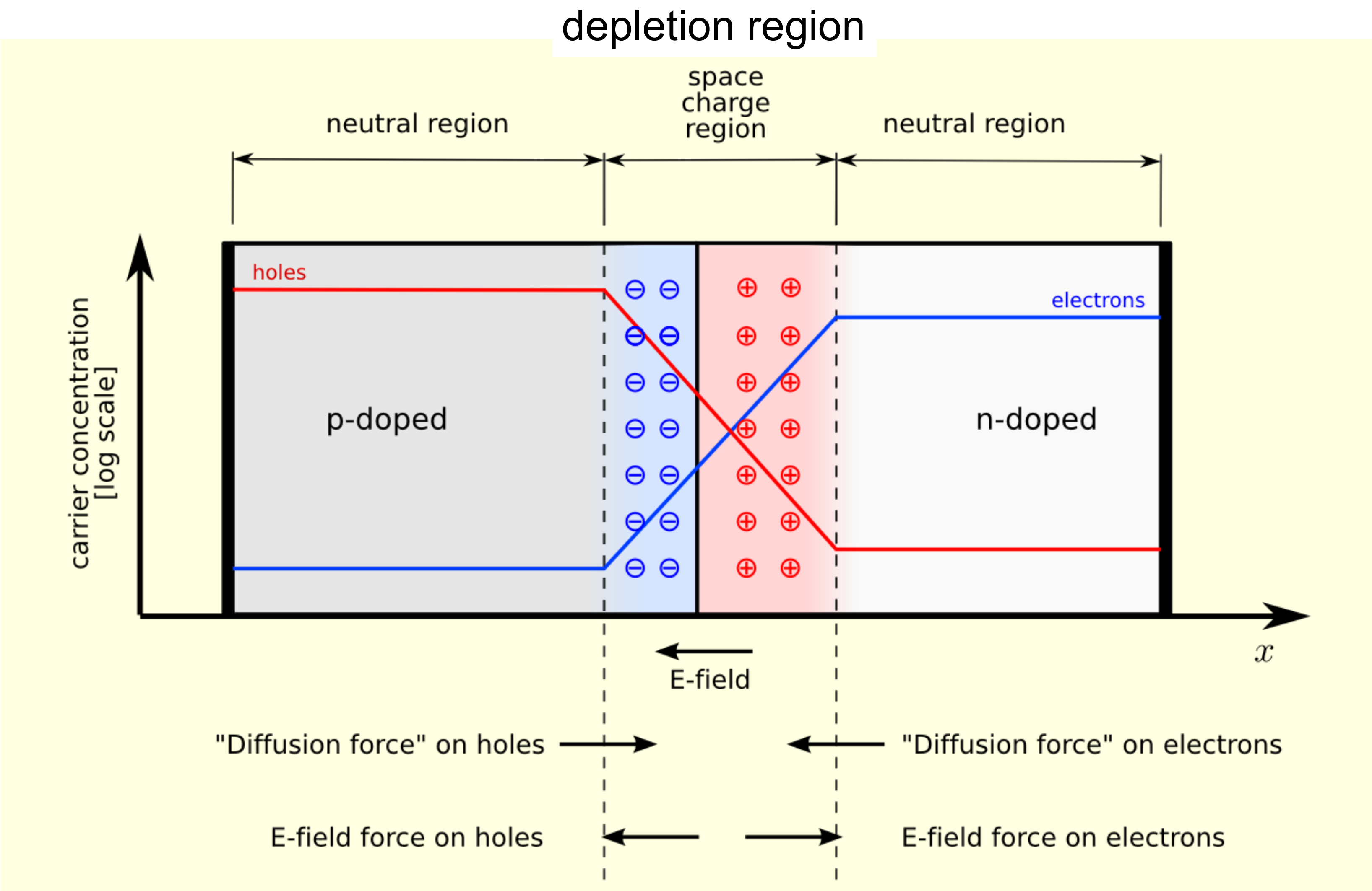

Depletion region of pn junctions and its electrical properties (no bias)

region over which the charge imbalance exist & extends into both the p & n side of the junction

low concentration of electrons and holes

in the **depletion region** the net charge is provided by the fixed ions (donors or acceptors) that have been left *uncovered* by majority carrier diffusion.

The electric field across the depletion region causes any electrons created in the region to be swept back towards the n-type material and any holes towards the p-type. Their motion constitutes a basic electric signal.

depletion region

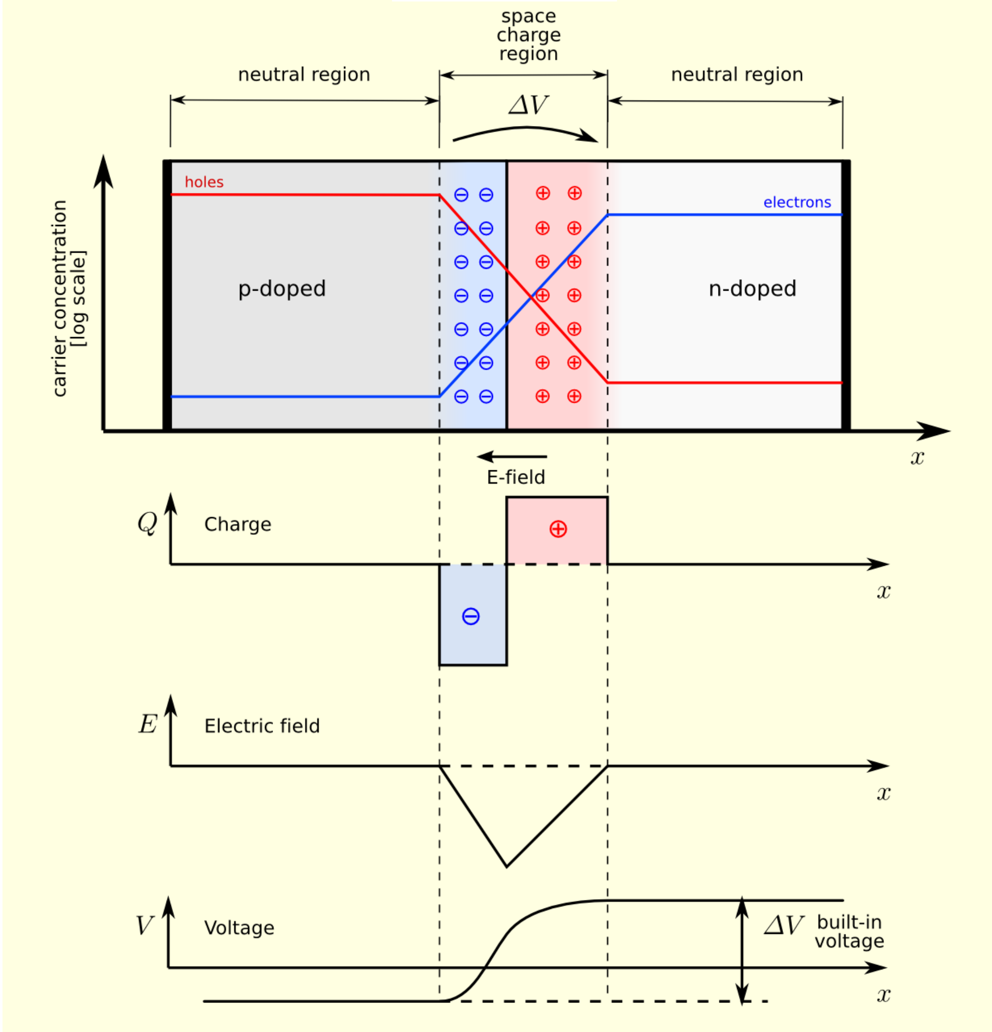

Depletion region of pn junctions and its electrical properties (no bias)

- When equilibrium is reached, the charge density is approximated by the displayed step function.
- Potential difference across the junction is called “contact potential” or “build in potential” and has values ~ 1V

This is already a detector but…

- very small active area (depletion region)
- Inefficient collection of electron and holes

not a good one!

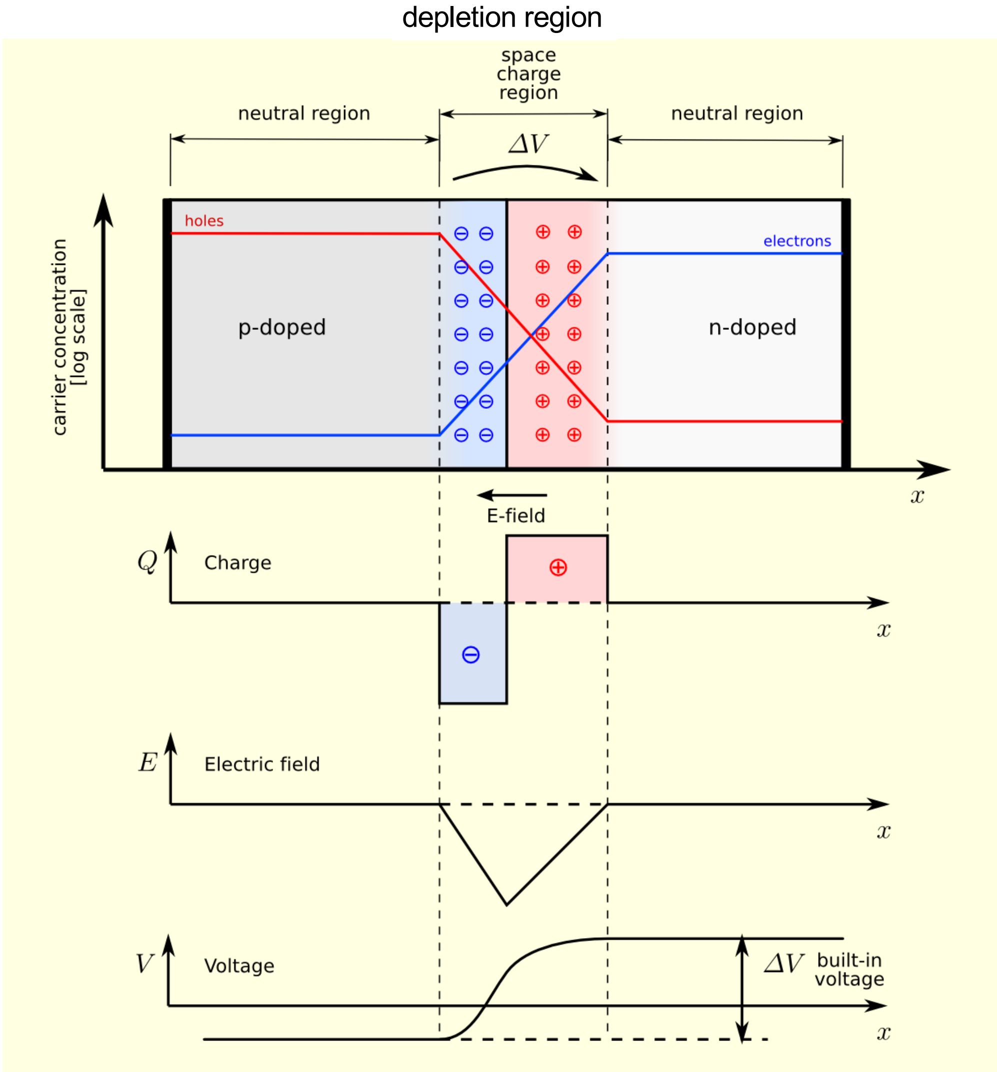

Depletion region of pn junctions and its electrical properties (reverse bias)

Solution: Apply reversed-bias voltage (negative voltage to the p-region and positive to the n-region)

- holes will move towards the p-contact and away from the junction
- Electrons will move towards the n-contact and away from the junction

increased depletion region +
faster and efficient charge collection

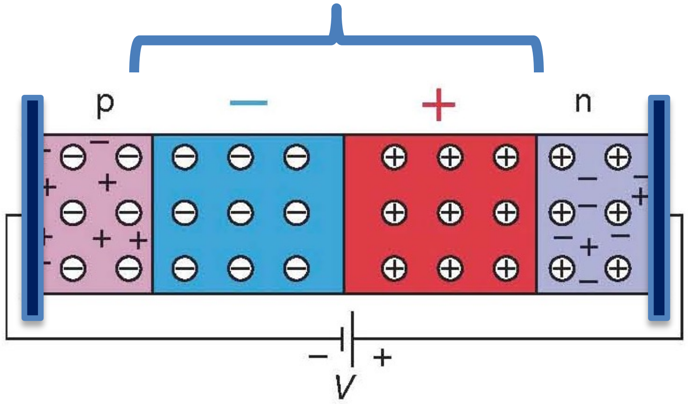

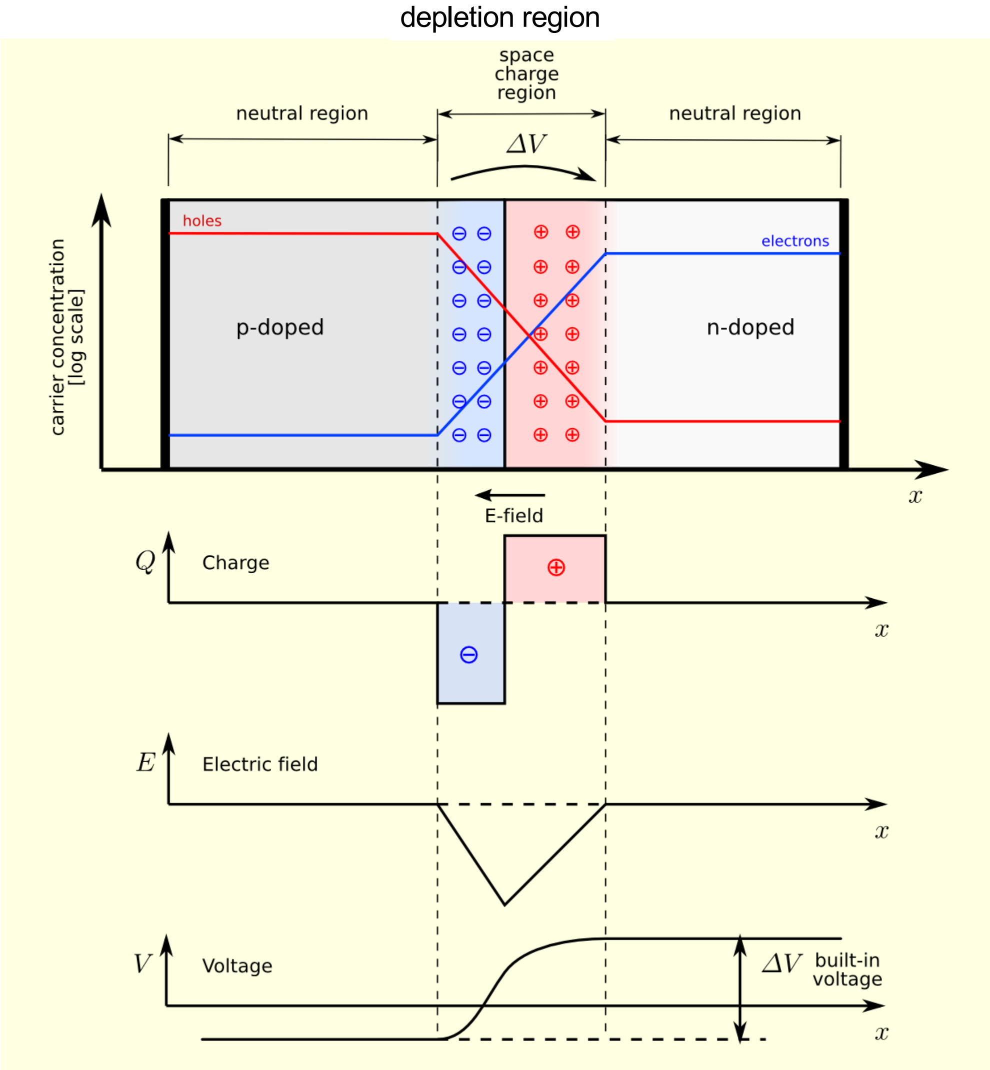

Planar HPGe detectors

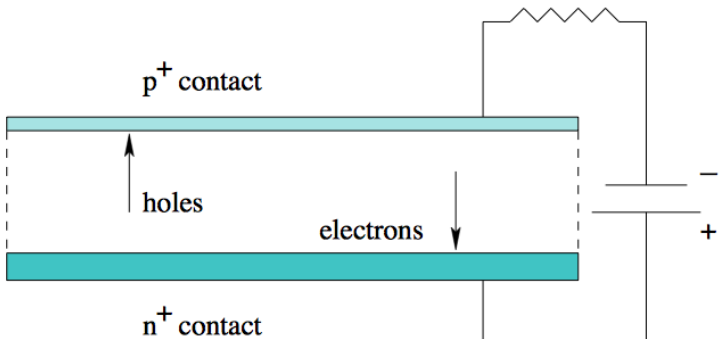

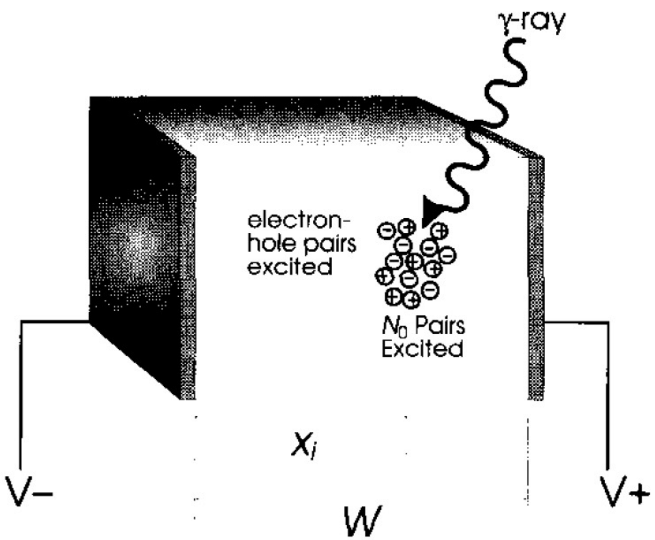

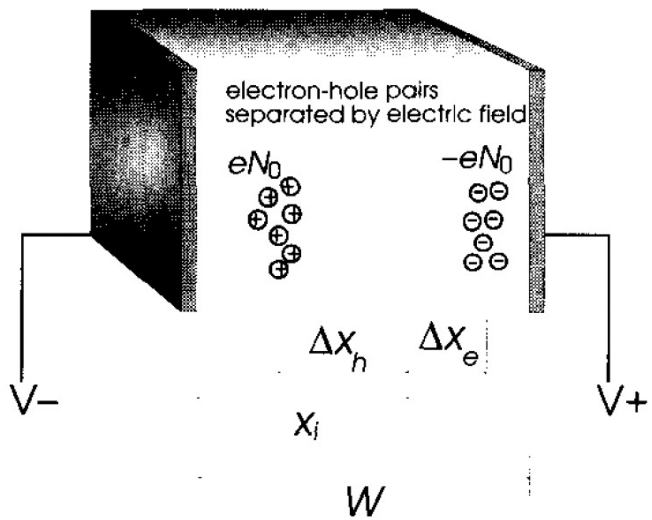

Coaxial HPGe Detectors

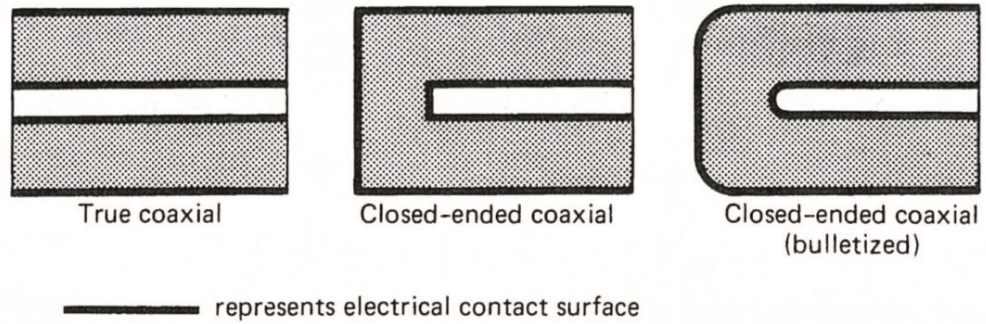

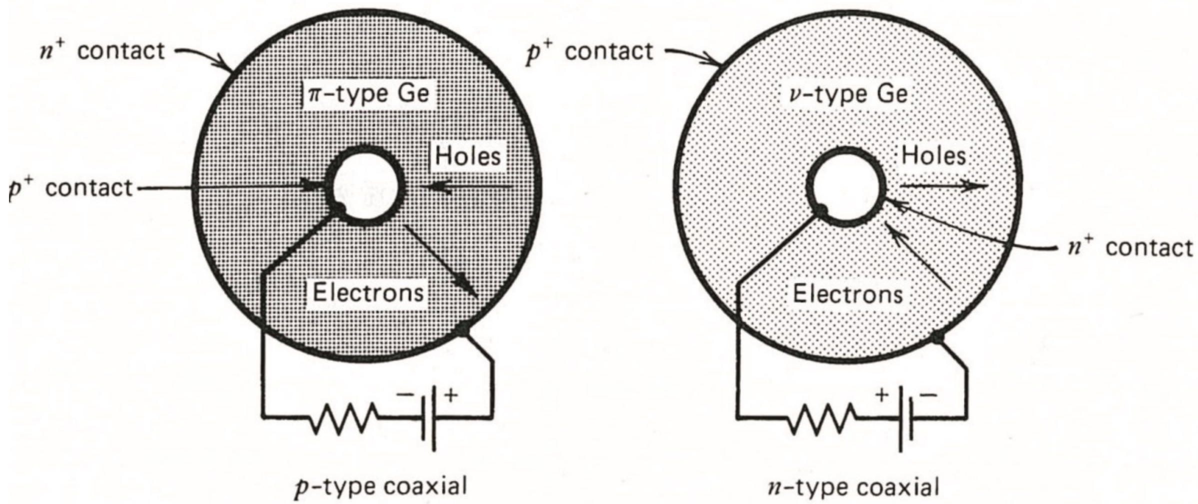

Depletion volume in a Coaxial Ge crystal (AGATA type)

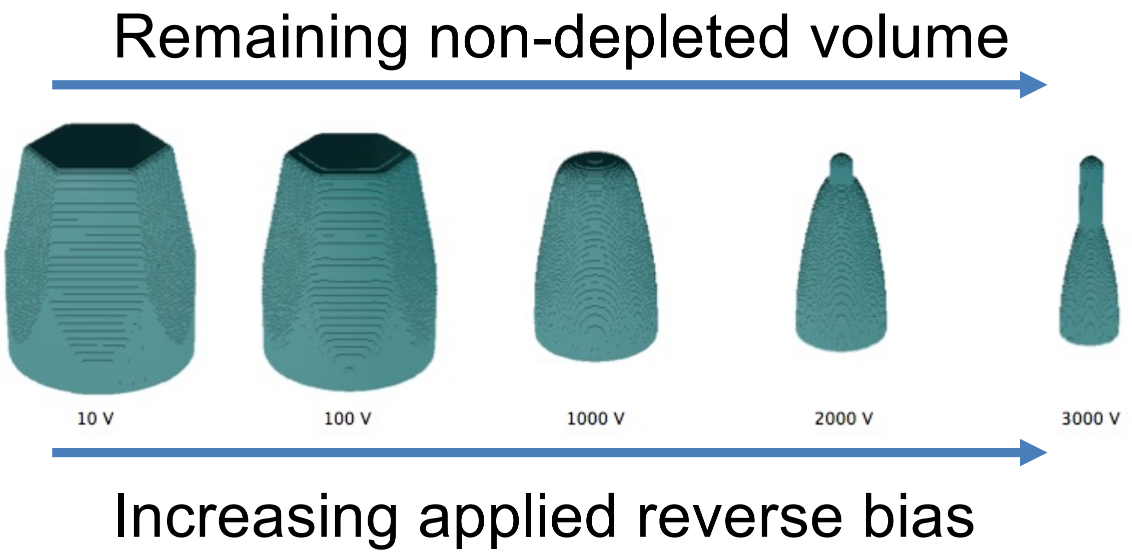

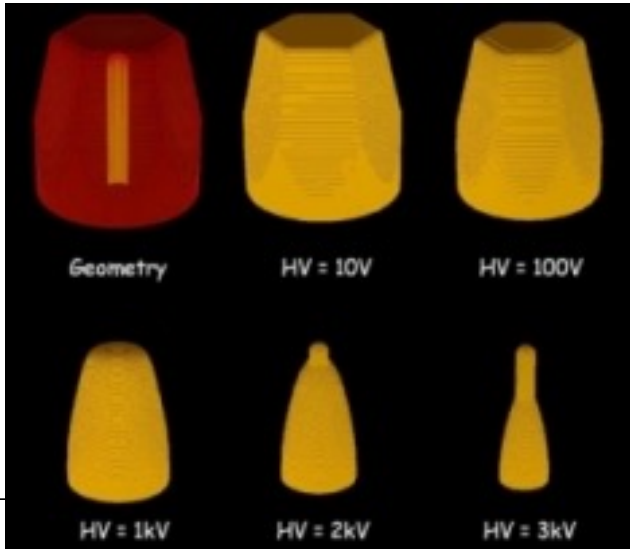

The basic ingredients ~~for detection~~ of this Lecture

- Interactions of ionizing radiation with matter
- Detection technology
- Electronic readout and signal processing
- Data analysis

position sensitive

The Shockley-Ramo theorem

The Shockley–Ramo theorem states:

The charge Q and current i on an electrode induced by a moving point charge q are given by:

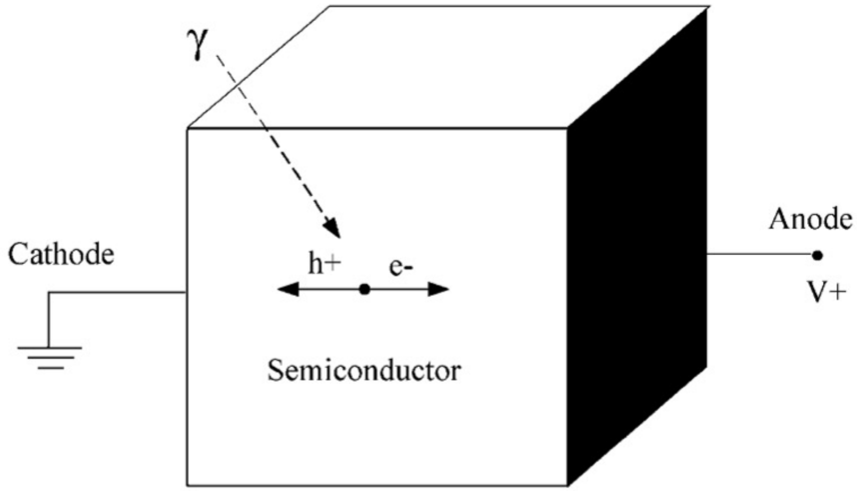

$$Q = -q\varphi_0(\boldsymbol{x})$$

$$i = q\boldsymbol{v} \cdot \boldsymbol{E}_0(\boldsymbol{x})$$

φ_0 and $\boldsymbol{E}_0$ are called the weighting potential and the weighting field, respectively.

where $\boldsymbol{v}$ is the instantaneous velocity of charge q. $\varphi_0(\boldsymbol{x})$ and $\boldsymbol{E}_0(\boldsymbol{x})$ are the electric potential and field that would exist at q's instantaneous position $\boldsymbol{x}$ under the following circumstances: the selected electrode at unit potential, all other electrodes at zero potential and all charges removed.

Remember
Drift and Mobility
slide

Shockley-Ramo theorem

Prescription :

1. **Apply V (Volts) to the electrode in consideration and ground (0V) to all the other electrodes.**
2. **The induced charge due to travel of a charge q over distance is**

$$Q(t) = \frac{q_0}{d}\left(\begin{array}{c}\text{electron drift}\\ \text{distance}\end{array} + \begin{array}{c}\text{hole drift}\\ \text{distance}\end{array}\right)$$

3. **Repeat this exercise with all the electrodes.**

Note:
Both electron and hole movement contributes to the signal!!
The charge induced/generated does not depend on the high voltage applied on the detector !

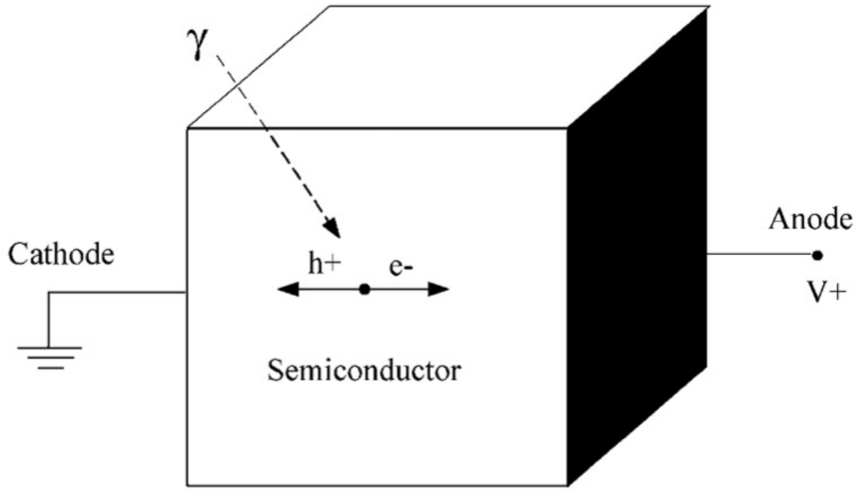

d : detector thickness

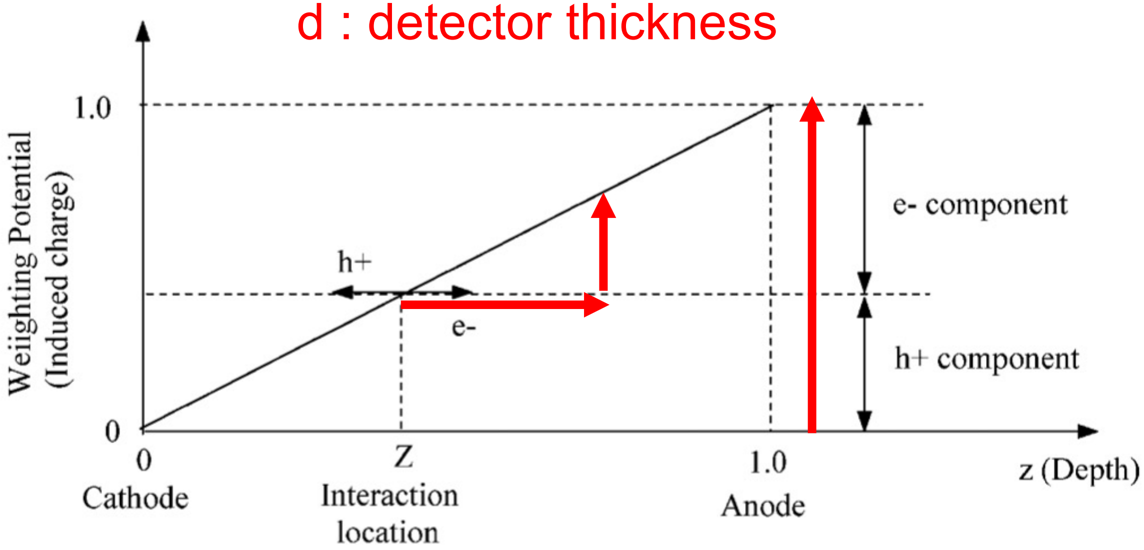

Planar detector: position sensitivity from pulse shape

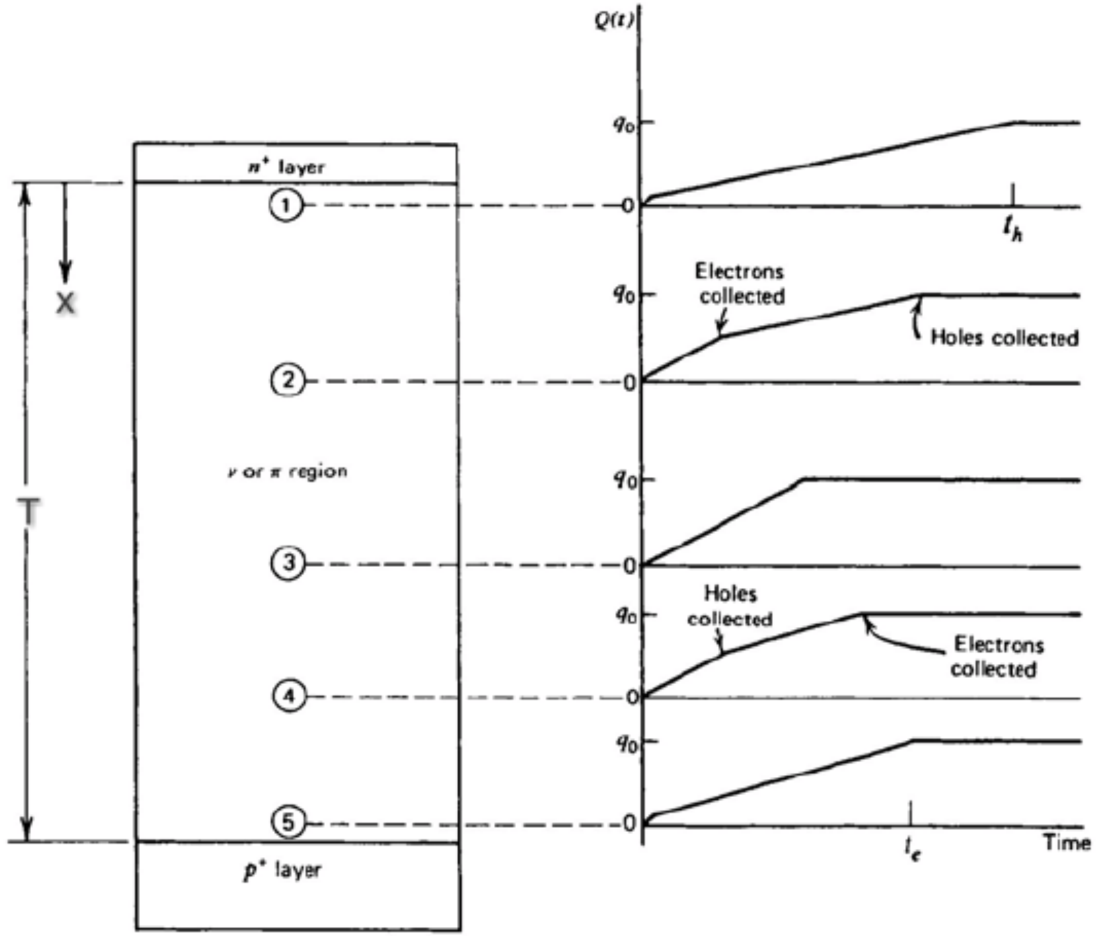

Time evolution of signal

pn$^+$-junction

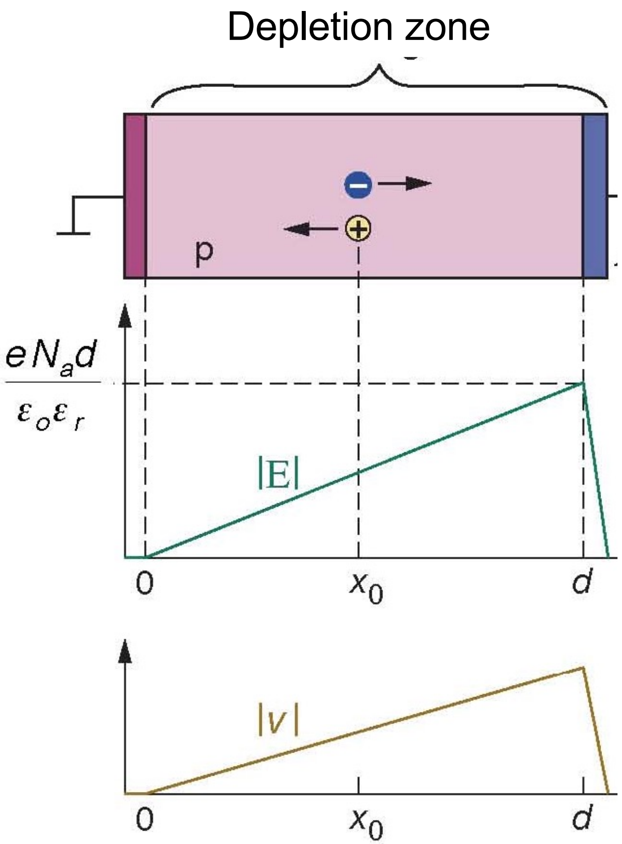

d : detector thickness

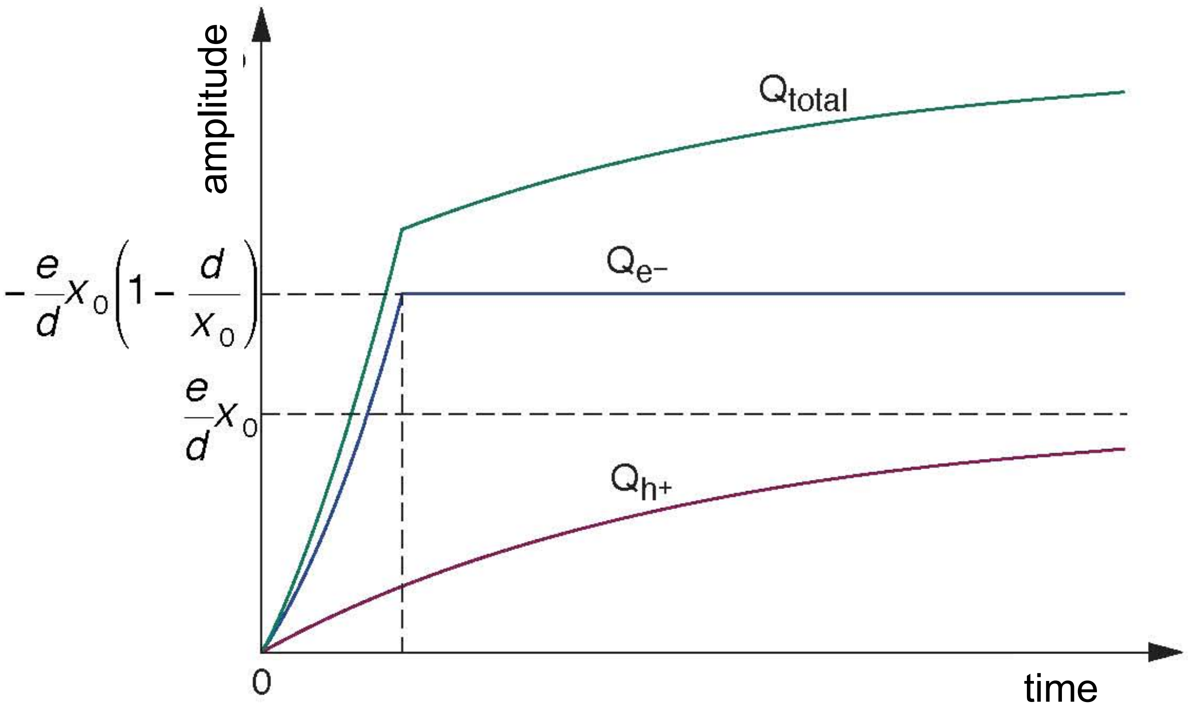

Coaxial detector: position sensitivity from pulse shape

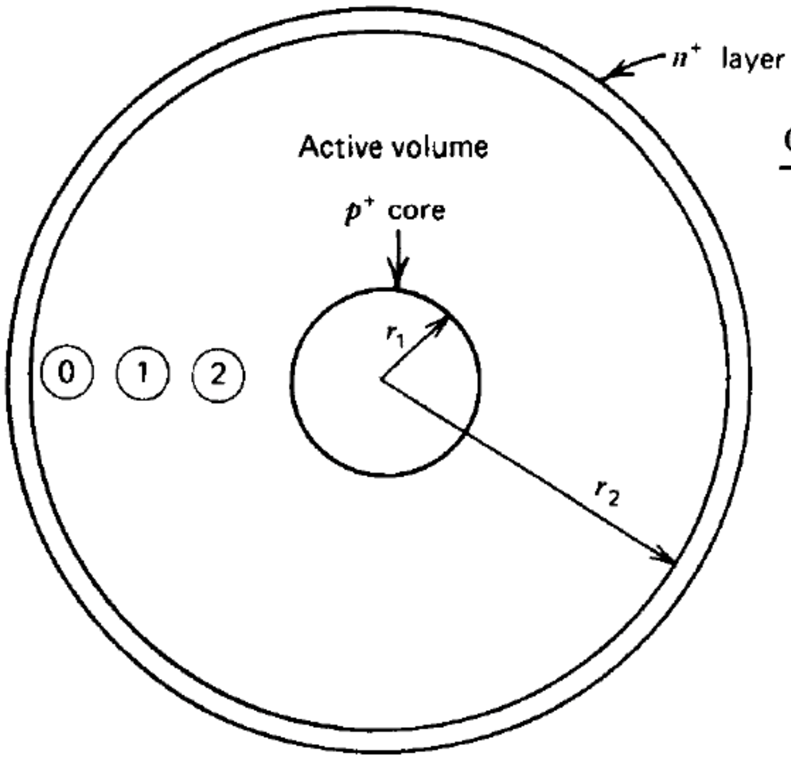

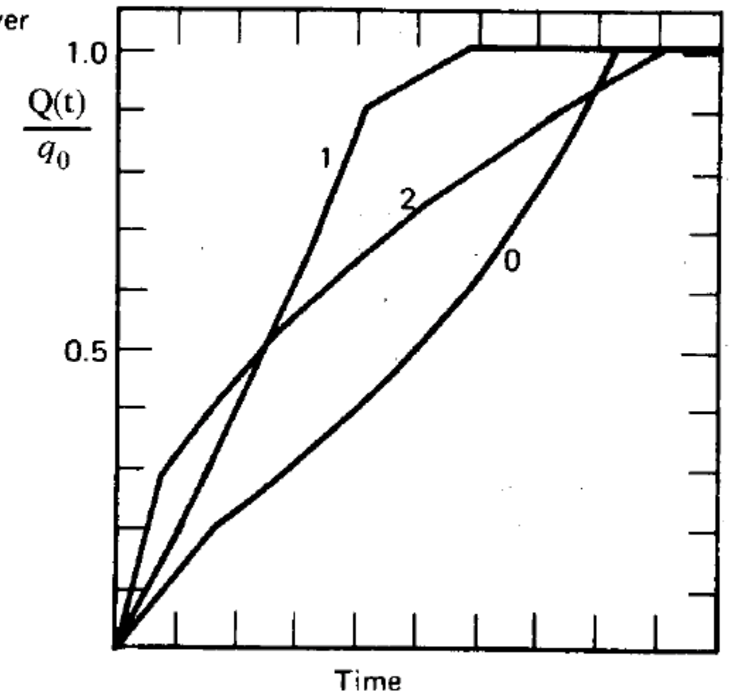

$$Q(t) = Q^-(t) + Q^+(t)$$

Knoll ch. 12

$$Q^+(t) = \frac{q_0\alpha}{V_0}\left[r_0^2 - r_h^2(t)\right] + \frac{q_0\beta}{V_0}\ln\frac{r_0}{r_h(t)}$$

$$Q^-(t) = \frac{\Delta E^-}{V_0} = \frac{q_0\alpha}{V_0}\left[r_e^2(t) - r_0^2\right] + \frac{q_0\beta}{V_0}\ln\frac{r_e(t)}{r_0}$$

$$\alpha \equiv \frac{eN_A}{4\epsilon} \quad \text{and} \quad \beta \equiv \frac{V_0 - \alpha(r_2^2 - r_1^2)}{\ln(r_2/r_1)}$$

NA (the acceptor concentration)

Coaxial detector with electrical segmentation: HPGe position sensitivity

36 segmented HPGe detector

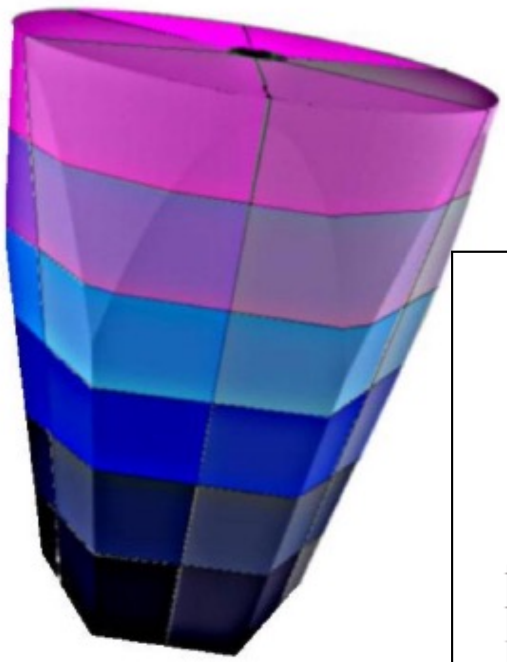

segment 4 where the γ-ray interaction occurred

neighbouring segment

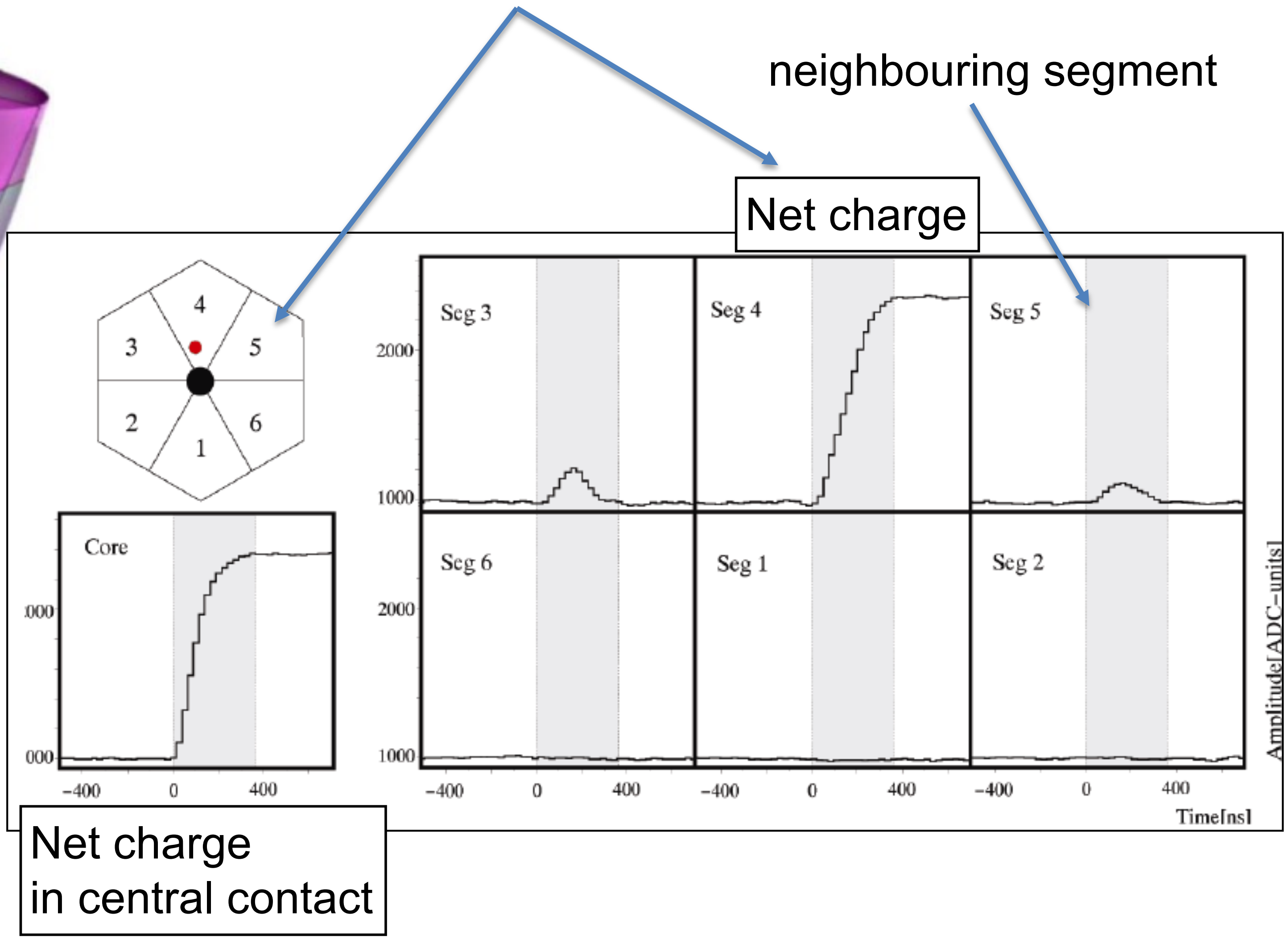

Digital signal processing:
to fully exploit the signal variety

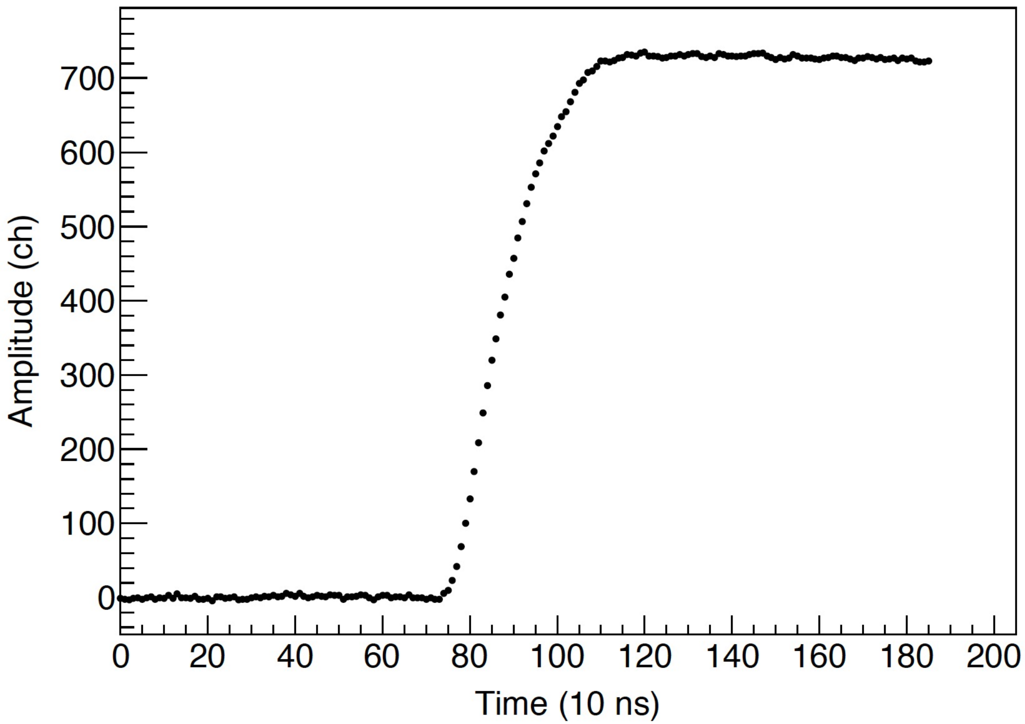

A digitised signal pulse
100 MHz → signal is sampled every 10 ns

CAEN desktop digitiser
DT5730 - 8 Ch. 14 bit 500 MS/s

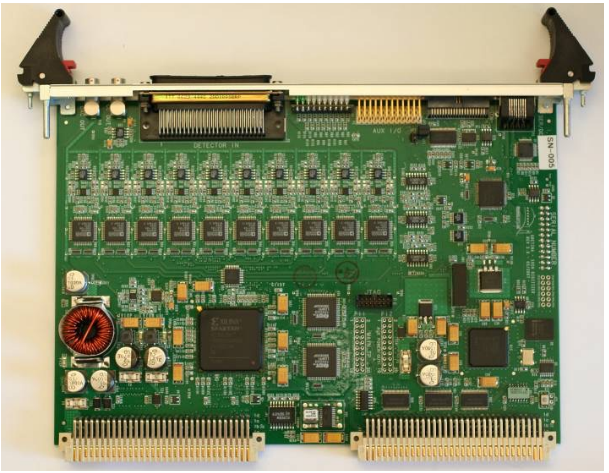

GRETINA Digitiser module
(designed & produced LBNL)
14bit, 100 MHz, Pulse shape

Pulse Shape Analysis for position reconstruction of γ-ray interaction

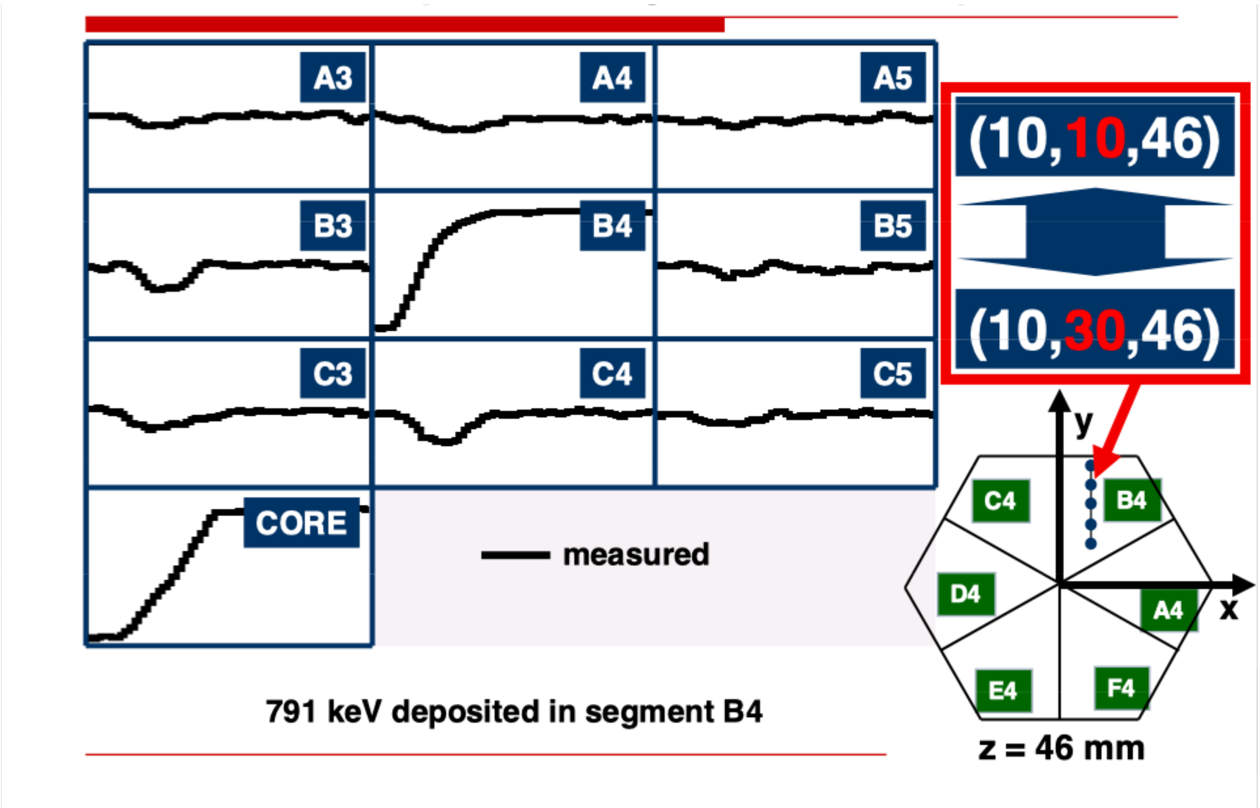

From F. Recchia, PSD8 conference

Pulse shape analysis concept

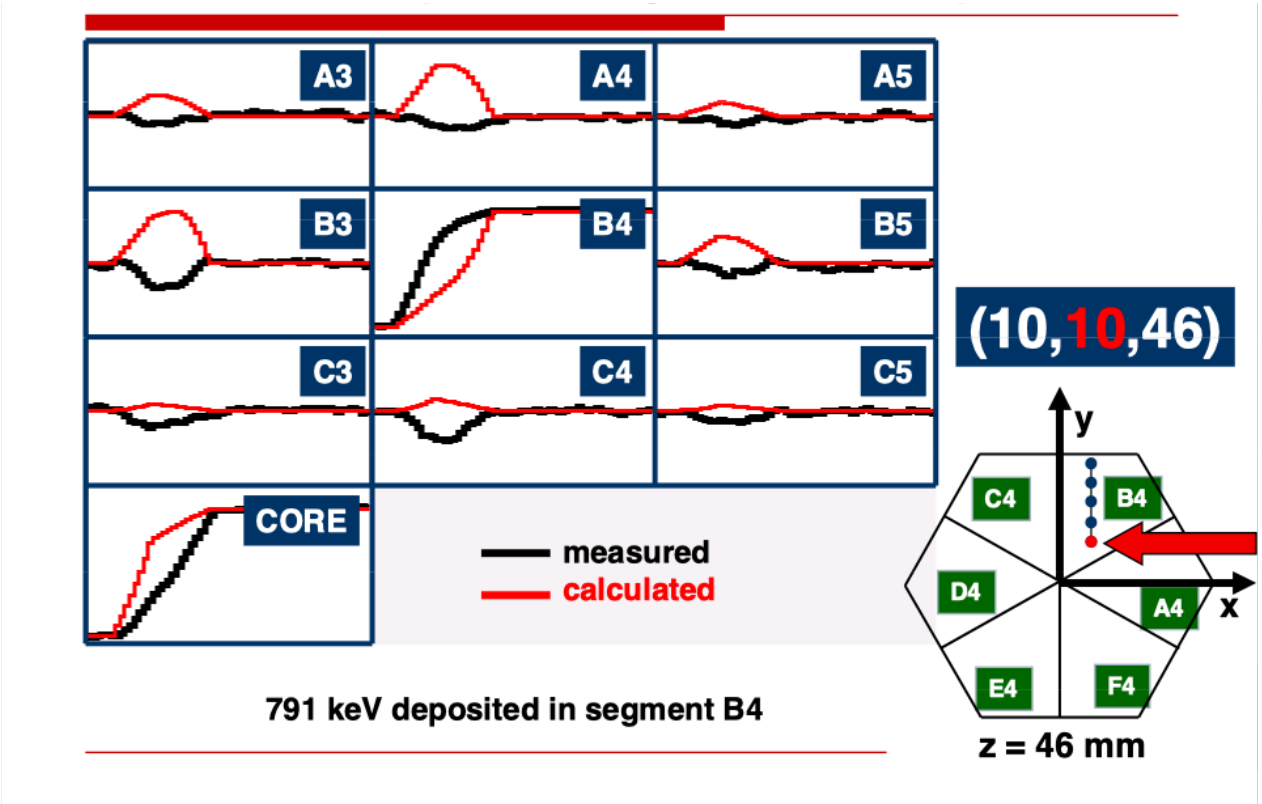

From F. Recchia, PSD8 conference

Pulse shape analysis concept

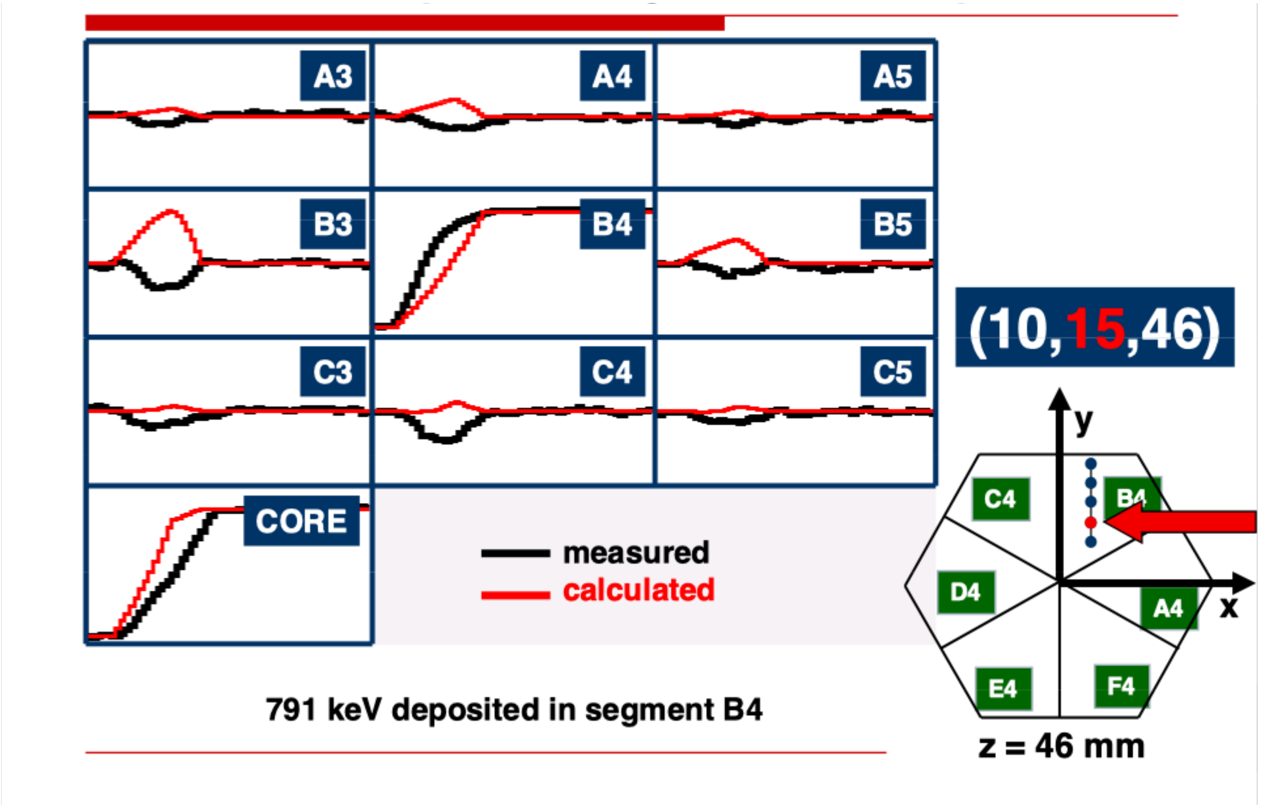

From F. Recchia, PSD8 conference

Pulse shape analysis concept

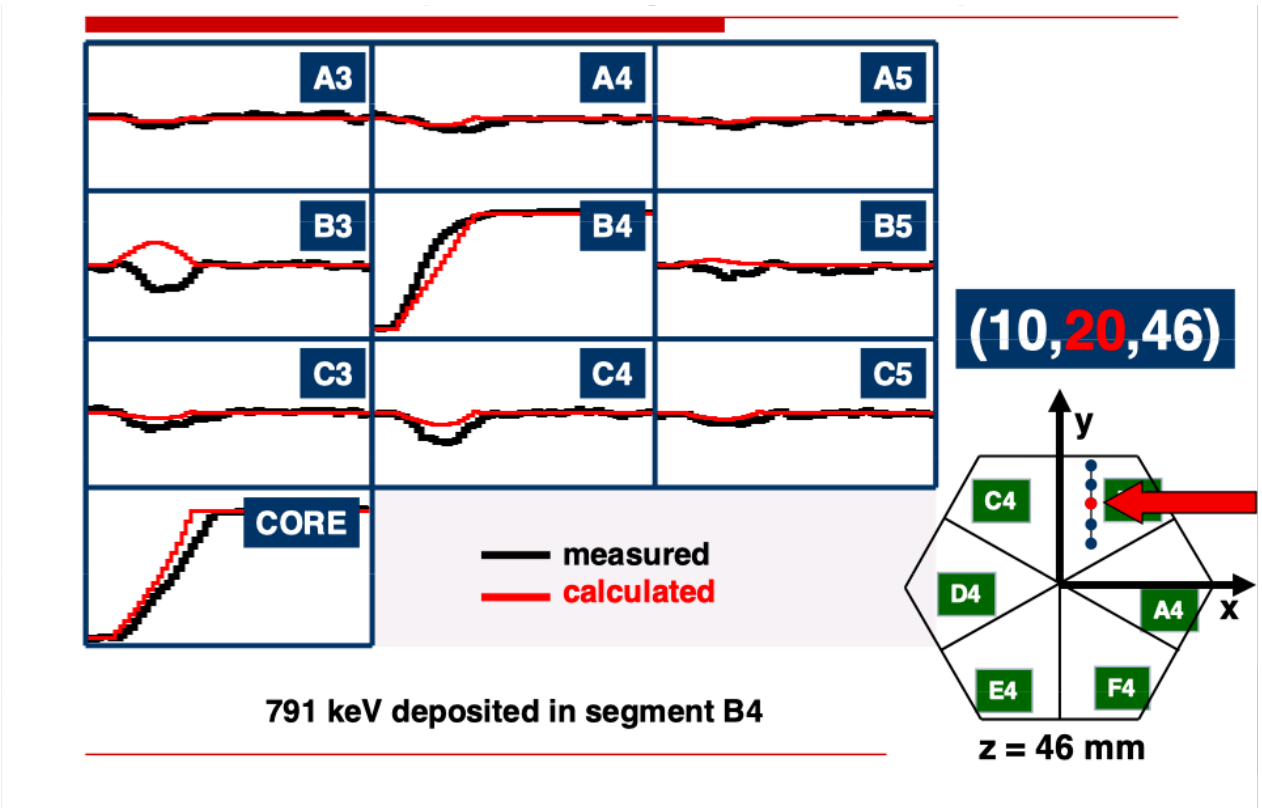

From F. Recchia, PSD8 conference

Pulse shape analysis concept

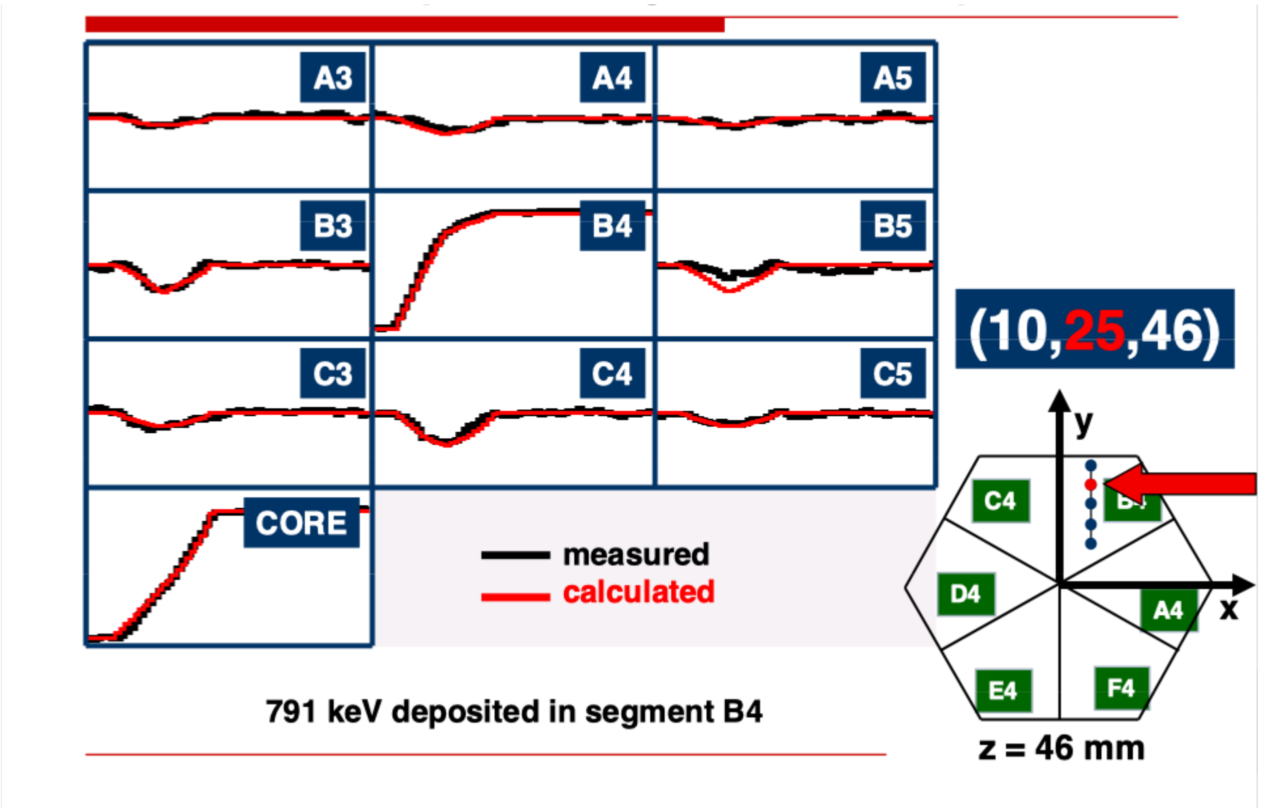

From F. Recchia, PSD8 conference

Pulse shape analysis concept

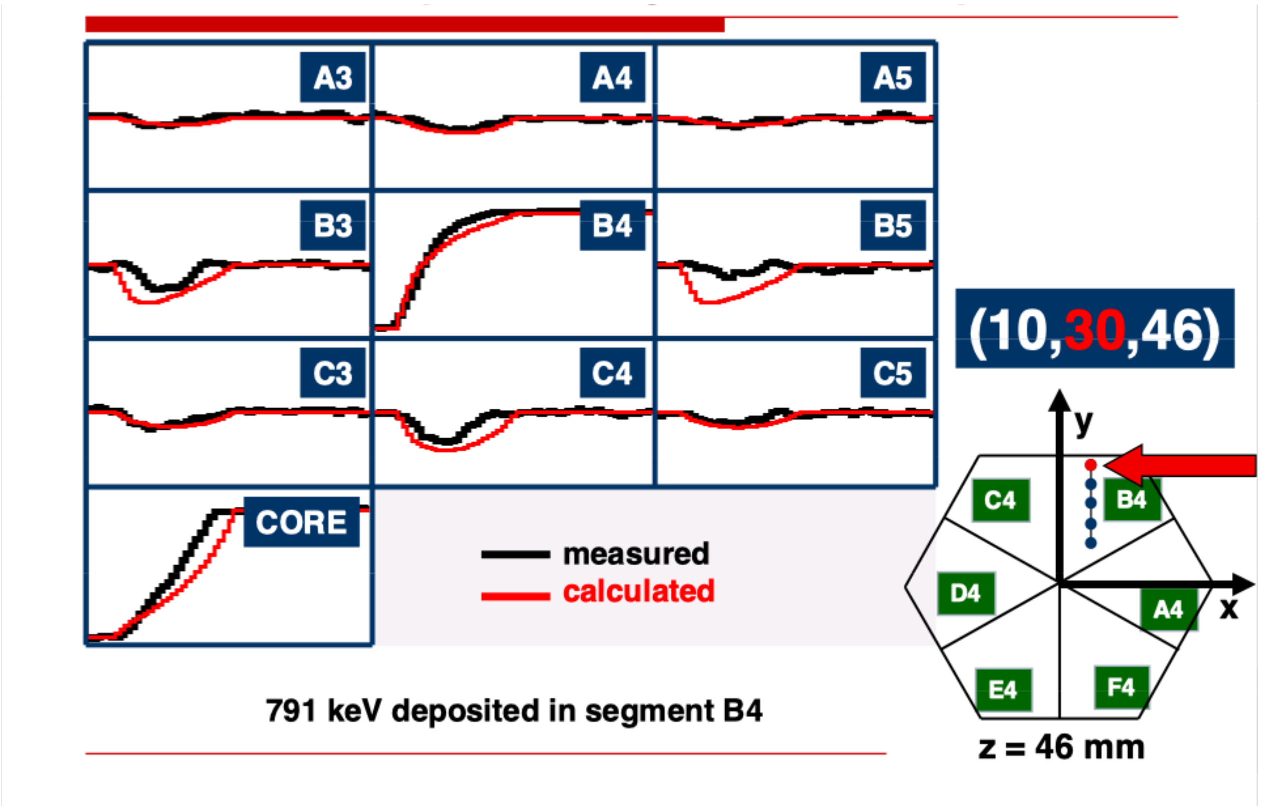

From F. Recchia, PSD8 conference

Pulse shape analysis concept

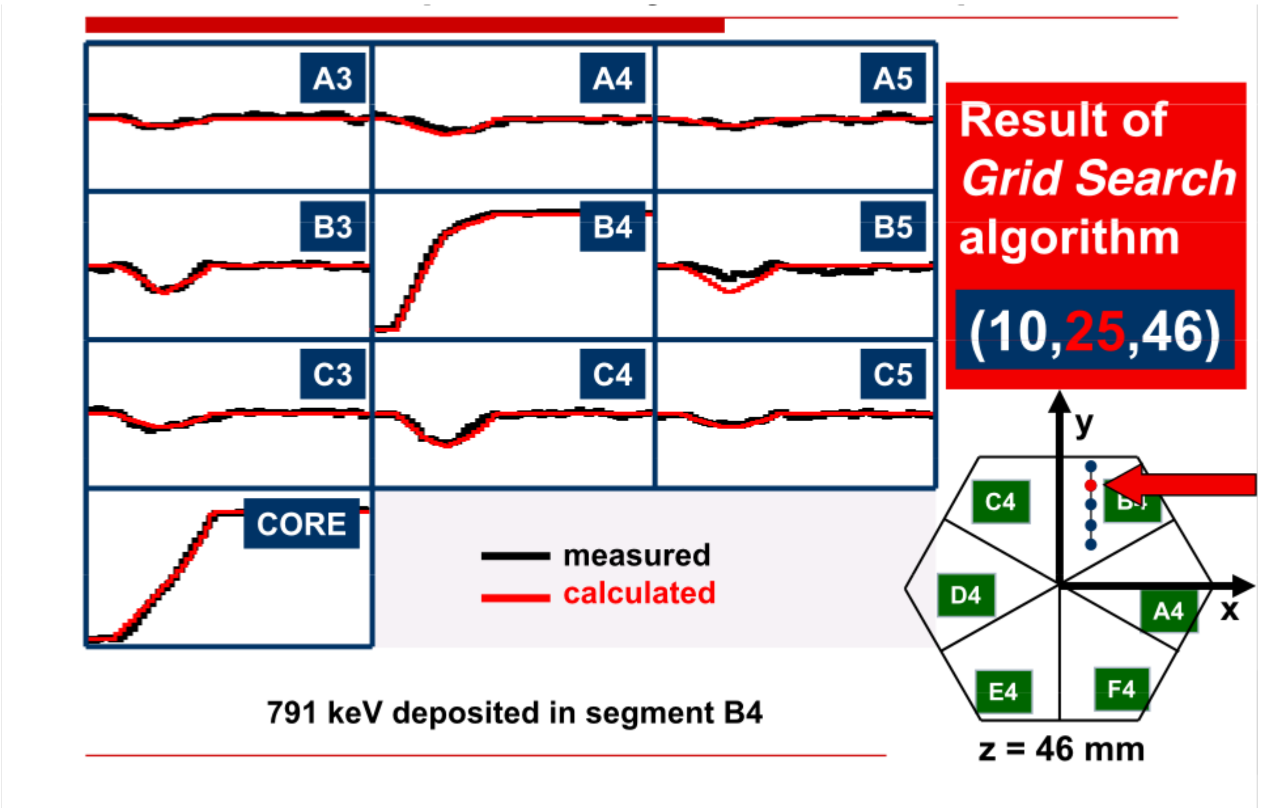

From F. Recchia, PSD8 conference

Exercise 3: Pulse-shape analysis (using chi2 minimisation)

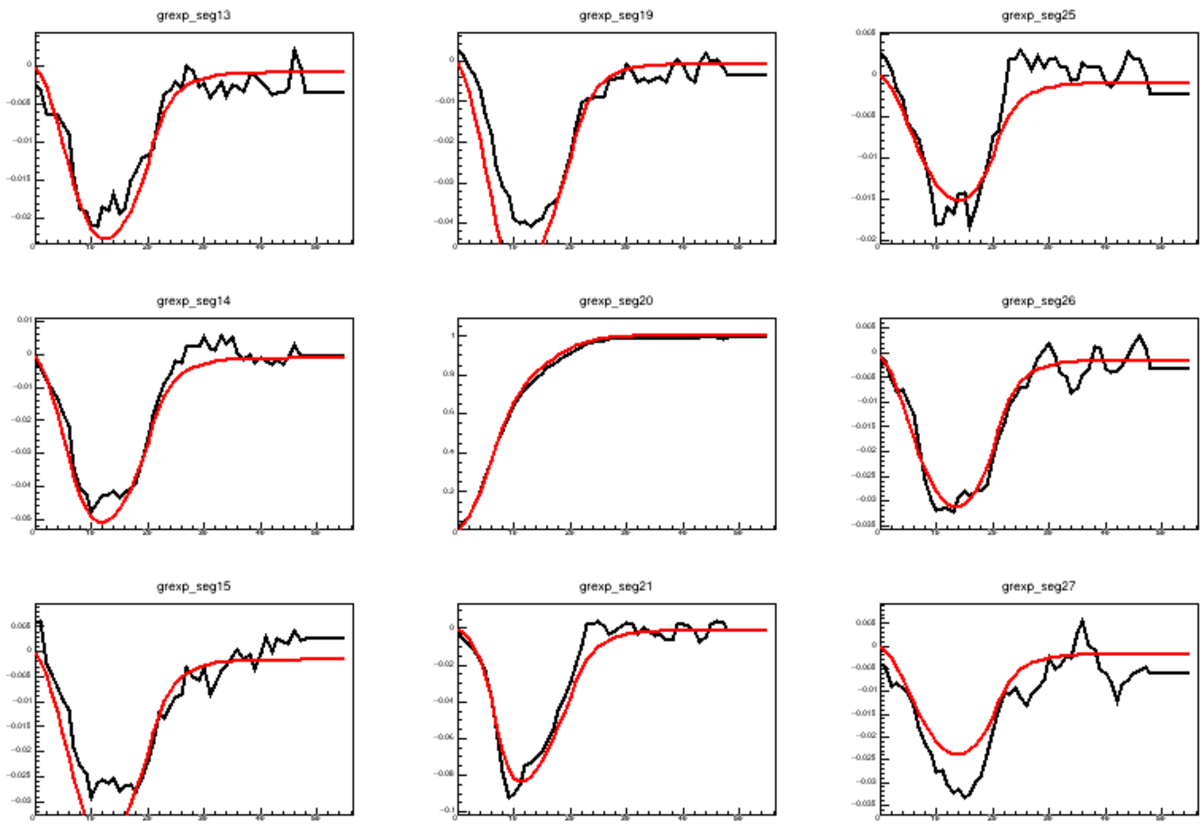

The text file contains:

- in the 2nd column the recorded waveforms in 9 neighboring segments and the CC for a single measured event
- in columns 3rd - 11th it has the same information for 9 pre-calculated basis points

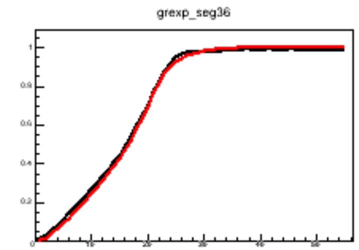

Compare the traces and extract the x, y, z interaction position (from the corresponding basis points) that gives the best-fit to the recorded data

Prepared by Sidon Chen

A realistic basis

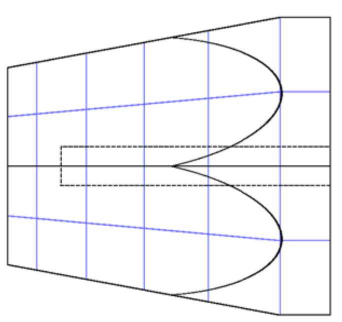

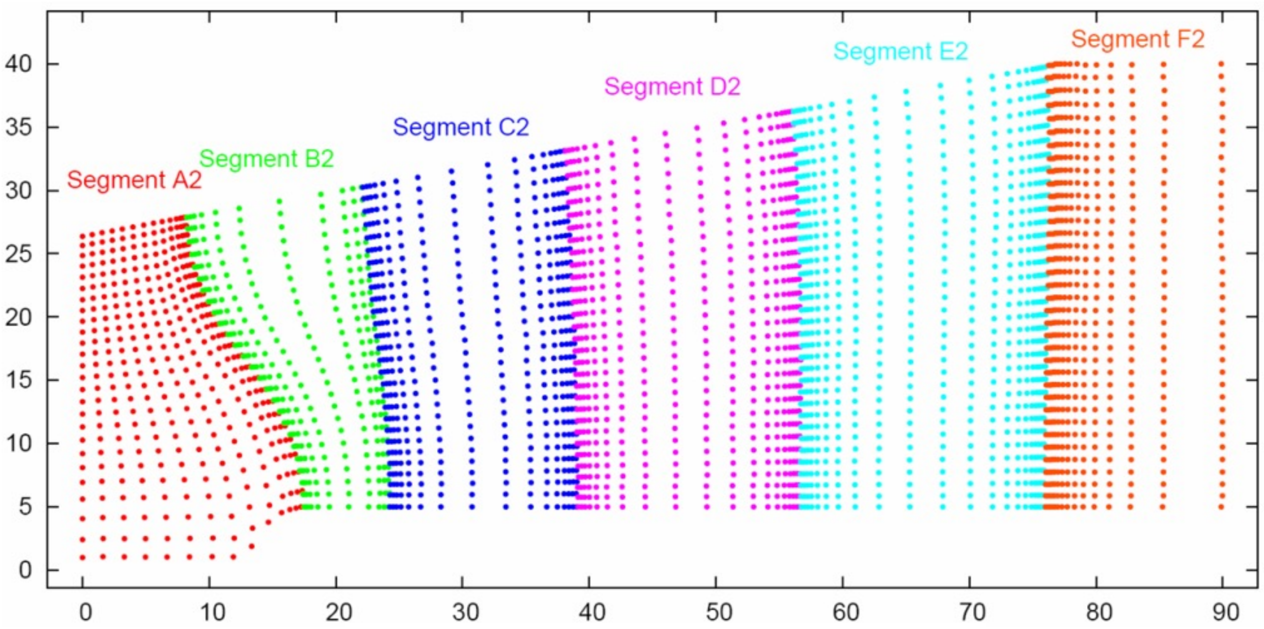

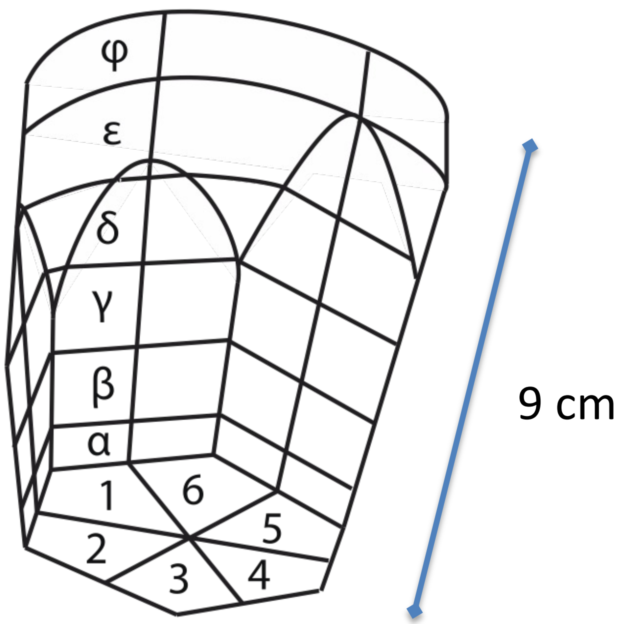

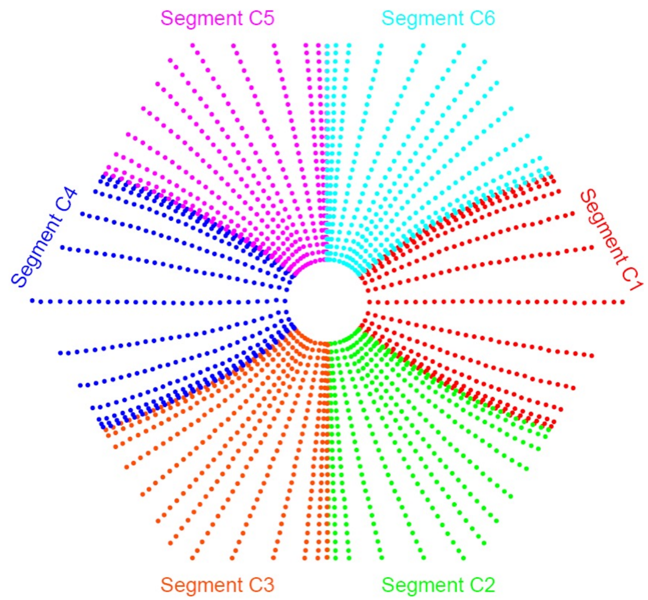

A realistic position reconstruction

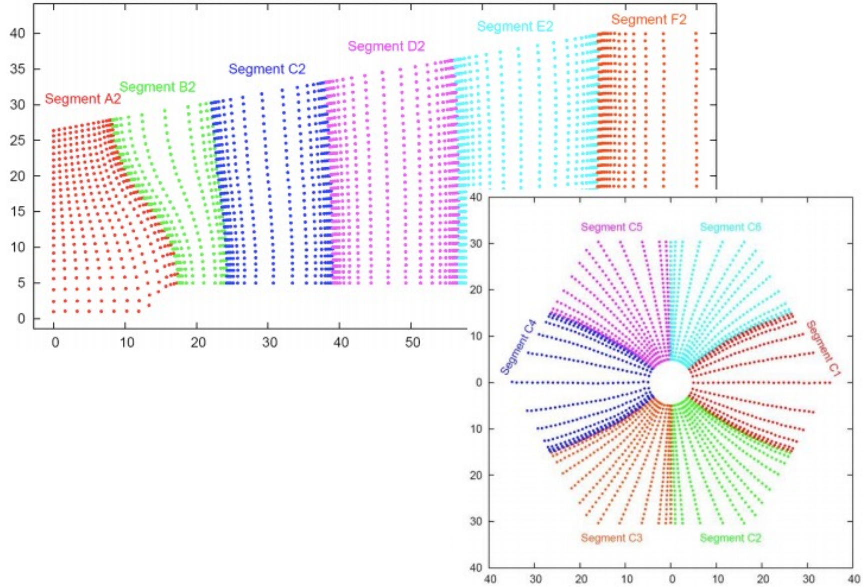

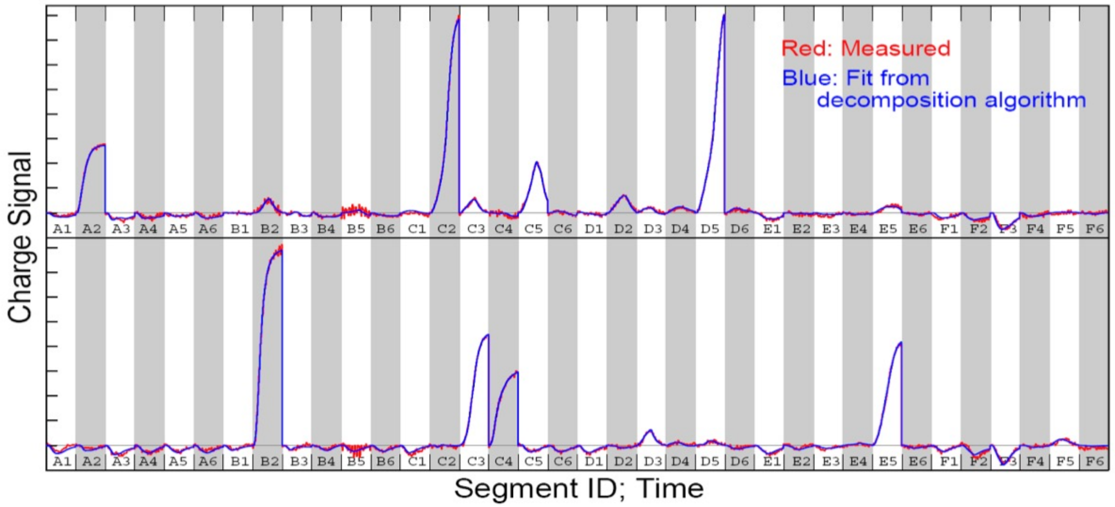

Collimated source of ^{137}Cs 662 keV

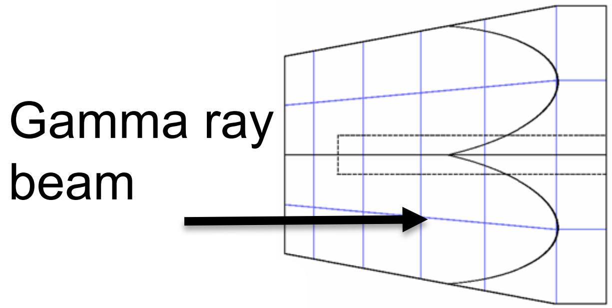

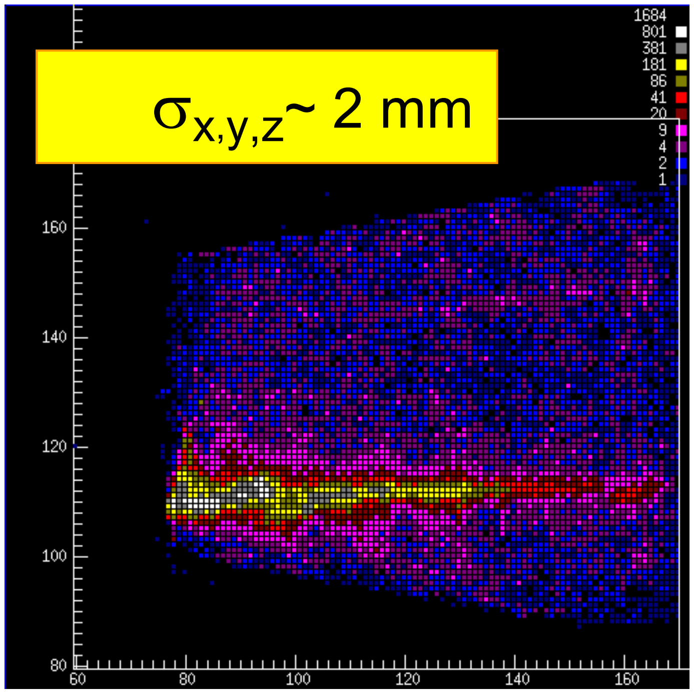

Position resolution

- Collimated beam of ^{137}Cs 663 keV
- Highest energy point from signal decomposition

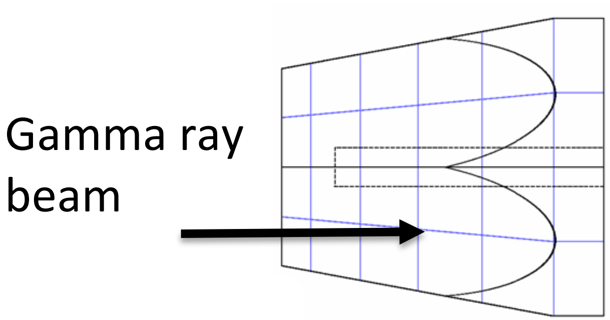

singles

$\sigma_{x,y,z}$~ 2 mm

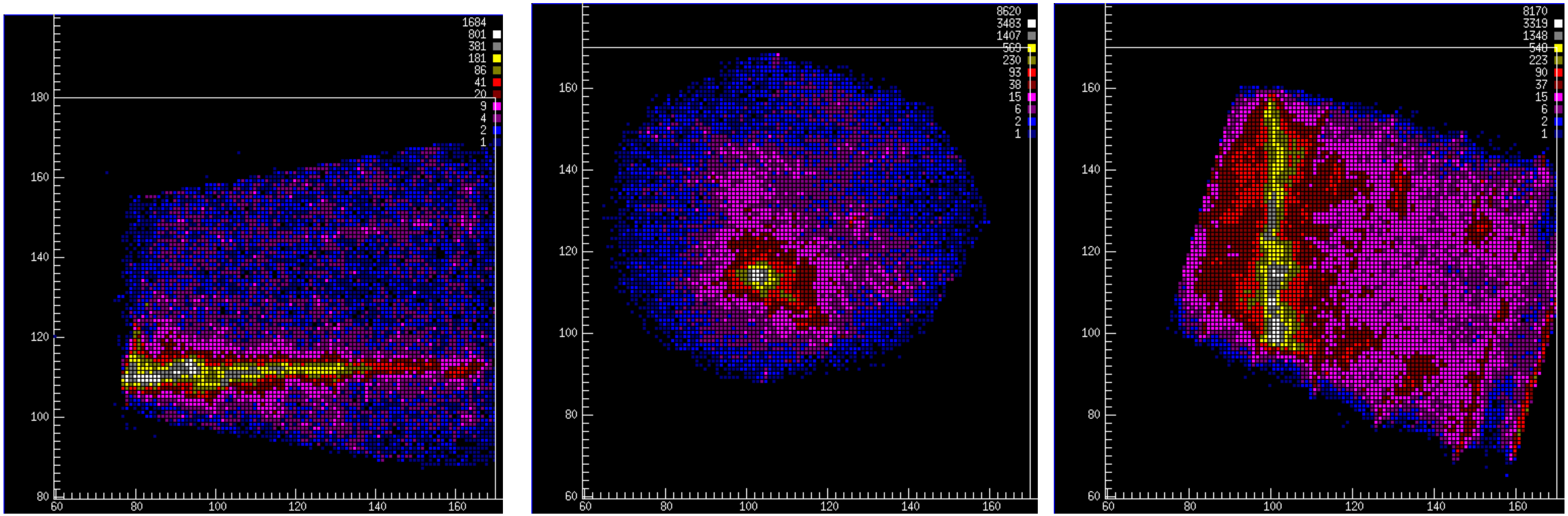

Gamma–Ray Tracking

1

Highly segmented HPGe detectors

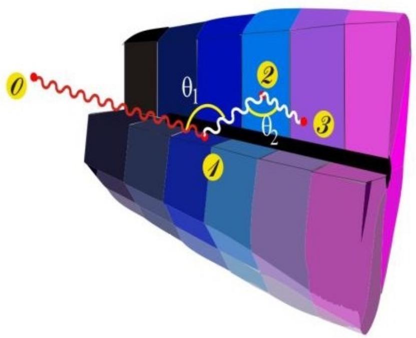

2

Digital electronics to record and process segment signals

3

Pulse Shape Analysis to decompose recorded waves

Identified interaction points

$(x,y,z,E,t)_i$

4

Reconstruction of tracks evaluating permutations of interaction points

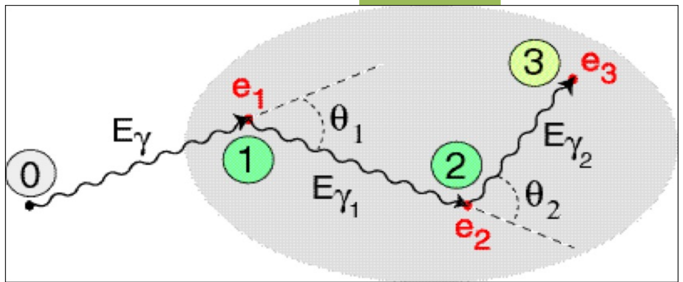

Reconstructed gamma-rays

Gamma-ray tracking: Principle of operation

A 3D position sensitive Ge detector
- Electrically segmented
- Pulse shape analysis

of position sensitive signals

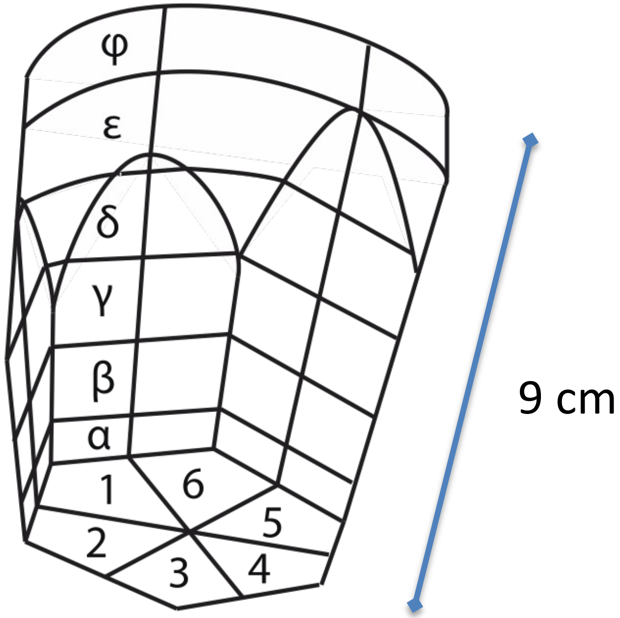

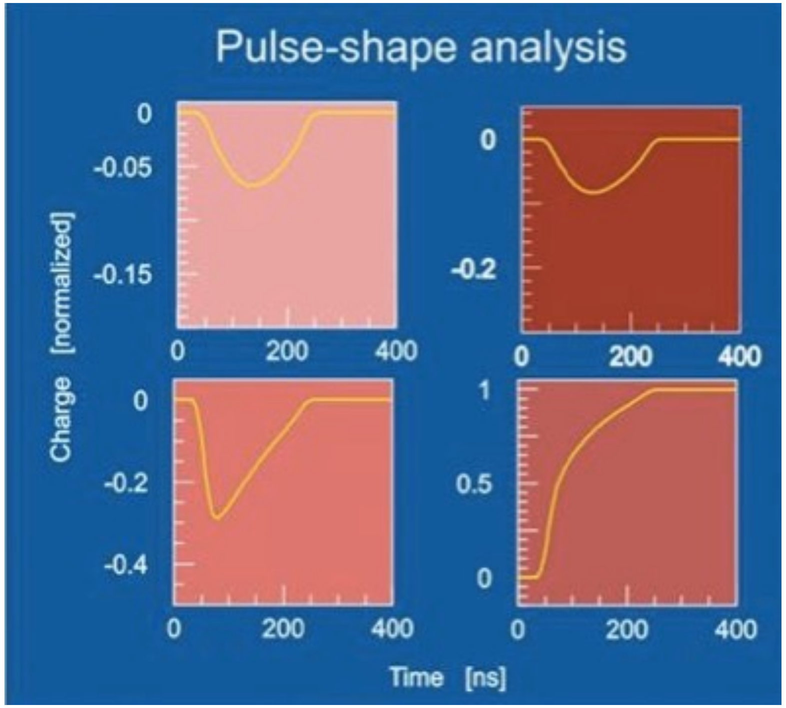

Determine interaction points

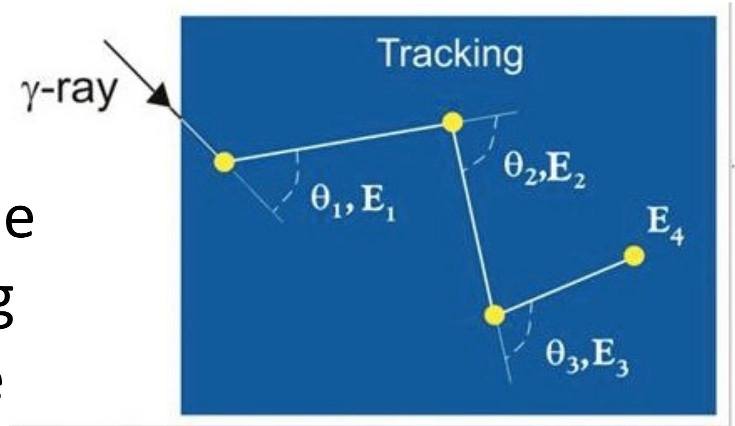

Determine scattering sequence

Tracking: clustering

First step in tracking is to find clusters of interaction points which likely belong to a single γ-ray scattering in the detector – based on opening angle into the Ge shell

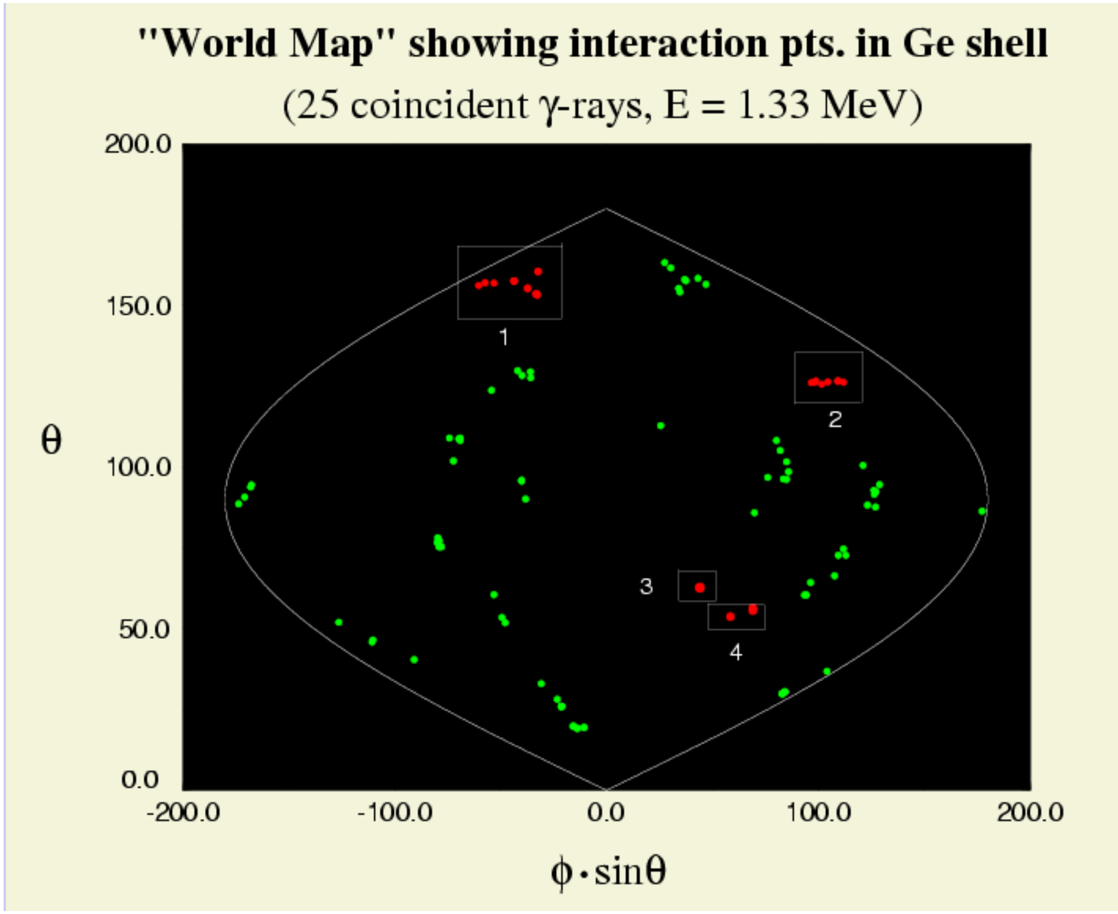

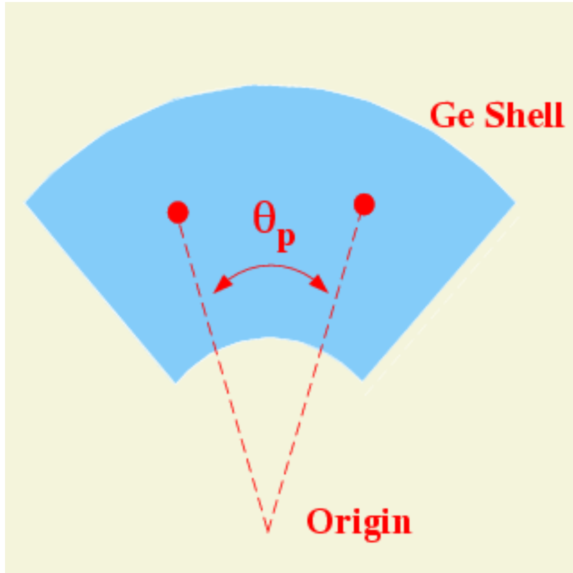

Any two points with $\Delta\theta < \theta_p$ are grouped into the same cluster

Tracking: Compton scattering formula

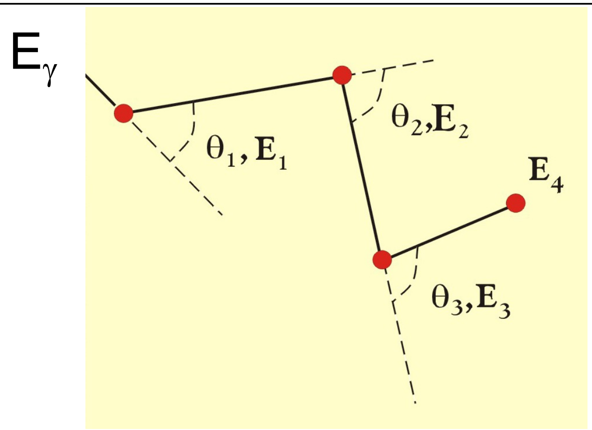

$$E_e = E_\gamma \left(1 - \frac{1}{1 + \frac{E_\gamma}{0.511}(1 - \cos\theta)} \right)$$

Assume:

- $E_\gamma = E_{e1} + E_{e2} + E_{e3}$
- γ-ray from the source

Problem: 3!=6 possible sequences

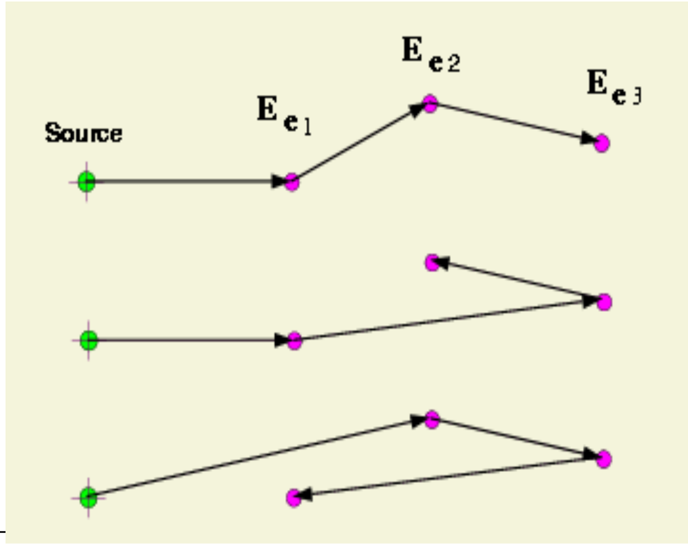

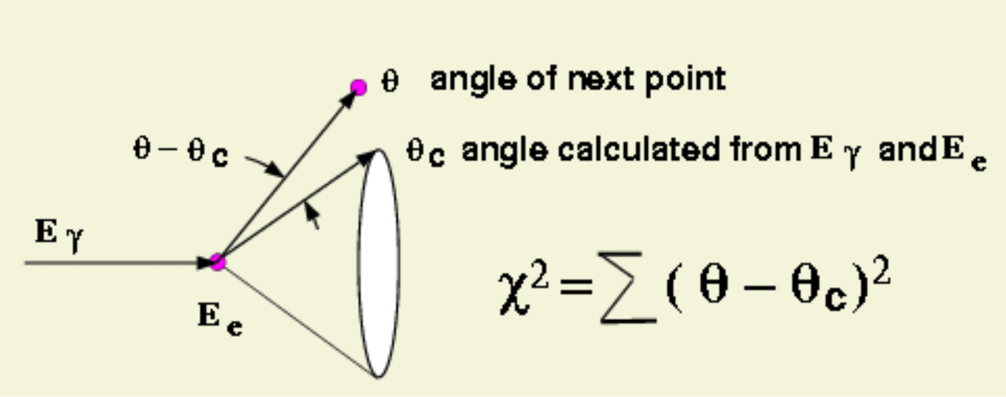

Sequence with the minimum χ^2
→ correct scattering sequence
→ rejects escaped (Compton) and wrong direction

Exercise 4: γ-ray tracking

A Geant4 simulation assumes a 2MeV gamma-rays emitted from 0.5c moving particles, and detected by 4Pai-AGATA array.

1,000,000 events are simulated.

The analysis is performed with OFT tracking and the Doppler correction is applied.

The branches in the tree are:

- **EntryID**: event id in simulation
- **Energy**: gamma energy without Doppler correction
- **EDopp**: gamma energy with Doppler correction
- **FOM**: in the OFT tracking, the FOM is calculated as the probability, so large FOM means tracking
- **ninter**: number of interactions in one event

Prepared by Sidon Chen

Doppler shift and broadening

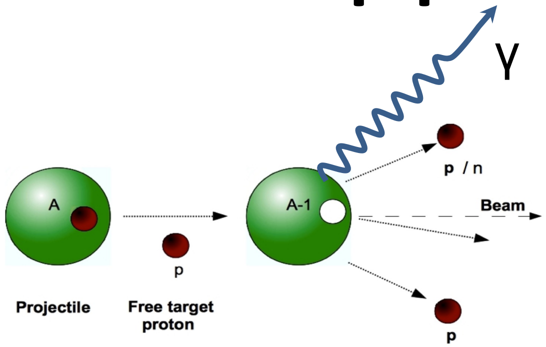

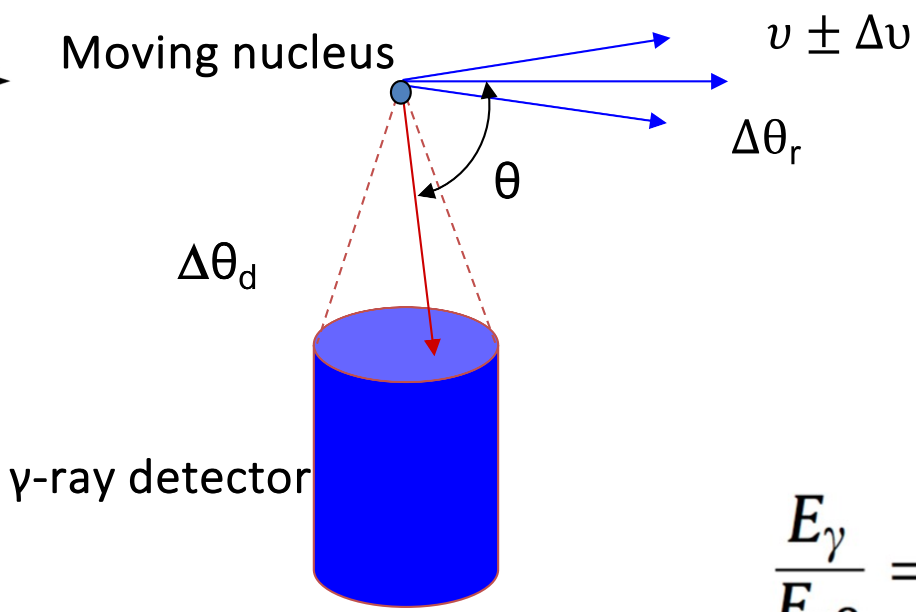

$$\frac{E_\gamma}{E_{\gamma 0}} = \frac{\sqrt{1-\beta^2}}{1-\beta\cos\vartheta_\gamma}$$

Broadening of detected gamma-ray energy due to:

- velocity change in target (unknown interaction depth), momentum spread
- $\Delta\theta$ due to opening angle detector and trajectory of nucleus

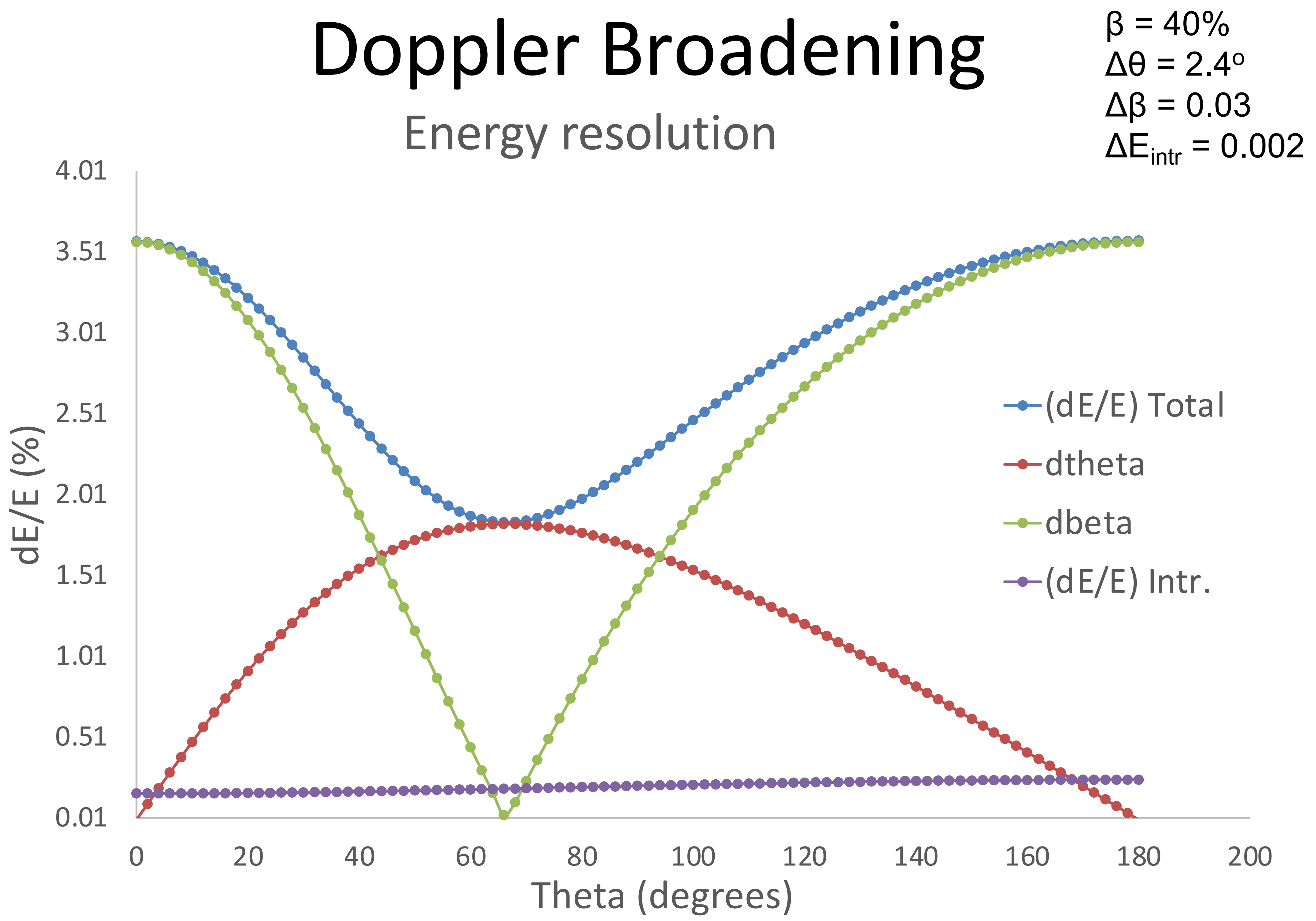
Doppler Broadening
Energy resolution
β = 40%
Δθ = 2.4°
Δβ = 0.03
ΔE_intr = 0.002
dE/E (%)
4.01
3.51
3.01
2.51
2.01
1.51
1.01
0.51
0.01
0
20
40
60
80
100
120
140
160
180
200
Theta (degrees)
(dE/E) Total
dtheta
dbeta
(dE/E) Intr.

Doppler Broadening

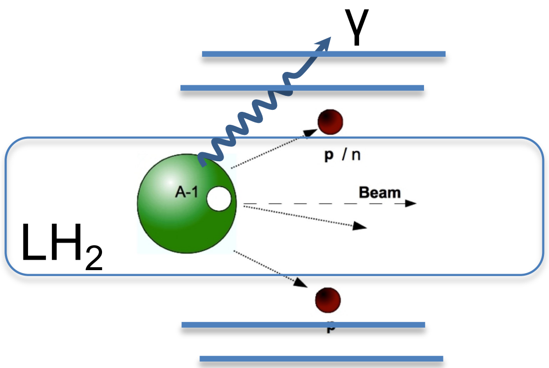

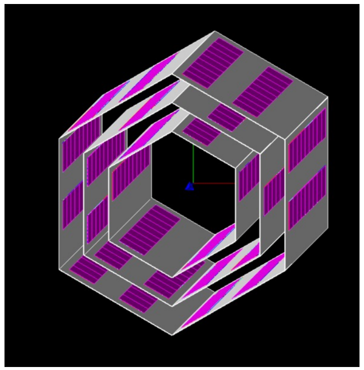

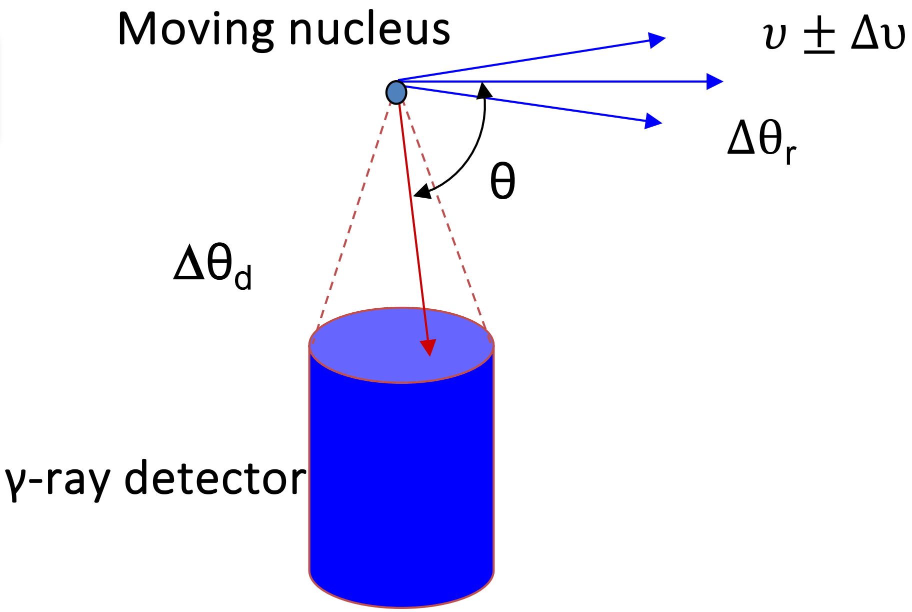

MINOS
Magic Numbers Off Stability

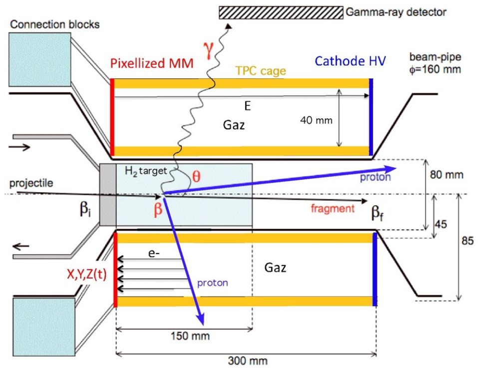

Broadening of detected gamma-ray energy due to:

- velocity change in target (unknown interaction depth), momentum spread
  - E.g. thin target (or MINOS)
- Δθ due to opening angle detector and trajectory of nucleus
  - E.g. position resolution of gamma-ray detector and Spectrometer/detector

Doppler correction using position information

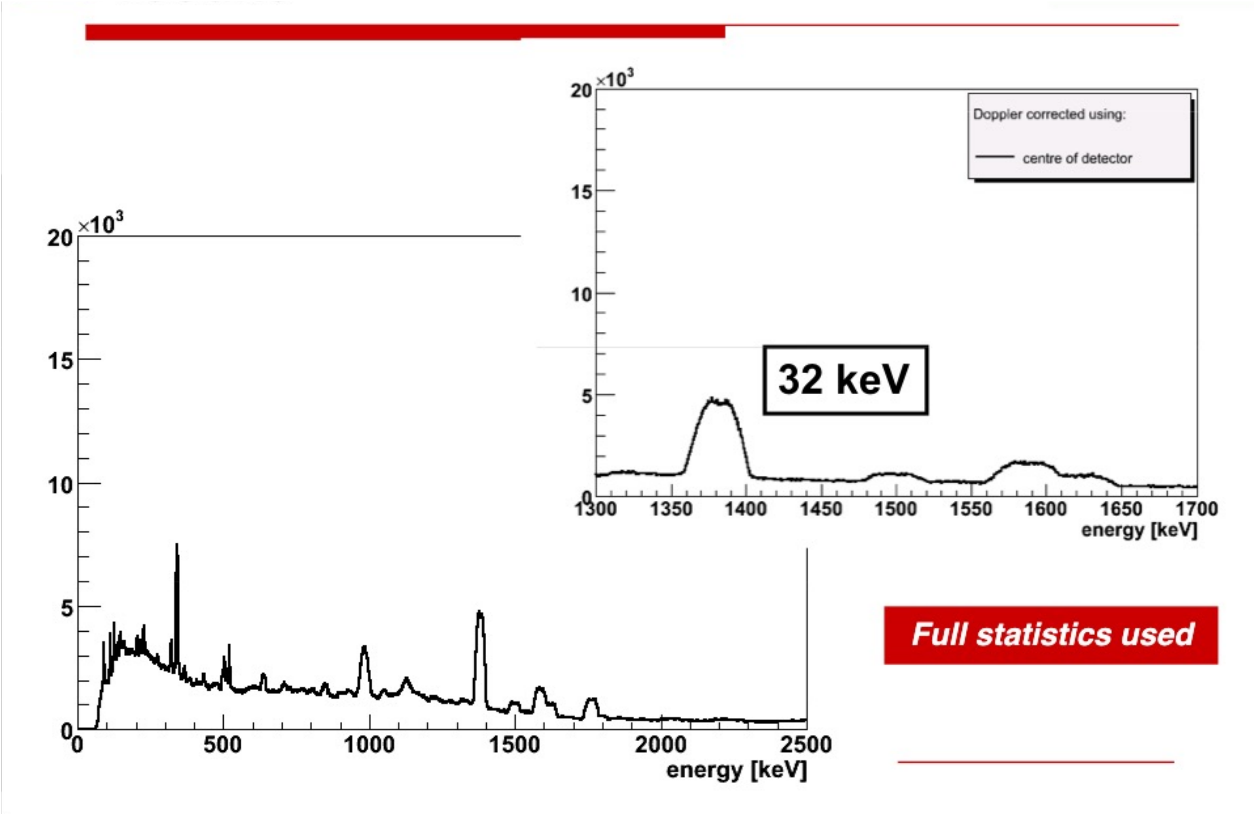

From F. Recchia, PSD8 conference

Doppler correction using position information

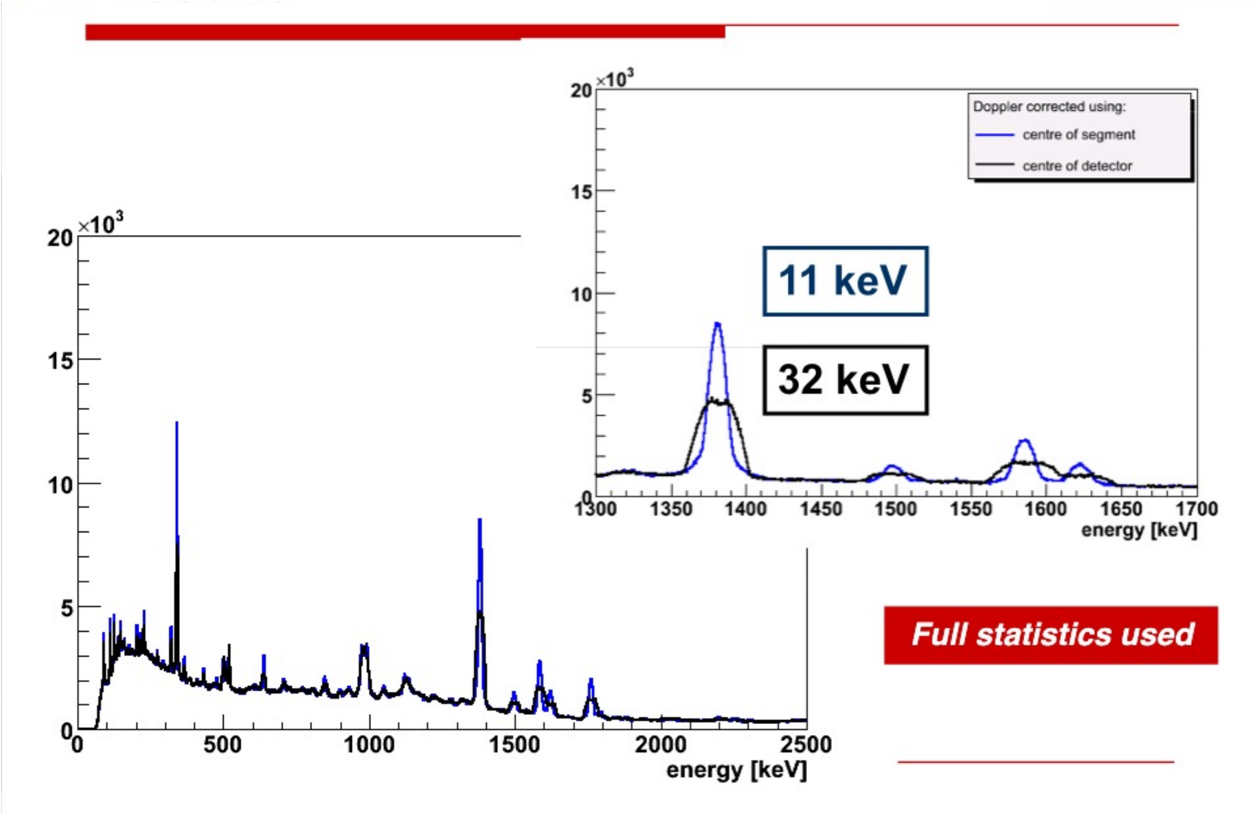

From F. Recchia, PSD8 conference

Doppler correction using position information

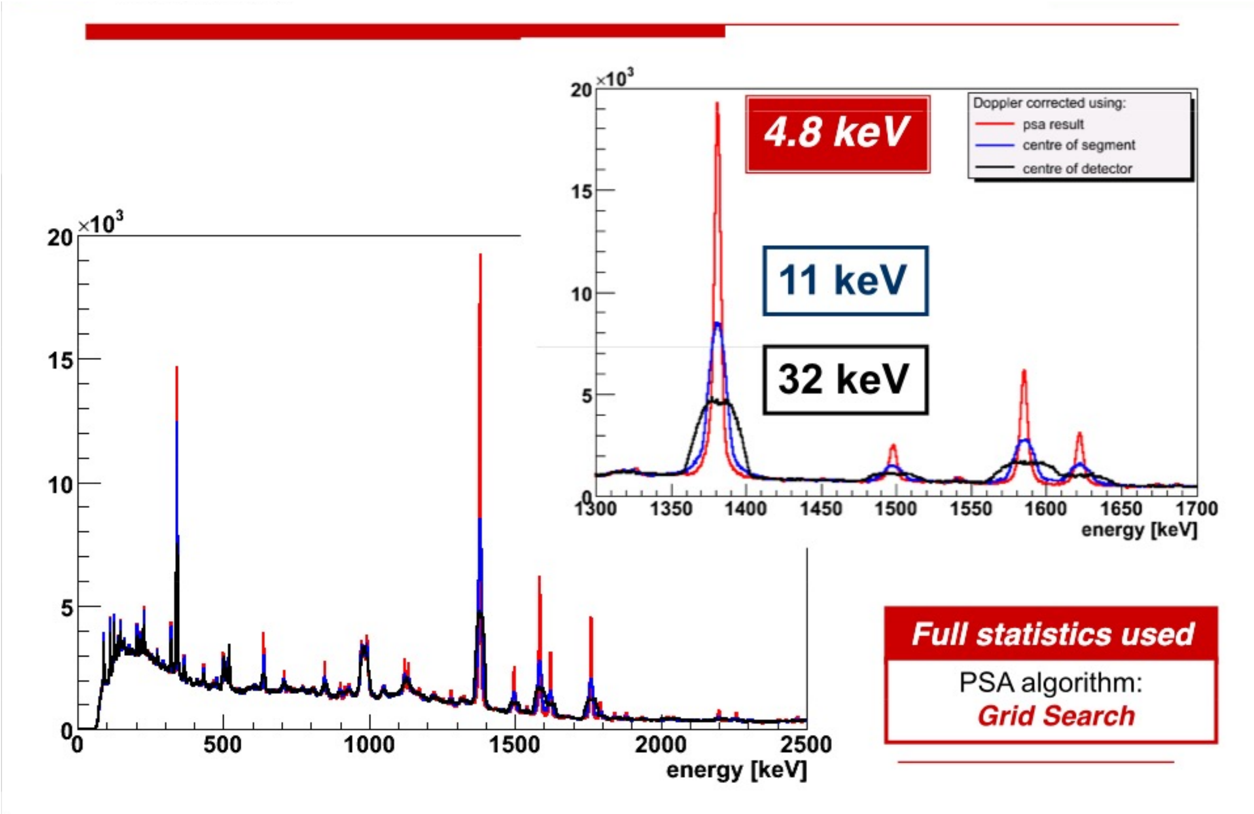

From F. Recchia, PSD8 conference

Advantages of Tracking

Advantages of Tracking	
Efficiency	No solid angle lost to suppressors
Peak-to-background	Reject Compton events
Doppler correction	Position of 1st interaction
Polarization	Angular distribution of the 1st scattering
Counting rate	Many segments

bonus

Particularly important for experiments with fast secondary beams delivered by the fragmentation facilities

Summary

In this Lecture we discussed:

- Interactions of ionizing radiation with matter
- Detection technology
- Electronic readout and signal processing
- Data analysis

Background and motivation

γ rays

Semiconductors, HPGe arrays

position sensitive

for g-ray tracking